

Data-Driven Approach for Personalization of Electropolishing Operations in Used Baths

Zahra Chaghazardi

A Thesis

In the Department of

Mechanical, Industrial & Aerospace Engineering (MIAE)

Presented in Partial Fulfillment of the Requirements

For the Degree of

Doctor of Philosophy (Mechanical Engineering) at

Concordia University

Montreal, Quebec, Canada

October, 2023

© Zahra Chaghazardi, 2023

**CONCORDIA UNIVERSITY  
SCHOOL OF GRADUATE STUDIES**

This is to certify that the thesis prepared

By: Zahra Chaghazardi

Entitled: Data-Driven Approach for Personalization of Electropolishing Operations in Used Baths

and submitted in partial fulfillment of the requirements for the degree of

**Doctor Of Philosophy**

**Mechanical Engineering**

complies with the regulations of the University and meets the accepted standards with respect to originality and quality.

Signed by the final examining committee:

<u>Dr. Pantcho Stoyanov</u>	Chair
<u>Dr. Philip Koshy</u>	External Examiner
<u>Dr. Alex De Visscher</u>	Arm's Length Examiner
<u>Dr. Martin Pugh</u>	Examiner
<u>Dr. Christian Moreau</u>	Examiner
<u>Dr. Rolf Wuthrich</u>	Thesis Supervisor (s)

Approved by \_\_\_\_\_

Dr. Muthukumaran Packirisamy Chair of Department or Graduate Program Director

12/06/2023  
Date of Defence

\_\_\_\_\_  
Dr. Mourad Debbabi

\_\_\_\_\_  
Dean, Dean of faculty

## **Abstract for PhD**

Data-driven approach for personalization of electropolishing operations in used baths

**Zahra Chaghazardi, Ph.D.**

**Concordia University, 2023**

Industrial electropolishing facilities can enhance their competitiveness in the market by embracing the concept of mass personalization, which involves closely integrating customers in the design process to accommodate their specific preferences. Traditional electropolishing operations rely heavily on skilled operators and costly trial-and-error experiments to determine the suitable process parameters for obtaining their target surface quality. The ongoing deterioration of the polishing bath further complicates achieving personalized outcomes. To adopt the mass personalization trend, electropolishing operations need to implement approaches that ensure consistent polishing results while enabling the rapid identification of optimal process parameters for achieving personalized surface finishes.

The goal of this work is to develop a prediction tool to determine the suitable polishing parameters in a deteriorating polishing bath to attain the target surface quality. The study uses surface roughness and brightness measurements, as well as SEM images of the parts to investigate the effect of bath conditions on the final surface finish of electropolished parts. Multiple explanations are suggested to justify the compromised performance of heavily-used baths. The study also proposes a current-voltage plot that can be used as a tool to determine the polishing voltages associated with the emergence of some surface defects under varying bath conditions.

A substantial dataset is next compiled from electropolishing experiments conducted under different bath states and using various polishing parameters. This dataset is later subjected to several machine learning algorithms to determine the model that best represents the data. The Random Forests model is selected as the foundation for the target prediction tool, which demonstrates excellent performance on both the dataset and previously unseen scenarios. The constructed tools offer a comprehensive perspective on electropolishing outcomes across different bath and part conditions and polishing process parameters.

Moreover, by facilitating the attainment of the desired surface finish even in heavily-utilized electrolytes, the developed tools diminish the need for frequent electrolyte replenishment and the expensive disposal of hazardous waste, thereby benefiting the environment

## **Acknowledgements**

I would like to express my heartfelt gratitude to the amazing individuals who have been with me every step of the way on this journey.

To my supervisor, Dr. Rolf Wuthrich, for his guidance, expertise, and mentorship.

To my thesis defense committee, Dr. Pantcho Stoyanov, Dr. Alex De Visscher, Dr. Martin Pugh, Dr. Christian Moreau, and Dr. Philip Koshy, for their valuable feedback and suggestions.

To my dear partner, for his never-ending support and encouragement.

To my two beloved friends, for their unwavering motivation and belief in me.

To my lab colleagues, for their friendship, knowledge-sharing, and assistance.

To my family for their boundless kindness and love.

And to all those who have contributed to my thesis in various ways, your support has been instrumental in my academic accomplishments. Thank you for being a part of this experience.

Woman-Life-Freedom

# Table of Contents

1. Introduction .....	1
1.2. Transition of manufacturing technologies towards mass personalization.....	1
1.3. Electropolishing, a promising candidate for mass personalization .....	2
1.4. Problem statement .....	3
1.5. Objectives.....	5
1.6. Significance of the study .....	7
2. Literature Review .....	9
2.1 Electropolishing process, potentials, challenges .....	9
2.1.1 Mechanism of electropolishing.....	10
2.1.2 Role of electropolishing parameters .....	11
2.1.3 Advantages and challenges of electropolishing process.....	14
2.2 Electrolyte ageing.....	18
2.2.1 What is electrolyte ageing?.....	18
2.2.2 How does aging affect the polishing quality?.....	18
2.2.3 What causes the decline in the quality of the surface in aged polishing baths? .....	19
2.2.4 Effect of electrolyte aging on increasing the consumed energy .....	20
2.2.5 Effect of aged solution disposal on environment .....	22
2.2.6 Evaluation of existing research on electropolishing in aged electrolyte .....	23
2.3 Quality control in electropolishing.....	25
2.3.1 Removing electrolyte sludge .....	26
2.3.2 Decanting the electrolyte .....	26
2.3.3 Monitoring bath properties .....	26
2.3.4 Quality control challenges .....	28
2.3.5 Quality control using data-driven approaches .....	28
3. Methodology.....	31
3.1. Introduction .....	31
3.2. Experimental set-up and procedure.....	31
3.2.1. Workpiece and bath preparation .....	31
3.2.2. Electropolishing.....	32

3.2.3.	Bath characterization .....	33
3.2.4.	Sample characterization.....	34
3.3.	Model development.....	36
4.	Polishing Bath History.....	38
4.1.	Introduction .....	38
4.2.	Bath analysis .....	38
4.3.	Sample analysis .....	40
4.3.1.	Surface roughness and brightness characterization .....	40
4.3.2.	Scanning Electron Microscopy .....	42
4.4.	Analysis of the results .....	43
4.5.	Concluding remarks .....	57
5.	Open Dataset for Stainless Steel Electropolishing .....	60
5.1	Introduction .....	60
5.2	Determining the correct process parameters in an ever-changing polishing bath.....	61
5.3	Dataset construction .....	65
5.4	Dataset exploration.....	71
5.5	Dataset preprocessing.....	77
5.6	Model development.....	77
5.6.1.	Definition of the target variable.....	78
5.6.2.	Feature selection .....	78
5.6.3.	Model training .....	82
5.6.4.	Hyperparameter tuning.....	82
5.7	Model selection .....	83
5.8	Concluding remarks .....	90
6.	Model Prediction of Polishing Parameters for Given Bath States.....	92
6.1.	Introduction .....	92
6.2.	Development of the prediction tool.....	92
6.3.	Performance of the prediction tool on previously seen solutions .....	93
6.4.	Generalization capacity of the prediction tool to unfamiliar polishing baths .....	94
6.5.	Concluding remarks .....	100
7.	Outlook .....	102
7.1.	Extending the scope of the study.....	102

7.2.	Increasing the size of the dataset for better generalization .....	102
7.3.	Application of the K Nearest Neighbors (KNN) algorithm .....	104
7.4.	Software architecture for actual deployment of the prediction tool in production .....	106
8.	Conclusion .....	108
9.	References .....	111
10.	Appendix .....	119



## List of Figures

Figure 2.1. Schematic of an electropolishing cell.....	9
Figure 2.2. Characteristic I-V curve of the electropolishing process according to Han et al. <sup>33</sup> ...	10
Figure 2.3. Variation of the mean surface roughness Ra of 316 stainless-steel surfaces with the duration of electropolishing process as (a) measured by AFM, and (b) measured by stylus profilometry <sup>52</sup> .....	13
Figure 3.1. A typical electropolishing cell utilized in this study.....	33
Figure 3.2. Specular and diffuse reflection.....	35
Figure 3.3. Surface gloss measurement angles.....	35
Figure 3.4. Model development steps.....	37
Figure 4.1. (a) Untreated sample and samples electropolished under 5 V, 300 s in (b) solution 3, (c) solution 2, and (d) solution 1.....	41
Figure 4.2. SEM images of a) untreated sample and samples electropolished in (b) solution 1, (c) solution 2, and (d) solution 3 under similar polishing parameters (5 V, 300 s).....	42
Figure 4.3. The change observed in the surface roughness (Ra) of samples electropolished in solutions 1, 2, and 3 under different polishing voltages for 300 s.....	45
Figure 4.4. Variation of the I-V behavior of the workpiece with electric conductivity of the bath. The polishing current shown in the plots is the average measured current over different durations of the polishing experiments (300 s, 600 s, and 900 s).....	46
Figure 4.5. (left) Current-voltage plot for water electrolysis process on a gas-evolving electrode, (right) bubble diffusion layers around a cylindrical electrode at various voltages <sup>103</sup> .....	47
Figure 4.6. Percolation model of the bubble nucleation sites on the lateral surface of an electrode <sup>103</sup> .....	48
Figure 4.7. The surface finishes obtained after electropolishing under increasing potentials (5, 6, and 7 V) for 300 s in solutions 1, 2, and 3. The orange peel effect and the gassing streaks are shown by red and green dashed lines, respectively. Note: the mechanical scratches (defects not highlighted with dashed lines) are due to the manipulation of the samples. ....	50
Figure 4.8. Surface finishes obtained at different regions of the current-voltage plot for samples electropolished in (a) solution 1, (b) solution 2, and (c) solution 3 (note: the mechanical scratches on the surface are due to manipulation and handling of the samples.).....	52
Figure 4.9. Samples electropolished under 5 V, 300 s in (a) solution A, (b) solution B, and (c) solution C.....	55
Figure 5.1. Up: Surface finishes obtained for titanium samples for (top) 20 minutes polishing duration and different polishing voltages (10, 15, 20, and 25V) and (bottom) 20 V polishing potential and different polishing durations (10, 20, 30, and 40 min) <sup>128</sup> .....	62
Figure 5.2. (top): Range of surface finishes obtained for stainless steel 316 samples by changing the electropolishing voltage and duration in solution 1, (bottom): variation of the corresponding surface gloss (the samples are organized in order of applied polishing voltage and polishing duration).....	64

Figure 5.3. (top): Range of surface finishes obtained for stainless steel 316 samples by changing the electropolishing voltage and duration in solution 3, (bottom): variation of the corresponding surface gloss (the samples are organized in order of applied polishing voltage and polishing duration).....	65
Figure 5.4. Boxplot of the standard deviation in conductivity measurements for different solutions (340 samples).....	66
Figure 5.5. Distribution of bath temperature in conducted experiments (249 samples).....	67
Figure 5.6. (left) Distribution of the standard deviation in bath temperatures, (right) effect of polishing duration on bath temperature standard deviation (249 sample).....	67
Figure 5.7. Standard deviation of surface roughness indexes before and after electropolishing treatment (249 samples).....	69
Figure 5.8. Standard deviation of surface gloss measurements before and after electropolishing (249 samples).....	70
Figure 5.9. Cumulative distributions of viscosity and conductivity for the investigated solutions. ....	72
Figure 5.10. Variation of the electric conductivity and viscosity among the studied electrolytes. ....	72
Figure 5.11. Surface roughness distribution of the samples (top) before, and (bottom) after electropolishing treatments (249 samples).....	73
Figure 5.12. Surface brightness distribution of the samples (top) before, and (bottom) after electropolishing treatments (249 samples).....	74
Figure 5.13. Correlation matrix for different variables of the electropolishing process.....	75
Figure 5.14. Effect of bath viscosity and electric conductivity on the average final roughness (Ra) of the electropolished samples.....	76
Figure 5.15. Effect of bath viscosity and electric conductivity on the average final roughness (Ra) of the electropolished samples.....	76
Figure 5.16. Correlation of the average final roughness (Ra) of the electropolished samples with the average surface gloss. ....	77
Figure 5.17. Dataset features in order of their importance in predicting Ra_rel using various feature selection methods.....	80
Figure 5.18. Dataset features in order of their importance in predicting H20_after using various feature selection methods.....	81
Figure 5.19. Hyperparameter tuning using cross-validation for (left) KNN algorithm and (right) Random Forests algorithm.....	83
Figure 5.20. The linear regression model used for the prediction of Ra-after, Rq-after, and Rz-after. ....	84
Figure 5.21. The KNN model used for the prediction of Ra-after, Rq-after, and Rz-after. ....	85
Figure 5.22. The Random Forests model used for the prediction of Ra-after, Rq-after, and Rz-after. ....	86
Figure 5.23. The Voting Regressor ensemble used for the prediction of Ra-after, Rq-after, and Rz-after. ....	87
Figure 5.24. RMSE distribution of different models for prediction of Ra-after, Rq-after, and Rz-after on the test set. ....	88

Figure 5.25. RMSE distribution of different models for prediction of final surface gloss on the test set.....	89
Figure 5.26. Results of Random Forests model in prediction of H2O_after. ....	90
Figure 6.1. Architecture of the prediction tool. ....	93
Figure 6.2. Predictions made by the tool outlined in Figure 6.1.....	93
Figure 6.3. Final surface roughness predictions for the for the sample polished in solutions 1, 2, and 3 of Chapter 4, under 5 V for 300 s. The blue line is the prediction tool, while the orange circles demonstrate the measured values. ....	94
Figure 6.4. Distribution of the tool's RMSE in prediction of Ra, Rq, and Rz for samples electropolished under 5 V for 300 s, and 3 V for 900 s in the studied solutions. ....	97
Figure 6.5. Samples electropolished under 5V and 300s in (a) solution 1, (b) solution 2, and (c) solution 3, and under 3V and 900s in (d) solution 1, (e) solution 2, and (f) solution 3.....	98
Figure 6.6. Samples electropolished in solution 7 under (a) 5 V and 300 s, and (b) 3 V and 900 s. ....	99
Figure 6.7. Samples electropolished under 5 V and 300 s in (a) solution 4, (b) solution 5, and (c) solution 6 and samples electropolished under 3 V and 900 s in (d) solution 4, (e) solution 5, and (f) solution 6.....	100
Figure 7.1. Variation of the tool RMSE error in prediction of Ra_after, Rq_after, and Rz_after with increasing the size of the dataset.....	103
Figure 7.2. Variation of the KNN model RMSE error in prediction of Ra_after, Rq_after, and Rz_after with increasing the size of the dataset.....	105
Figure 7.3. Example of a software architecture of actual deployment of the prediction tool in production. ....	107
Figure 10.1. The linear regression model used for the prediction of Ra-rel, Rq-rel, and Rz-rel. ....	119
Figure 10.2. The KNN model used for the prediction of Ra-rel, Rq-rel, and Rz-rel. ....	120
Figure 10.3. The Random Forests model used for the prediction of Ra-rel, Rq-rel, and Rz-rel. ....	121
Figure 10.4. The Voting Regressor ensemble used for the prediction of Ra-rel, Rq-rel, and Rz-rel. ....	122
Figure 10.5. RMSE distribution of different models for prediction of Ra-rel, Rq-rel, and Rz-rel on the test set.....	123

## List of Tables

Table 4-1. Measured properties for different bath states. ....	39
Table 4-2. Concentration of dissolved metals measured by ICP-MS analysis. ....	39
Table 4-3. Surface characterization and weight loss measurements for three samples electropolished under the same process parameters (5 V, 300 s) in solutions 1, 2, and 3. ....	41
Table 4-4. Electropolishing results for samples treated in polishing baths with different compositions. ....	55
Table 5-1. Electropolishing process parameters used for the construction of the dataset. ....	67
Table 5-2. Average number of measurements conducted for dataset construction. ....	71
Table 6-1. Characteristics of studied baths. ....	95
Table 6-2. Composition of the fresh electrolytes used in the preparation of baths 1, 2, and 3. ....	95

# Nomenclature

## Symbols

$D$	Diffusion coefficient of a species
$\eta$	Viscosity of the electrolyte
$T$	Absolute temperature
$i_L$	Limiting current density
$n$	Number of electrons involved in an anodic dissolution process
$F$	Faraday constant
$\nu$	kinematic viscosity of the electrolyte
$\omega$	Rotation speed of a rotating disk electrode
$\Delta C$	Concentration difference of the diffusing species between the anode surface ( $C_s$ ) and the bulk electrolyte ( $C_b$ )
$U$	Terminal voltage of an electrochemical cell
$U_0$	Equilibrium potential of an electrochemical cell
$\eta_a/\eta_b$	Anodic/Cathodic electrode overpotential
$R_0$	Electrical resistance of the electrolyte
$\rho$	Electric resistivity of the electrolyte
$l$	Distance between the working and the reference electrodes
$A$	Area of the exposed electrode surface
$\Omega$	Lateral surface of a gas-evolving electrode
$S$	Size of the bubbles generated on the electrode surface
$\theta$	Fraction of the electrode surface covered by bubbles
$\beta$	Coefficient of faradaic gas generation
$d_n$	Mean distance between two bubble nucleation sites on the electrode surface
$\xi$	Bubble flatness index
$\Delta t_b$	Bubble detachment time from the electrode surface
$i_{local}$	Local current density
$I^{crit}/U^{crit}$	Critical current/voltage for formation of a gas film on a gas evolving electrode
$Ra$	Arithmetic mean surface roughness
$Rq$	Root mean square of the surface roughness
$Rz$	Ten point mean surface roughness
$H20/H60$	Surface gloss index at 20°/60° angle
$Sa$	Arithmetic mean height of the surface
$Sq$	Root mean square height of the surface
$Ssk$	Skewness
$Sku$	Kurtosis

# Nomenclature

## Acronyms

AI	Artificial Intelligence
RSM	Response Surface Methodology
ML	Machine Learning
SRF	Superconductivity Radio Frequency
XPS	X-ray Photoelectron Spectroscopy
SEM	Scanning Electron Microscopy
EDX	Energy Dispersive X-ray Spectroscopy
ER	Electrochemical Reduction
ICP-MS	Inductively Coupled Plasma Mass Spectroscopy
IC	Ionic Chromatography
AAS	Atomic Absorption Spectrometry
GRA	Grey Relational Analysis
ANN	Artificial Neural Network
BP	Backpropagation
ECM	Electrochemical Machining
DI Water	Deionized Water
MSE	Mercury Sulfate Electrode
ABS	Acrylonitrile Butadiene Styrene
FDM	Fused Deposition Modeling
GU	Gloss Units
ANOVA	Analysis of Variance
KNN	K-Nearest Neighbors
RMSE	Root Mean Squared Error
$y_{pred}$	Prediction made by the machine learning algorithm

# 1. Introduction

## 1.1. Mass personalization, a new consumption trend

Nowadays, the customers' urge to identify themselves via the products they purchase and consume is an increasing trend in consumer behavior. Customers are increasingly seeking customizable and personalized goods that allow them to put their mark on the products and create something that feels uniquely theirs. Technological advances and evolving customer demands are driving an emerging trend known as “mass personalization”, which enables large-scale product customization to meet individual consumer preferences. Nowadays, companies leverage digital platforms to allow consumers to personalize and customize products. The fashion industry has embraced mass personalization by allowing customers to select colors, patterns, and materials, and even add personalized engravings or messages to create unique products tailored to their tastes. For instance, the popular watch company Swatch offers clients to choose from a variety of parts and design features to build their own unique Swatch watch <sup>1</sup>. Another example is Nike brand’s customization platform where customers select their favorite design elements to create their own unique shoes <sup>2</sup>. Several other industries including beauty and cosmetics, food and beverage, home furnishing, automotive, and consumer electronics are also experiencing significant mass personalization growth.

## 1.2. Transition of manufacturing technologies towards mass personalization

With the advent of the second industrial revolution, mass production methods enabled manufacturers to produce large quantities of standardized parts at a lower cost and in a shorter time. Industries could benefit from the mass production of products with high demand rates such as automobiles and electronic items. Upon the emergence of the third industrial revolution, mass automation, automation technologies, and assembly lines were employed to rapidly manufacture tremendous numbers of standard parts or their variations <sup>3-6</sup>. Nonetheless, the main disadvantage of such processes was the lack of diversity in the final products since it was difficult to adapt a production line to changing demands <sup>7,8</sup>.

The move to a new manufacturing strategy, mass customization, was driven by the ever-rising need of the companies to satisfy the various demands of the customers. This strategy makes use of advancements in information and manufacturing technology to combine the increased diversity of the products with near-mass production efficiency <sup>9</sup>. However, in mass customization, it is the manufacturer who presents the customer with various designs and feature combinations to choose from, rather than the other way around, making it impossible to fully satisfy the individual preferences of the customers or offer personalized products <sup>10,11</sup>. To remain competitive in the market today, companies must implement tactics to enhance both the quantity and degree of their

customized products. This has shifted the mass customization strategy towards a novel paradigm known as mass personalization. The foundation of this concept is the close involvement of the consumers in the design process to accommodate their specific preferences <sup>10,12,13</sup>.

From a technological standpoint, there are no significant impediments to manufacturing individualized products. However, transitioning from large batches of massively identical products to small batches of massively individualized items has proven financially challenging. Given that mass producers often invest heavily in specialized machinery and that shifting to more flexible production strategies raises the manufacturing overhead dramatically, it is becoming exceedingly difficult to make highly diversified products at prices comparable to mass-produced ones <sup>14</sup>.

Another significant factor that raises the cost of the mass personalization strategy is the optimization of manufacturing technology. Manufacturing processes require optimum operating parameters to achieve cost-effective production. Therefore, various optimization strategies are employed, including model-based parameter calculations, implementation of technology vendor's instructions, or experimental optimization using systematic approaches like the Taguchi method. However, since the mass personalization strategy demands flexible manufacturing technologies capable of swiftly adapting to new designs, process parameter re-calibration and re-determination are unavoidable <sup>15</sup>. In contrast to mass production, where the cost of optimizing process parameters may be spread over a large number of identical products, these costs could become prohibitive for the cost-effective production of low-volume and high-variety parts.

The manufacturing processes that are more suited to the idea of mass personalization typically share similar traits such as:

- Consist of adaptable operations and systems
- Do not require specialized tooling or lengthy set-up, re-programing, and re-calibration processes
- Can handle complex geometries

### **1.3. Electropolishing, a promising candidate for mass personalization**

The electropolishing process is an example of a manufacturing technology that is well-suited to the notions of mass production and mass personalization. Electropolishing is an electrochemical method for improving the surface finish of metal objects, as well as their corrosion resistance and surface cleanliness <sup>16</sup>. The flexible yet effective nature of this process makes it highly appealing to many industries such as pharmaceutical, medical devices, aerospace, automotive, and food processing, where high-quality surface finishes and cleanliness are critical. The electropolishing process does not require a sizeable set of equipment or a complicated manufacturing system. In addition, the key process parameters including the applied polishing voltage/current, polishing time, bath temperature, and cell geometry can be easily adjusted to handle various component materials and geometries.



The electropolishing services on the market do not, however, offer a variety of options in terms of the final surface quality, let alone the possibility of providing the customer's specific selection of surface finish. This is true even though it is theoretically possible to adjust the process parameters to easily achieve target surface qualities. Moreover, despite its flexible and affordable nature that facilitates the transition toward the mass production strategy, the electropolishing process has certain limitations.

One of the major issues affecting the performance of industrial electropolishing processes is the electrolyte's "aging" or gradual degradation due to extensive usage. It has been demonstrated that high levels of dissolved metal in heavily-exploited electrolytes have a negative impact on the polishing rate and the ultimate roughness and brightness of the surface<sup>17-21</sup>. Since the polishing bath is considered one of the main tools of the electropolishing process, the continuous change in its chemical composition and physical properties makes it more difficult to maintain the consistency of the polishing quality. As a result, large-scale manufacturing of standardized parts is hampered by inconsistent surface quality. The continuous and inevitable deterioration of the polishing electrolyte also adds to the already considerable process optimization costs that stand in the way of the mass personalization strategy. Although various process optimization approaches may be used for the electropolishing process, constant changes in the polishing tool (electrolyte) would necessitate repeated re-calculation of the optimum process parameters even for previously manufactured parts. Identifying the optimum polishing parameters for obtaining desired surface attributes typically necessitates time-consuming and costly trial-and-error experiments and is strongly reliant on the operator's prior expertise and competence.

There seems to be a lack of publicly available information about electropolishing in deteriorated electrolytes because companies prefer to keep this information private to maintain their competitive edge in the market. Additionally, a review of the literature reveals that there is limited research that concentrates on the impact of electrolyte deterioration on the final surface finish or practical solutions for sustaining and enhancing polishing results in heavily-used baths.

#### **1.4. Problem statement**

Finding the right process parameters for achieving the desired product quality in the mass production paradigm can be challenging. This complexity becomes even greater when it comes to mass personalization due to a higher level of variability and a lack of previous data.

Producing a large series of identical parts with well-defined surface finishes is a daily task that the electropolishing industry masters very well. The real challenge arises when processing a new part (different geometry, metal, etc.) or producing a new surface finish. As a result, a great number of trial-and-error experiments are required to optimize the process parameters. This is especially the case in industrial settings where the state of the electropolishing bath isn't well controlled and it is not uncommon to see polishing baths that have been in use for many years. Such baths have very different properties than the ideal lab-scale electrolytes or recently acquired polishing baths. As long as the optimization process is conducted for the production of large series, the associated

manufacturing overhead can be distributed over the large numbers of parts. However, as the series gets smaller the additional cost per part becomes too large to be economically viable. The electropolishing industry is therefore actively seeking strategies to expedite the lengthy and costly optimization process required for processing new types of parts or surface finishes.

If the electropolishing process is to adopt the mass personalization trend, effective approaches should be considered for a) maintaining the consistency of polishing results by real-time adjustments of process parameters based on visual and experimental feedback, and b) rapid identification of optimum process parameters for achieving personalized surface finishes.

Several challenges need to be addressed in this context:

### I. Rapid identification of optimum process parameters

Manufacturing operations are usually run by strict schedules and production objectives. The time spent on trial-and-error experimentations to find the optimal process parameters can cause production delays and affect overall efficiency. Furthermore, trial-and-error methods that manually modify parameters could not thoroughly investigate the entire parameter space, and may lead to suboptimal results or missed opportunities for process optimization.

When a new order is submitted to a polishing facility, optimum process parameters need to be identified as fast as possible. Finding the right process parameters through a series of trial-and-error experiments is not time efficient, especially when the order size is small. The ideal approach identifies optimum process parameters for achieving a target surface quality with the minimum number of experiments.

### II. Adjusting process parameters at a reasonable cost

As was already discussed, the cost of optimizing process parameters challenges the profitable production of small-size orders with a high variety of parts. Conducting numerous trial-and-error experiments to find the best process parameters consumes significant resources, including materials, equipment, energy, and labor. The ideal approach will enable tuning the polishing process parameters at a reasonable cost.

### III. Lack of qualified workforce willing to work in demanding conditions

Electropolishing is a specialized process that requires specific expertise and skills to operate the equipment, handle chemicals, and ensure the desired results. Finding individuals with the necessary training and expertise in electropolishing techniques can be quite challenging. In addition, the hazardous working environment of electropolishing facilities can further limit the pool of competent candidates. Finding a qualified workforce that is willing to work in such environments despite the safety concerns or the need for additional training and certifications can be quite challenging.

Given the above-mentioned challenges, the application of an intelligent process for quality control and optimization of the electropolishing process can be a promising solution. Intelligent tools, such as artificial intelligence (AI) algorithms can analyze vast amounts of data to improve the overall efficiency of manufacturing processes<sup>15</sup>. In addition, these tools facilitate real-time data monitoring, enabling early detection of quality deviations from intended standards and speedy identification of underlying causes of process issues. Another important feature of intelligent tools is the ability to learn from historical data and make adaptive control decisions to continuously improve manufacturing processes<sup>22–24</sup>.

A strategy that employs previous production experience to help determine acceptable process parameters shows significant potential for advancing the electropolishing process towards mass production and mass personalization methods despite the deteriorating state of the polishing electrolyte. The guiding principle of this strategy is that a manufacturing process may progressively enhance its performance just as a junior operator advances to a senior operator over time. By incorporating artificial intelligence and machine learning algorithms, the intelligent process can analyze collected data and dynamically adjust process parameters to compensate for changes in bath conditions, ensuring consistent and high-quality results. This intelligent process can also identify correlations between the bath conditions and the resulting surface quality and optimize process parameters based on the intended outcome<sup>25</sup>.

## 1.5. Objectives

The objective of this study is to employ machine learning methods to quickly identify the optimum polishing parameters for achieving the desired surface finish in an aging solution. Several uncertainties need to be addressed to solve this problem:

- *Establishing a methodology for quantifying the state of an aging bath and determining relevant electrolyte properties:*

Research of the literature indicates that certain metal concentrations or electropolishing ampere-hours thresholds have been suggested in industrial studies for the onset of the decline in the polishing performance of some baths. There is, however, a scarcity of available data concerning the definition of an aged bath and important measurable electrolyte properties to identify its state. To determine what is considered a deteriorated or an “aged” bath, it is necessary to establish baseline parameters and benchmarks relevant to the electropolishing process and used electrolytes. Only after establishing an effective method for quantification of the bath state will we be able to investigate the effect of bath aging on the outcomes of the electropolishing process. In this regard, relevant physicochemical properties of the electrolyte need to be identified and prioritized in terms

of their importance for the performance of the bath as well as their simplicity and ease of use in fast-paced industrial electropolishing settings.

- *Exploring the possibility of employing the physicochemical properties considered relevant to the state of the polishing bath for maintaining the consistency of electropolishing results:*

Upon understanding the effect of variations in the physicochemical properties of an aging bath on the ultimate surface finish of electropolished samples, we aim to ascertain whether these properties may be used to make necessary adjustments to the polishing process parameters, such as voltage and time, in order to maintain consistent surface properties (i.e., roughness and appearance) of the workpiece. This investigation requires an adequate number of electropolishing experiments with different process parameters at varying bath states, followed by precise surface characterization of electropolished parts.

- *Building a comprehensive dataset of the polishing process parameters and resulting surface qualities:*

The first step towards a prediction tool for the identification of process parameters required for obtaining a target surface quality in an aging bath is building a comprehensive dataset. Such a dataset must encompass a wide range of polishing bath states, process parameters, and surface finishes. In addition to a significant number of polishing experiments, the construction of this dataset requires precise measurements of the electrolyte states, process parameters, and surface properties. The dataset can then be thoroughly analyzed to acquire an in-depth understanding of the key contributors to the ultimate surface quality of the parts and their potential correlations.

- *Developing a tool to predict the optimum process parameters for achieving a target surface quality at a given bath state:*

The target prediction tool of this study shall be based on a machine learning model chosen among various algorithms based on its accuracy in representing the constructed dataset. After developing the tool, we also aim to evaluate its predictive power and generalization capability to unseen situations.

## 1.6. Significance of the study

In order to remain competitive and fulfill the demands of today's customers in a timely manner, manufacturing industries are embracing the Industry 4.0 philosophy where automation is pushed beyond robotics to new technologies emerging from data science and artificial intelligence<sup>26</sup>. The adoption of Industry 4.0 technologies, such as automation and sophisticated data analytics, may greatly benefit surface treatment operations by significantly increasing their productivity and efficiency. In addition, Industry 4.0 enables advanced quality control and process optimization by collecting and analysis of vast amounts of data from different phases of the surface treatment process<sup>22,25</sup>. Traditional industries, such as electropolishing, need to find ways to automate their often heavily artisanal-based techniques to increase the efficiency and quality of their operations. They also need to develop an intelligent network of machines and processes to cut down on the time spent on non-value-added tasks and learn from previous experience. In addition, the possibility to choose from a variety of attainable surface finishes rather than a one-size-fits-all "shiny" or "smooth" surface can be a strong steppingstone for the "mass personalization" of the electropolishing services.

Moreover, development of a smart process to find the optimum polishing parameters in a degrading bath can significantly decrease the costs of electropolishing operation. One considerable expense for electropolishing operations is the cost of electrolyte replenishment and disposal of the degraded baths<sup>20,27,28</sup>. Electropolishing facilities require replacing the polishing bath periodically with fresh electrolytes to maintain an acceptable quality of the polished parts<sup>28-31</sup>. Also, the disposing of heavily-exploited electrolytes typically requires following proper disposal procedures and contracting licensed waste management services to ensure compliance with environmental regulations<sup>29</sup>. Determining the suitable polishing parameters that allow obtaining the target surface quality at any given bath state can reduce the frequency of bath renewal and disposal, thereby cutting a substantial share of these expenses.

Another major expense for electropolishing facilities is the labor cost including the cost of training and certifications for personnel handling hazardous chemicals and wages of highly skilled operators that can determine the optimum process parameters for achieving required surface finish. Indeed, the technicians who perform electropolishing operations have training and experience levels that are significantly higher than those of other workers in the electropolishing facility. Developing a smart tool that can automate labor-intensive process optimization tasks and enable data-driven decision-making can reduce the reliance on human labor and lead to significant cost savings for electropolishing facilities.

Finally, the disposal of extensively-used electrolytes with high concentrations of heavy metal ions exposes contaminants into the environment and endanger the ecosystem and human health<sup>28,32</sup>. This smart process reduces the frequency of bath renewal and the subsequent disposal of hazardous electrolytes to the environment by extending the service life of degraded polishing baths.

In the upcoming chapter, an in-depth examination of the electropolishing process mechanism, the significance of key process parameters, and some advantages and limitations of electropolishing are detailed. Chapter 2 also summarizes the existing knowledge on the electrolyte aging mechanism and its impact on the polishing process outcomes. In addition, conventional quality control methods in electropolishing, along with their potential drawbacks, are explored.

Chapter 3 presents the experimental methodology employed in this study and briefly outlines the steps taken to develop the predictive tool, which is the target of this research. Chapter 4 utilizes various experimental results to elucidate the influence of electrolyte degradation on the surface quality of polished components and proposes a methodology for quantifying the bath state.

The details of the dataset construction process are presented in Chapter 5, followed by an analysis of the dataset and an evaluation of different machine learning algorithms based on their ability to reproduce it. Chapter 6 outlines the development process of the prediction tool derived from the findings of Chapter 5. The performance of the constructed prediction tool is then assessed in both familiar and previously unseen situations.

Chapter 7 offers suggestions for potential future research directions, and finally, the most significant conclusions are summarized in the concluding chapter.

## 2. Literature Review

### 2.1 Electropolishing process, potentials, challenges

Electropolishing is an electrochemical finishing process for the removal of surface impurities and irregularities from a metallic component. In this process, the workpiece is polarized as the anode of an electrolytic cell (a two electrodes cell in general) with a suitable material serving as the cathode. Electrochemically dissolved metal cations diffuse through the electrolyte towards the cathode, where reduction reactions generally produce hydrogen<sup>33,34</sup>. Figure 2.1 illustrates a typical electropolishing cell.

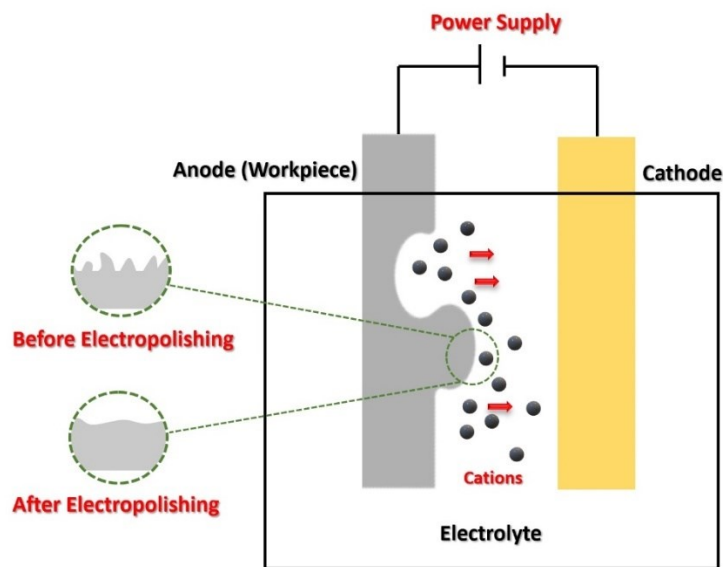


Figure 2.1. Schematic of an electropolishing cell.

Electropolishing produces smooth and bright surface finishes by removing surface imperfections, such as microburrs, scratches, and scale, resulting in a clean and aesthetically appealing surface<sup>35,36</sup>. In addition to leveling surface irregularities, electropolishing can greatly enhance corrosion resistance by removing defective and corrosion-promoting surface oxides and nonmetallic inclusions and replacing them with a dense, stable, and chemically homogeneous protective passive layer<sup>37-39</sup>.

### 2.1.1 Mechanism of electropolishing

Figure 2.2 depicts the typical current density-voltage curve exhibited by many electropolishing systems, with each part of the curve representing a different step of the electropolishing process. In the first region of the curve, preferential etching of the surface occurs, and grain boundaries are attacked. This may be explained by the fact that for a given potential, the rate at which different planes of a metal crystal dissolve depends on their orientation. Therefore, in the active potential region, the anodic dissolution of metals with crystal planes at random orientations results in faceting and the formation of crystallographic patterns on the surface. In this region, raising the applied voltage increases the current density. In the passivating region, however, increasing the applied voltage causes a slight decrease in current density, indicating the formation of a passive oxide layer on the workpiece surface. The passive layer is stabilized in the polishing region, and the process becomes mass transfer-controlled. Since the current remains nearly constant with increasing voltage, this area is also known as the limiting current plateau. As the applied voltage increases in the last region (the transpassive region), the passive layer begins to break down and the anodic dissolution is accompanied by the evolution of gas bubbles and pitting of the workpiece surface<sup>33,40,41</sup>.

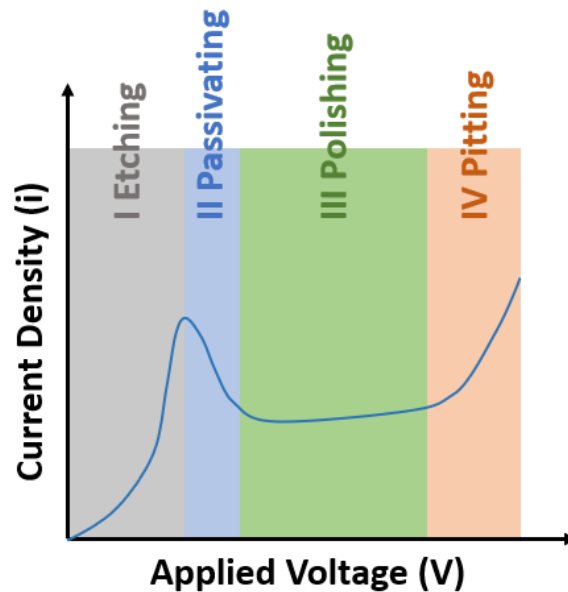


Figure 2.2. Characteristic I-V curve of the electropolishing process according to Han et al.<sup>33</sup>

During the electropolishing process smooth and bright surfaces are achieved by eliminating surface roughness as well as crystallographic and grain-boundary attack. It is generally agreed upon that electropolishing occurs through two processes of anodic levelling (elimination of surface roughness of height  $> 1 \mu\text{m}$ ) and anodic brightening (elimination of surface roughness  $< 1 \mu\text{m}$ ). Anodic leveling results from varying dissolution rates at metal surface peaks and valleys



depending on the current distribution or mass-transport conditions. Anodic brightening results from suppressing the influence of surface microstructure (crystallographic orientations, surface defects, etc.) on the dissolution process. It is achieved under mass transfer-controlled elimination of microscopic irregularities<sup>40,42</sup>.

Although electropolishing has been used for decades, its mechanism is still debated in the literature. Based on the oxidation, dissolution, and diffusion processes observed during electropolishing, it is generally accepted that the mass transport-controlled anodic dissolution of metal is responsible for the electropolishing process<sup>43</sup>. Two mass-transport mechanisms have been proposed to explain the polishing process: (i) the establishment of a viscous boundary layer or (ii) the formation of a salt film on the workpiece surface<sup>33,40</sup>.

It is generally believed that when a current passes across the electrolyte, metal dissolution products form a viscous boundary layer (or as some researchers postulate, a salt film) on the workpiece surface. Since this surface layer has a higher viscosity and electrical resistivity than the bulk of the solution, it reduces the current density and metal dissolution rate. The thickness of the surface layer and hence, the diffusion rate of metal cations to the solution are different at protrusions and valleys of the surface. As a result, the non-uniform current distribution and different dissolution rates on the surface lead to anodic leveling<sup>33,40</sup>.

Anodic brightening, on the other hand, is achieved by the random removal of cations from the metal lattice given the random and rare chance of cation vacancies in the anodic film. Thus, in contrast to the surface etching observed in the active potential region, where the rate of metal crystal dissolution depended on crystallographic orientation, the effect of workpiece microstructure is suppressed in the mass transfer-controlled region, and sub-micrometer scale and specular reflectivity metal finishes are obtained<sup>44-46</sup>.

Although mass transport control is common to all brightening systems, the transport limiting species may vary from one system to another. According to the review conducted by Landolt<sup>42</sup>, three possible transport limiting species have been suggested: anodically generated metal ions, acceptor anions, and water. The answer to the question which species is limiting in each brightening system can be difficult to determine.

### **2.1.2 Role of electropolishing parameters**

Optimizing the electropolishing process necessitates a thorough understanding of the effect of process variables, such as polishing current, potential, duration, or electrolyte temperature, on the final surface quality of the parts. Some of the main process parameters and their speculated functions are as follows:

Electropolishing current It is commonly accepted that the polishing process is accelerated at high currents, leading to nonuniform dissolution and possible pitting of the part surface. Applying lower polishing currents is, however, not favorable given the considerably lower material removal rates<sup>47</sup>.

For instance, during the electropolishing of aluminum samples, it was observed that with increasing the applied polishing current density, the formation rate and thickness of the oxide layer increased, and the diffusion-controlled dissolution regime was attained faster. Also, under excessively high current densities, a much thicker and deformed oxide layer was formed on the workpiece through dramatic bubble evolution, leading to non-uniform metal dissolution and eventually, surface roughening. It was argued that at the optimum current density, the surface brightness reaches a maximum because the formation and dissolution rates of the oxide layer are balanced<sup>48,49</sup>.

Awad<sup>36,50</sup> claimed that achieving the limiting current region for increasing the surface smoothness and brightness of AISI-304 stainless steel samples requires adequate electric current distribution over the surface, regular dissolution of surface asperities, and homogenous filling of surface depressions by metal oxide layer. According to the author, low current densities are not sufficient for ionic mobility through the viscous electrolyte, which results in low anodic reaction rates, incomplete surface oxidation, and ultimately, matt surfaces.

Electropolishing potential The application of sufficient electric potential is necessary for the polishing electrode reactions to proceed at an acceptable rate. For a given overvoltage, increasing the distance between the anode and cathode of the electrochemical cell lowers the flowing current due to the increased electrical resistance between the electrodes. Further, the electropolishing system's ohmic drop and current efficiency can both be negatively impacted by the development of a passive layer on the anode surface<sup>34,47</sup>.

During the charge transfer-controlled anodic dissolution of the workpiece, increasing the applied polishing potential was shown to increase the surface roughness of the workpiece (etching) and decrease the surface brightness. Further increasing the potential leads the anodic dissolution process to become mass transfer-controlled, allowing for the generation of highly reflective and smooth surfaces. However, while low voltages might not activate the polishing electrode reactions, applications of very high potentials are generally avoided. At very high cell potentials, the significant increase in current density leads to considerable evolution of gas bubbles, resulting in a dramatic deterioration of surface finish quality (increased surface roughness and decreased surface brightness) due to excessive defects and local pit formation. Overpolishing due to high voltages can also diminish the part's dimensional accuracy<sup>36,47,51</sup>.

Electropolishing duration During the electropolishing process, the surface roughness of the samples has been observed to undergo a rapid decrease at first and reach a limiting value with further extension of the process<sup>47</sup>. Figure 2.3 depicts the change in surface roughness of 316L stainless steel samples as a function of electropolishing duration presented in a study by Haïdopoulos et al<sup>52</sup>. Prolonging the electropolishing process is typically known to further reduce the surface roughness of the workpiece. However, it has been shown that electropolishing a part for excessively long durations does not improve its surface finish significantly and may potentially result in severe part dissolution<sup>47</sup>.

The surface brightness of the workpiece has also been observed to initially improve and decline later with increasing the electropolishing duration. It has been reported that prolonged polishing processes and the continuous electric potential applied to the surface can result in severe and irregular surface dissolution leading to distortion of the workpiece and deterioration of surface brightness<sup>39</sup>.

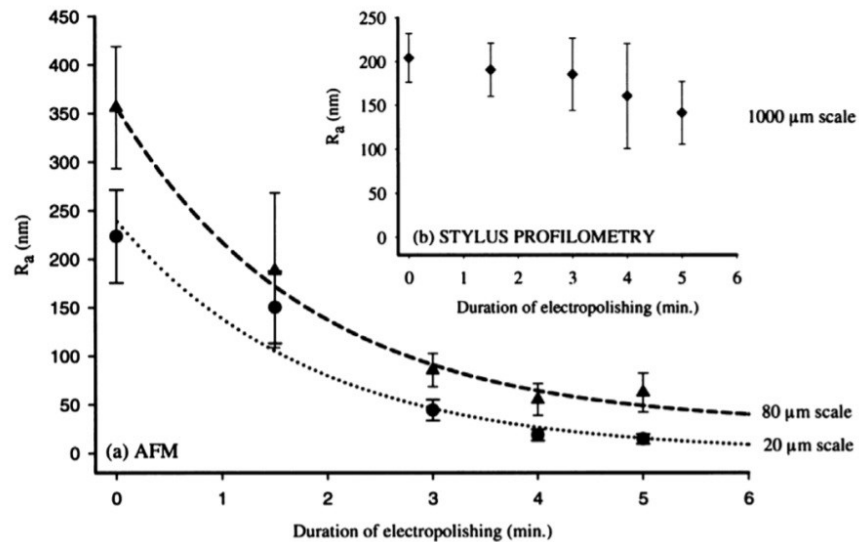


Figure 2.3. Variation of the mean surface roughness  $R_a$  of 316 stainless-steel surfaces with the duration of electropolishing process as (a) measured by AFM, and (b) measured by stylus profilometry<sup>52</sup>.

Electropolishing Bath Temperature One of the key factors that can significantly affect the electropolishing process is the temperature of the polishing bath. Higher bath temperatures result in faster ion diffusion, greater metal solubility, and lower electrolyte viscosity, all contributing to an increase in polishing current density<sup>33</sup>.

It has been reported that increasing the temperature of the polishing bath results in an increase in limiting current density and improvement of the surface brightness. This observation has been justified by the fact that increasing the bath temperature increases the solubility of dissolution products in the bulk solution and therefore higher current densities are required to obtain a bright surface<sup>53</sup>. Higher temperatures were also reported to facilitate the electropolishing process and shift the polishing mechanism to mass-transfer controlled. The time required to obtain a bright polished surface is reportedly shorter at higher temperatures<sup>38</sup>. It has been justified that since polishing baths are typically composed of highly viscous electrolytes that are very resistive to ionic mobility, an effective polishing process requires an adequate temperature to overcome their ohmic resistance and increase the ionic mobility towards the working electrode<sup>36</sup>.

In addition, according to the literature, at lower bath temperatures, the oxide layer generated during electropolishing has a high formation rate and a low dissolution rate. As a result, the thickness and resistance of the oxide layer are increased. Conversely, at higher temperatures, the formation and

dissolution rates of the oxide layer are balanced, and the optimum oxide thickness and surface quality are achieved <sup>49</sup>. However, at very high temperatures, the viscosity of the diffusion layer is significantly reduced, making it difficult to maintain a viscous layer on the workpiece surface. Therefore, it has been suggested that excessively high temperatures should be avoided to prevent the development of etching pits and the deterioration of surface quality <sup>33,34</sup>.

Other factors, such as bath agitation, interelectrode distance, and polishing current signals can also affect the ultimate surface quality of electropolished samples <sup>47</sup>. Considering the diversity of the adjustable parameters and their rather complicated influences on the outcomes of the electropolishing process, considerable research has been devoted over the years to identifying the most reliable and efficient process optimization methods. For example, several studies have compared the surface quality obtained with various levels of process parameters to optimize the electropolishing process <sup>54,55</sup>. Other studies employed statistical methods for the systematic optimization of the electropolishing process. Such methods help to identify the key process parameters and their optimal settings to achieve the desired surface finish, material removal rates, or other performance metrics. For instance, some studies have utilized the Taguchi design of experiments to determine the optimum level of process parameters that yield high surface quality parts <sup>56,57</sup>. Kao et al. <sup>58</sup> used grey relational analysis to optimize electropolishing process parameters such as temperature, current density, and electrolyte composition to achieve optimal surface roughness and passivation strength for 316L stainless steel parts. The response surface methodology (RSM) has also been used in several studies for the optimization of the electropolishing process parameters <sup>59,60</sup>.

### **2.1.3 Advantages and challenges of electropolishing process**

Various surface polishing technologies based on mechanical, chemical, or electrochemical approaches have been proposed for improving the appearance and performance of metallic parts. Compared to other polishing methods, electropolishing offers advantages that make it an appealing process to some demanding applications including biomedical, food and beverage, aerospace, and electronics and semiconductor industries.

For instance, one of the major advantages of electropolishing over mechanical polishing is that no tool contact is required, and it can potentially handle much more complex geometries. In principle, any part of the workpiece within the electrolyte's reach may be treated with electropolishing, provided that a cathode can be placed in the vicinity of the surface. Such flexibility can be quite beneficial in the treatment of small or complicated geometry parts with internal spaces, hidden surfaces, and intrusions that are otherwise inaccessible <sup>47,61,62</sup>.

Furthermore, as a non-contact polishing process, electropolishing does not cause further mechanical stresses, oxide contamination, or surface hardening <sup>63,64</sup>. In fact, it can be used for the treatment of hardened materials which is challenging for mechanical machining considering the contact between the tool and the workpiece <sup>65</sup>. In addition, contrary to some polishing methods

like laser polishing, electropolishing operates at low temperatures and does not subject the parts to excessive heat, thereby minimizing the risk of thermal stress and distortion <sup>66</sup>.

Electropolishing is usually a faster process compared to chemical polishing due to the application of anodic current densities <sup>38</sup>. Utilization of anodic current densities in electropolishing also helps to reduce the need for strong or highly concentrated acidic solutions that are typically used in chemical etching, which makes the working conditions safer and the resulting hazardous waste less harmful to the environment <sup>63,67</sup>. Electropolishing also offers better control over the process, whereas, in chemical etching, mere modification of chemical bath concentration and polishing time cannot render parts with the desired accuracy <sup>38,68</sup>.

Aside from its great potential for effective improvement of surface qualities, the electropolishing process bears limitations that can challenge adopting mass-production and mass-personalization strategies. Some major drawbacks of the electropolishing process are inconsistent polishing quality caused by electrolyte deterioration, the artisanal nature of the process, and the complexity of process optimization due to the high number of process parameters to fine-tune <sup>47</sup>.

Electrolyte ageing The "aging" or degradation of the electrolyte over time due to repeated usage is one of the main issues in industrial electropolishing operations. Significant amounts of dissolved metal in heavily used electrolytes have detrimental effects on the polishing rate and the ultimate roughness and gloss of the surface. <sup>18,69,70</sup>. Studies have shown that the accumulation of metal ions in electrolytes increases consistently with increased usage to the point where higher voltage/current or longer polishing times are needed to maintain the consistency of polishing quality <sup>20,69,70</sup>. Increasing the polishing voltage/current or the duration of the electropolishing process results in higher energy consumption, bath overheating, development of surface defects, and formation of byproducts <sup>71</sup>. An alternate approach is to replace the electrolyte when a specific amount of metal content is reached or when the process begins to yield unacceptable results <sup>28,69</sup>. However, since electrolyte mixtures are expensive frequent bath renewal can be financially burdensome for industrial electropolishing facilities <sup>20,27</sup>. Other potential strategies, according to the literature, include:

- Altering the electrolyte composition to create a more affordable alternative with a longer lifespan <sup>20</sup>
- Detecting the onset of the "aging" by continuously monitoring the changes in the electrolyte and reversing the process by adding fresh electrolyte <sup>31,70</sup>
- Removing the metal content using chemical or electrochemical methods or by means of natural sorbent materials <sup>18,28,31</sup>
- Lowering the amount of metal ions in the electrolyte by obtaining the optimum polishing parameters for minimum weight loss of the workpiece <sup>32,72</sup>.

In addition to the financial drawback of bath aging, the disposal of aged electrolytes with high concentrations of heavy metal ions exposes contaminants to the environment, endangering the ecosystem and human health <sup>28,32</sup>. A detailed discussion of this issue, including the effect of various

electropolishing parameters on bath aging and its consequences on the final surface quality of the parts, will be provided in the next section.

Artisanal process and complicated process optimization The term "artisanal" refers to a process or technique that requires skilled craftsmanship, attention to detail, and a high level of manual expertise. Electropolishing is considered an artisanal process due to the high level of skill and craftsmanship needed to precisely select and control the process parameters that deliver the desired results.

Industrial electropolishing facilities usually rely on highly skilled operators with a deep understanding of the process, including knowledge of the workpiece material, electrolyte composition, and the role of process parameters. The operator's ability to monitor and control various parameters, such as polishing voltage, current, time, and bath temperature, is critical to the success of the electropolishing process. Over their many years of experience, skilled operators acquire the ability to make real-time decisions and adjustments based on the specific requirements of each workpiece. Considering their important responsibilities and the hazardous working environment of the electropolishing facilities, these operators must be paid highly competitive wages<sup>73</sup>.

Such heavy reliance on the knowledge and expertise of the operators can be a significant obstacle to the automation of electropolishing operations and their ultimate transition to mass production and mass personalization strategies. Transitioning to the mass production paradigm calls for streamlining processes, increasing production speed, and reducing dependence on manual labor to achieve higher efficiency and cost-effectiveness. Indeed, streamlining electropolishing procedures necessitates rapid and low-cost parameter optimization strategies. In addition, since the customers of mass-produced products expect uniformity across the parts, ensuring reproducibility and consistent quality of the products is another crucial requirement. This concern may be addressed through establishing standardized procedures and automated quality control measures.

Another obstacle for artisanal processes like electropolishing is handling the complexity and variety of products in the context of mass personalization. Electropolishing operations must adopt parameter optimization methods that can accommodate product customization requirements while maintaining efficiency and cost-effectiveness. This can be a challenging task because:

- Different electropolishing operators may have unique approaches and preferences, leading to variations in the process control strategy and the final surface quality. This subjectivity and variability make it difficult to establish standardized procedures and optimize the process for efficiency and quality.
- The knowledge and expertise are generally stored in the operator's memory rather than in documented instructions or process manuals. This lack of formal documentation makes it challenging to analyze and improve the process systematically.
- In electropolishing, like most artisanal processes, data collection and feedback mechanisms are limited or nonexistent. Without accurate and comprehensive databases on process

parameters and final surface characteristics, making decisions for process optimization becomes difficult.

- The electropolishing process involves complex interactions between various parameters that can affect the final surface finish of the parts. These interactions can be hard to quantify and understand, especially when they involve subjective judgments of the operator.
- At some point, the experienced operators will retire, and transferring their knowledge to a broader workforce or new generations of operators can be challenging. It takes time and effort to train new operators to achieve the same level of skill and expertise, and even then, variations in individual performance can still occur.

To the best of our knowledge, no research has been conducted on the possibility of personalizing the electropolishing process. However, the literature on the electropolishing process indicates that it is indeed possible, albeit probably not affordable. For instance, some studies have focused on electropolishing optimization for accommodating workpieces of different materials and geometries. The results of such works may be guidelines for determining the specific process parameters required for achieving desired surface finishes for various types of parts. Further, some studies have shown that different electropolishing process parameters can generate diverse surface finishes, such as high gloss, mirror-like surfaces, or matte ones. It can thus be concluded that it is possible to achieve a range of polished surface finishes by manipulating process variables such as the polishing voltage, current, and time. Moreover, several researchers have employed process monitoring methods such as in-situ measurement of process parameters that can be useful for quality control of the electropolishing results.

Despite the demonstrated potential for personalization of the electropolishing operations, the artisanal nature of the process and dynamic changes of the polishing bath can undermine the feasibility of this approach. Even if the electropolishing operations succeed in producing large batches of identical parts with well-defined surface qualities, the real challenge emerges when a new surface finish or a new type of part (different geometry, material, etc.) is to be processed. In such cases, the process parameters must be optimized again by considerable trial-and-error experiments to accommodate the new target. This is especially the case in industrial facilities where the state of the electropolishing bath is not well-controlled, and it is not uncommon to see polishing baths that have aged for several decades. Such baths have very different properties than the ideal lab-scale or freshly set up electrolytes. From a financial viewpoint, as long as the optimization process is conducted for large batches, the resulting manufacturing overhead can be spread out over the large numbers of parts to be produced. But when the batch size becomes small, the additional cost per part grows too large to be economically viable. This can prove quite challenging in the context of mass personalization, where small orders of individually personalized products are common.

Recently, manufacturing processes have benefited from data-driven approaches like machine learning (ML) algorithms as a valuable tool for reducing the cost of parameter optimization/calibration. Machine learning algorithms can analyze large amounts of data, identify patterns, and make predictions based on those patterns. They can, hence, automate the optimization

process by learning from historical data and identifying the optimal parameters for attaining a given objective. As a result, manual trial-and-error optimization approaches are no longer needed, and considerable resources are saved. In addition, data-driven methods can continuously analyze data from sensors and monitoring systems to optimize process parameters in real-time. This enables dynamic adjustment and fine-tuning of parameters based on changing conditions, thereby improving efficiency, and reducing waste or errors.

There have been few instances of employing data-driven approaches for electropolishing process optimization or the prediction of final surface finish. For instance, Krishna et al.<sup>74</sup> developed a multilinear model to predict final surface roughness of 316 stainless steel samples using the main bath properties. Lochyński et al.<sup>75</sup> devised a multifactorial mathematical model for the prediction of the surface quality based on the metal content of the polishing bath and process parameters. An in-depth review of these works is provided in the next section.

## **2.2 Electrolyte ageing**

### **2.2.1 What is electrolyte ageing?**

The electropolishing process is accomplished through metal dissolution. As a result, oxidized metal ions form soluble and insoluble (recognized as dark sediments<sup>69</sup>) chemical compounds in the electrolyte<sup>31</sup>. A growing amount of sludge (metal precipitates) builds up in the bath as the polishing process progresses due to a rise in the concentration of metal ions in the electrolyte<sup>28,70</sup>. The expression "aging" of the electrolyte refers to the contamination of electropolishing baths with metal ions upon prolonged use.

### **2.2.2 How does aging affect the polishing quality?**

It has been observed that electropolishing of parts in aged electrolytes can result in the appearance of surface defects and deterioration of part's roughness and gloss<sup>18,76,77</sup>. According to Chatterjee<sup>28</sup>, during electropolishing of stainless steel parts, the surface brightness of the parts drops when the iron content of the acid bath exceeds about 6 wt. %, because the electrolyte becomes saturated with metal salts of stainless steel. Therefore, to keep an ideal process, the iron in the solution during electropolishing should be maintained below 5 wt. % to reduce sludge formation. Similarly, during electropolishing of niobium Superconductivity Radio Frequency (SRF) cavities used for particle acceleration, Eozénou et al.<sup>76</sup> observed that when the polishing process was extended, the surface brightness of the samples reached a maximum and subsequently began to decrease after around 7.7 g of niobium was dissolved in the bath (after 2580 minutes of electropolishing). However, when the polishing bath was replaced with a fresh solution, the maximum surface brightness improved even further until roughly the same quantity of niobium was dissolved again (after 2490 min of electropolishing). Using XPS (X-ray Photoelectron Spectroscopy), SEM (Scanning



Electron Microscope), and EDX (Energy Dispersive X-ray Spectroscopy) analysis, Tyagi et al.<sup>77</sup> demonstrated that as the electrolyte ages, the surface finish of niobium samples deteriorates, and a significant amount of sulfur particles is generated on their surface. These sulfur particles are known to limit the SRF cavity performance. The sulfur generation rate at the cavity surface was also found to be proportional to the aging of the EP electrolyte. While studying the effect of the Electrochemical Reduction (ER) process on reducing the contamination in aged polishing baths, Lochynski et al.<sup>18</sup> observed that the surface roughness of 304 stainless steel samples increased after electropolishing in an aged bath, while for a bath subjected to the ER process, the surface roughness was gradually improved with increasing the polishing duration. The samples electropolished in the aged bath were also found to exhibit a higher weight loss. Krishna et al.<sup>74</sup> obtained similar results showing that the surface quality of stainless steel samples drops as the polishing electrolyte ages. In addition, the SEM images of the samples electropolished in aged solutions indicated a very rough and irregular surface with traces of bath contamination.

### **2.2.3 What causes the decline in the quality of the surface in aged polishing baths?**

Generally, as polishing solutions are used, some of their properties change. Such changes can significantly affect the surface finish of the electropolished samples:

Increased viscosity- Decreased ionic conductivity According to the theories suggested for the mechanism of electropolishing and given the crucial role of the viscous film of metal salts formed at the anode surface, the viscosity of the solution is believed to be the key element in the control of electropolishing. The viscosity, in turn, is dependent on the composition of the polishing solution and its temperature<sup>31</sup>.

Electropolishing baths are often selected from viscous acidic solutions<sup>28,40</sup>. It should be pointed out, nonetheless, that an overly high solution viscosity brought on by excessive metal dissolution can also be detrimental to the results of electropolishing<sup>74</sup>. Not only may it cause the solution's electric conductivity to decrease due to the slower movement of charge carriers, but it can also thicken the viscous layer that has developed on the anode's surface and increase its electric resistance, reducing the rate of material removal<sup>36,40</sup>.

Indeed, since a fresh electrolyte only contains a few ions, its electric conductivity may be insufficient to deliver an acceptable polishing effect, but after a few polishing processes, the rate of material exchange at the workpiece/electrolyte interphase is enhanced<sup>69</sup>. However, as previously mentioned, prolonged polishing processes may result in excessive metal dissolution and an increase in solution viscosity, which eventually increases the ohmic resistance of the electrolyte<sup>36</sup>. Consequently, higher current densities or longer polishing times are required to obtain satisfactory results. This is consistent with the results of electropolishing niobium SRF cavities, in which the intensity and etching rate of the samples drop dramatically with bath aging<sup>76</sup>. Additionally, as the ohmic resistance of the electrolytes decreases at elevated temperatures, aging of the polishing bath increases the optimum process temperature<sup>69</sup>.

Moreover, according to the Stokes–Einstein equation, higher viscosity of aged solutions decreases the diffusion coefficient of ions and hence the mass transfer-controlled metal dissolution rate <sup>78</sup>:

$$\frac{D\eta}{T} = \text{constant} \quad 2.1$$

where  $D$  is the diffusion coefficient of particles ( $\text{cm}^2 \text{s}^{-1}$ ),  $\eta$  is the viscosity of solution ( $\text{g cm}^{-1} \text{s}^{-1}$ ) and  $T$  is its absolute temperature.

#### Change in the electrolyte composition:

Aside from the changes in physical properties of the polishing bath, the solution composition also changes upon excessive exploitation <sup>38,70,74</sup>. As the polishing electrolyte ages, the concentration of metal cations in the bulk of the solution is increased. For a mass transfer-controlled anodic dissolution process, the limiting current density measured by a rotating disk electrode can be described by the Levich equation <sup>79,80</sup>:

$$i_L = 0.62nFD^{\frac{2}{3}}v^{-\frac{1}{6}}\omega^{\frac{1}{2}}\Delta C \quad 2.2$$

where  $n$  is the number of electrons involved in the reaction,  $F$  is the Faraday Constant equal to  $96500 \text{ C/mol}$ ,  $D$  is the diffusion coefficient,  $v$  is the kinematic viscosity,  $\omega$  is the rotation speed of the disk, and  $\Delta C$  is the difference between the concentration of the diffusing species at the anode surface ( $C_s$ ) and the bulk electrolyte ( $C_b$ ).

As can be noticed in equation 2.2, the limiting current density is a function of the concentration gradient of the diffusing species. The increase in the bulk concentration of metal cations will, therefore, decrease the concentration gradient across the cell, which, in turn, reduces the limiting current density. As a result, longer polishing times are needed to achieve an acceptable surface finish. Aside from increased energy consumption concerns <sup>38</sup>, the extension of the polishing process increases the likelihood of bath contamination from various sources. Such contaminations can result from the dissolution of different parts with different manufacturing processes, the environment of the polishing facility, and accidental bath contamination by operators. These impurities may find their way to the surface of the electropolished samples and affect their quality. For instance, it has been proved that impurities found on the surfaces of polished aluminum samples can absorb light and affect the reflection of the specimens <sup>49</sup>.

#### **2.2.4 Effect of electrolyte aging on increasing the consumed energy**

In addition to its impact on the surface quality of electropolishing samples, electrolyte aging can increase the energy consumption of the process. It has been reported that the decline of the electrolyte efficiency upon prolonging the electropolishing process leads to a constant decrease in

the polishing intensity and material removal rate<sup>20,81,82</sup>. Seeing as the renewal of the polishing bath has shown promising results in terms of improving the surface quality of the samples, one might consider renewing the polishing bath to be a practical solution to the issue of electrolyte aging<sup>76</sup>. However, changing the polishing bath frequently would be to be very costly given the significant amount of electrolyte required (for example, the 2,000 L polishing bath tank at the KEK plant in Japan or a ton of electrolyte for a single batch in industrial Cu electroplating))<sup>20,27</sup>.

As previously mentioned, in order to provide satisfactory surface results in aged electrolytes, higher currents/voltages or longer polishing times are necessary due to the considerable decline in polishing rate and intensity. Neither option is financially viable considering the significant electric energy consumption<sup>38,72,74</sup>, which is why industries usually prefer polishing baths having a long lifetime and requiring low voltages<sup>76</sup>. Aside from the financial cost of increased energy consumption, raising the polishing voltage/current to compensate for the aging of electropolishing baths may result in other issues such as:

a) Exacerbation of surface conditions

Tyagi et al.<sup>27</sup> investigated the effect of increasing the polishing current density to improve the electropolishing results of niobium surfaces in an aged solution. The results of the study showed that despite a 25% increase in the rate of niobium removal, a significant amount of sulfur (up to 10.3 at. %) was generated on the samples at a higher current density of 50 mA/cm<sup>2</sup>, whereas the sulfur amount reduced drastically to 0.3 at. % for the surfaces treated with lower current density (33 mA/cm<sup>2</sup>). Additionally, SEM analysis of the samples subjected to high current densities revealed a significant number of particles larger than 10 μm at the surface. EDX analysis determined the particles' composition to be sulfur and oxygen. Hence, it was concluded that EP in aged electrolytes should be carried out with a low current density to ensure the minimum sulfur particles at the surface. Similar observations were reported in a study by Lochyński et al.<sup>18</sup>, where the application of higher current densities for electropolishing 304 stainless steel samples in a strongly contaminated industrial bath resulted in the emergence of smudges on the entire exposed area, leading to a significant deterioration of their surface roughness.

b) Reducing the lifetime of the polishing bath

A study by Éozénou et al.<sup>76</sup> on electropolishing niobium SRF cavities in an aging solution showed that the polishing rate increased with higher polishing voltage and the maximum surface gloss was reached earlier. However, the deterioration of the surface gloss also started at lower concentrations of dissolved niobium in the solution, indicating that the lifetime of the polishing bath had decreased<sup>83</sup>. The higher polishing potential was also found to result in increased bath contamination and the formation of significant amounts of sulfur particles at the workpiece surface. Another study by the same authors on electropolishing niobium SRF cavities indicated that a lower polishing voltage increased the lifetime of the EP mixture<sup>84</sup>. This observation was justified by the fact that overheating of the solution under higher potentials resulted in intensive evaporation of the hydrofluoric acid, HF, present in the

polishing bath, which, from previous experience, was identified as the key element in determining the final surface finish of the samples.

c) Additional cost of cooling system

The viscosity of the polishing solution is known to decrease at elevated temperatures. According to the Stokes-Einstein equation (2.1), a lower viscosity leads to greater diffusion of ions and molecules in the solution, higher polishing rates, and increased bubble generation. However, since the acidic electrolytes usually used in electropolishing have high electrical resistivity, applying a higher polishing voltage/current could lead to overheating of the solution and damage to the surface quality. Consequently, cooling devices and large amounts of acid would be necessary to prevent overheating of the solution and further deterioration of surface quality<sup>84,72</sup>.

According to the study by Éozénu et al.<sup>84</sup>, the only drawback to low-voltage electropolishing is the decreased niobium removal rate, which could be improved by increasing electrolyte agitation, or increasing the concentration of hydrofluoric acid in the polishing bath. In this regard, some studies have investigated the effect of altering the polishing bath composition to extend its service life. For instance, Éozénu et al.<sup>76</sup> observed that raising the concentration of hydrofluoric acid in the polishing bath, improved the niobium removal rate even with a lower polishing voltage. It was concluded that electropolishing in a hydrofluoric acid-concentrated bath yielded a higher polishing current without the need for supplying more electrical power or overheating of the solution. In addition, the lifetime of the polishing bath was found to significantly increase upon increasing the hydrofluoric acid concentration. Nevertheless, an upper limit had to be determined for hydrofluoric acid concentration in the polishing bath, because previous experiments showed that a too high hydrofluoric acid content led to the loss of the diffusion plateau and nonuniform etching inside the cavities. Also, at higher hydrofluoric acid concentration, an efficient cooling system had to be provided to control the temperature<sup>81</sup>. Finally, despite all advantages, working with a hydrofluoric acid-concentrated bath was not favorable due to the safety concerns<sup>83</sup>.

### 2.2.5 Effect of aged solution disposal on environment

Heavily-used electrolytes are known to contain very high concentrations of heavy metal ions, mainly iron, chromium, and nickel ions, that are eventually introduced to the natural environment through wastewater<sup>32,72,85</sup>. Heavy metals exhibit high mobility, relatively high chemical stability, and carcinogenicity in natural ecosystems<sup>86</sup>.

In surface treatment facilities, the parts are transferred to a rinse tank after the electropolishing process to remove the anodic film formed on their surface with deionized water. The parts are then thoroughly rinsed with fresh deionized water to remove any remaining trace of the anodic film. During this rinsing step, significant amounts of wastewater are generated that must be properly

treated before disposal <sup>28</sup>. The non-biodegradable and toxic heavy metals present in the aged electrolytes and electropolishing wastewater can accumulate in living organisms, causing many diseases and disorders <sup>85,86</sup>.

The situation worsens as the polishing bath ages. A higher concentration of contaminants in a polishing bath increases its specific gravity, allowing more concentrated solutions to come out from the surface and enter the wastewater <sup>72</sup>. In addition, the high viscosity of the polishing electrolytes results in more corrosive wastewater, which can cause problems its neutralization process <sup>32</sup>.

The disposal of huge quantities of aged polishing baths and contaminated wastewater from electropolishing facilities is very challenging due to the high concentrations of heavy metals.

### **2.2.6 Evaluation of existing research on electropolishing in aged electrolyte**

As it was previously discussed, some industrial reports have emphasized the importance of process monitoring for maintaining the desired surface quality of electropolished parts <sup>28,70</sup>. These technical papers describe the important electrolyte-related process parameters for monitoring; however, they are rather brief and do not generally give the readership a clear understanding of the issue. Thanks to the insights of skilled operators with decades of hands-on experience, throughout the years, electropolishing companies have established specialized knowledge and proprietary techniques that give them a competitive advantage in the market. Therefore, companies consider such information valuable trade secrets and do not share them with the public to avoid compromising their competitive edge.

An investigation of the academic papers published in this field indicates that very little knowledge is available regarding electropolishing in aged electrolytes and its effect on the final surface quality of the parts. The research conducted so far is limited both in the range of the investigated process parameters and target surface characteristics. This section will discuss some of the major shortcomings of the existing literature:

#### Lack of a clear definition of an aged electrolyte

It is commonly said that the solution is aged once the polishing results deviate from the target specifications. However, an in-depth understanding of the variations in different properties of the polishing electrolyte upon prolonged exploitation is missing. The few papers that have discussed electrolyte aging have almost unanimously described aging by the dissolved metal content of the solution, and very seldom have they studied the change over time in other bath properties such as specific gravity, electric conductivity, and viscosity. Without a clear understanding of the mechanism of electrolyte deterioration, one cannot modify the process parameters to maintain the quality level of electropolished parts.

### Necessity of more efficient electrolyte analysis methods

Almost all the research conducted so far on electropolishing with aged solutions has used methods such as Inductively Coupled Plasma (ICP) testing or Ionic chromatography (IC) for determining the metal and ion content of the electrolyte, respectively. These methods are usually costly and time-consuming. Since only some facilities have the required equipment for these tests, sample solutions must be sent to outside laboratories for analysis, which could take up to several days. Given that the mass personalization approach requires real-time adjustments of process parameters based on visual and experimental feedback, simpler and faster methods are required for investigating electrolyte deterioration. In addition to their significant influence on final electropolishing results, electrolyte properties such as specific gravity, electric conductivity, and viscosity can be easily and rapidly measured on-site without the need for sophisticated equipment or advanced interpretation skills<sup>74</sup>.

### Limited range of bath states and polishing results

Most of the conducted studies have focused on either handling the detrimental effects of electrolyte aging on the surface finish or achieving minimum surface roughness or maximum surface brightness in an aging bath. For instance, the body of the works by Éozénou et al.<sup>76,81–84,87</sup> on electropolishing niobium cavities in aged solutions, while quite enlightening, is focused on reducing the generation of sulfur particles on the surface of the cavities upon aging of the electrolyte. These studies provide a basic understanding of the effect of solution aging on mass transport phenomena in the solution and, consequently, deterioration of surface gloss. However, they are mostly focused on finding the optimal electrolyte composition with a higher lifetime and less chance of impurity generation. Similarly, the works of Tyagi et al.<sup>27,77</sup> on low-current-density electropolishing of niobium cavities in aged solutions only aim to alleviate high levels of sulfur generation on the surface. The studies by Lochyński et al.<sup>18,32,72,88</sup> on the electropolishing process in aged solutions focus on achieving the highest surface quality (highest gloss, lowest surface roughness) and/or lowest sample weight loss. However, as already stated, shifting the electropolishing operations towards mass personalization calls for accommodating various surface qualities (e.g., matt, semi-bright, or mirror reflection). Different applications require different levels of surface quality, and developing an efficient approach for obtaining a vast range of results in an aging electrolyte can be a huge advantage for electropolishing companies in today's market.

Further, the research conducted so far does not encompass a wide range of aged solution conditions or final surface qualities. For instance, the study by Surmann et al.<sup>69</sup> on the application of a fuzzy logic controller for automating the electropolishing process considers only four states of the polishing bath, namely, new, good, medium, and bad, which is estimated based on the ampere-hours of the polishing process. It may be argued that the ampere-hours of polishing treatment may not always be a reliable indicator of a bath's condition as the bath is frequently replenished and modified during its service life. Therefore, it seems more logical to assess the state of the polishing bath based on its usage and modification history. The work of Lochyński et al.<sup>32</sup> also only deals

with aged baths that have a metal content of up to 6%. The study by Krishna et al.<sup>74</sup> investigates the variation in electrolyte properties upon aging, however, the range of the changes in the properties is quite limited compared to the actual deteriorated bath states encountered in industry. Even if industries can maintain acceptable polishing bath quality by different countermeasures like decanting, establishing a more flexible electropolishing process that can deliver acceptable results even at higher levels of bath contamination is strongly justified.

#### Limited size of electropolishing database

An experienced operator may be able to estimate the required process parameters given a certain bath state. However, this process can be highly subjective, time-consuming, and limited regarding the scope of explored process parameters. The constant variation of the polishing bath can further complicate this process. The aim of this study, as mentioned several times, is to automate the parameter optimization process in aging solutions by means of data-driven approaches. In this regard, detailed analysis of studies that have employed models for the prediction of final surface characteristics or optimal electropolishing process parameters in aged baths is of utmost importance. Krishna et al.<sup>74</sup> developed a mathematical model to predict the final surface roughness of electropolished samples based on the properties of the aging bath, such as specific gravity, viscosity, and electric conductivity. However, given the limited range of studied bath parameters, the lack of surface appearance (gloss) investigations, and the fixed level of electropolishing process parameters (5V, 10 min), this study does not yield a comprehensive analysis of the topic. The study by Lochyński et al.<sup>32</sup> developed models of surface characteristics as affected by process parameters, based on a limited number of actual observations. The majority of data utilized in this study for determining the optimum process parameters required to achieve the target surface quality was generated by the model. A limited number of actual observations and a lack of model evaluation experiments undermine the validity of the results. Given the existing knowledge gap on optimization of electropolishing process parameters in aging electrolytes, and the importance of this knowledge in maintaining the consistency of the results and reducing the overall costs of electropolishing operations, a comprehensive study of the issue is required. This study shall be based on a sizeable database of experimental results, encompassing a wide range of surface qualities and bath states. The results of the study shall be assessed with different evaluation methods, and its extendibility to new operating conditions shall be studied.

### **2.3 Quality control in electropolishing**

The quality and consistency of electropolishing results depend on the degree to which the electropolishing process is controlled<sup>28</sup>. Given that electrolytes are known to significantly deteriorate with repeated application, a lack of process control may result in inconsistent and unpredictable qualities<sup>28</sup>. Various methods are used in electropolishing facilities to maintain the effectiveness of the polishing electrolyte as it ages. The general practice involves monitoring certain properties of the bath, removing the sludge, and regular decanting of the electrolyte.

### **2.3.1 Removing electrolyte sludge**

As part of the routine preventative maintenance, it is advised that the sludge formed from metal precipitation during electropolishing should be removed regularly<sup>28,31,74</sup>. Filtration methods can also be employed to remove suspended particles, debris, or contaminants that may have accumulated in the electrolyte during usage<sup>85</sup>. The excessive metal ions dissolved in the polishing bath can also be precipitated out by different techniques such as lowering the temperature, chemical precipitation (use of precipitating agents), or electrodeposition (electrochemical reduction)<sup>28,31</sup>.

Failure to remove the sludge can have a severe impact on the polishing process. For instance, some metal ions tend to plate out at the cathodes, which reduces the polishing quality and dissipates electrical energy. Consequently, periodic cathode cleaning is required<sup>18,31</sup>. In addition, when the sludge covers the cathodes, the power supply undergoes an extra workload to compensate for the wasted electrical energy and may ultimately burn out<sup>31</sup>.

### **2.3.2 Decanting the electrolyte**

The simplest and most common method for restoring the quality of aged polishing baths is to replenish the electrolyte with a fresh solution or specific bath components to restore the proper composition. The frequent practice followed in the industry is to use the bath up to the point where the polishing quality is known to be impaired. At this point, 10 – 20% of the solution is removed and replaced with fresh electrolytes to maintain the optimum chemical balance of the electrolyte (decanting). Except for electrolytes with a high sludge volume, it is typically not necessary to replace 100% of the used electrolyte because it is known from experience that polishing baths perform better with some metal already dissolved into the solution<sup>28-31</sup>.

### **2.3.3 Monitoring bath properties**

Good electropolishing is proven to depend on maintaining the concentration of total acid and dissolved metal in the polishing bath, as well as the bath's specific gravity, viscosity, and temperature<sup>28,31,69,70</sup>. Regular evaluation of the bath state can determine the time of decanting. Additionally, after bath adjustment, continuing the assessments for a while can help to establish the appropriate schedule for electrolyte decanting and other restorative activities (such as acid addition) based on polishing ampere-hours<sup>70</sup>.



Some typical bath control measurements include:

### **Viscosity**

The polishing bath viscosity is considered an important factor in controlling the electropolishing process. The viscosity depends on dissolved metal content, ratio of bath constituents, and temperature of the polishing bath <sup>28,31</sup>. It is important to maintain the solution viscosity necessary for optimum electropolishing results by accurately regulating the specific gravity, metal concentration, and temperature.

### **Specific gravity**

The specific gravity of the solution increases with the accumulation of ampere-hours, which is attributed to an increased concentration of dissolved metals in the solution. A typical method of monitoring the electrolyte quality is the routine measurement of its specific gravity and comparing it to the operating range recommended by the manufacturer. In the absence of a guideline, it is suggested to simply decant the electrolyte on a regular basis (monthly) <sup>29,30</sup>.

### **Analysis of dissolved metal concentrations**

As previously mentioned, the electrolyte's specific gravity and tendency for sludging increase as its dissolved metal content grows. The build-up of certain metals in the solution (such as iron during stainless steel electropolishing) is known to adversely affect the polishing results. In such cases, Atomic Absorption Spectrometry (AAS) is recommended for determining the concentration of elements such as iron, copper, nickel, and chromium in the solution <sup>30</sup>.

### **Titration of acids**

In an aging polishing solution, the acid concentration drops as the concentration of the dissolved metals in the solution increases, which might lead to an unfavorable polishing quality <sup>38,70</sup>. Acid titration can be used to monitor the concentration of various acids in the polishing solution. For instance, the electropolishing solution for stainless steel typically contains at least two inorganic acids, namely, sulfuric acid and phosphoric acid. The concentration ratio of the acids can be analyzed by titration with different pH endpoints to ensure it remains within the desired range for optimal performance <sup>30</sup>.

## **Electrical conductivity**

Electrical conductivity measurement is another useful parameter for assessing the quality of the electrolyte. The conductivity of the bath can vary with changes in the concentration of ions, dissolved solution byproducts, or contaminants. Monitoring conductivity can help detect changes in the bath's composition and guide corrective actions <sup>74</sup>.

### **2.3.4 Quality control challenges**

For practical applications, it is important to characterize the electropolishing bath state using quantities that can be measured on-site, such as viscosity, specific gravity, and electrical conductivity <sup>74</sup>. In an electropolishing facility it is usually the operator's responsibility to record the variations in the electrolyte quality and estimate the state of the bath for each electropolishing treatment <sup>69</sup>. Determination of the proper polishing parameters based on the bath condition relies to a great extent on the "art of electropolishing", i.e., the ability of the operator <sup>28</sup>. Maintaining the consistency of polishing results in an ever-changing bath can become a great challenge, even for a skilled operator. Particularly, if different users operate the same polishing bath, there is high uncertainty about the electrolyte quality <sup>69</sup>.

Aside from requiring a great level of knowledge and experience of the process, sustaining an acceptable quality of the polishing bath is quite costly. Given the relatively high cost of polishing electrolytes and the considerable amount to which they are consumed in electropolishing facilities (for instance, the capacity of the electrolyte reservoir tank at the KEK facility in Japan is 2,000L), changing the polishing solution frequently reveals very expensive <sup>20,27</sup>. Another significant cost for quality control of electropolishing services is the cost of disposing of the used electrolytes <sup>27,28</sup>. Since aged electrolytes have high metal content, they are considered hazardous waste and cannot be simply neutralized and flushed <sup>32</sup>. The same applies to the sludges formed during the electropolishing and rinsing waters used for removing electrolyte residues from the polished parts. Therefore, their disposal is usually handled by certified waste hauling services to ensure compliance with environmental regulations <sup>29</sup>. Some electropolishing facilities conduct a standard in-house waste treatment process consisting of pH adjustment, removal of metals from the solution, sludge filtration, drying, bagging, and shipping by a certified waste hauler <sup>89</sup>. Either way, waste disposal and replenishment of the electropolishing tanks with fresh acid are costly and impose environmental issues.

### **2.3.5 Quality control using data-driven approaches**

The main goal of all the discussed efforts is to maintain the consistency of the surface qualities despite electropolishing in an aging solution. This would be a great improvement, especially for an electropolishing facility looking to establish the mass production paradigm. As previously stated, effective process control is essential for maintaining product consistency and quality. In

addition, trained and skilled operators are required to optimize the process to achieve efficient and cost-effective mass production. In theory, if all of the requirements are met, and the process parameters can be adjusted to obtain consistent results, the electropolishing process gets one step closer to implementing the mass production strategy. The transition to mass production might be complicated, nevertheless, by some circumstances. For instance, determining the correct process parameters to reproduce a surface finish obtained in a previous order in a bath that has perhaps changed significantly since then. Another instance would be finding the basic polishing parameters to accommodate a new surface finish that has not been produced before. Relying on the previous experience of the operator is the only imaginable way to address such situations. Indeed, most electropolishing facilities still rely on skilled operators' judgment for critical decision-making about the polishing process.

The transition from mass production to a mass personalization approach requires developing a range of product customization options. For instance, in the case of the electropolishing process, the customers may be provided with a menu of surface roughness, surface brightness, or acceptable workpiece weight loss options to choose from. In addition, considering the importance of learning from the operator's experience for successful quality control, utilization of tools that enable data-driven decision-making is crucial for electropolishing treatments.

An essential aspect of the mass personalization approach is data collection, storage, and analysis, which would enable manufacturing new concepts based on previous knowledge and experiments. Proper management and exploitation of this huge amount of data is outside the capabilities of human operators. This is why embracing digital technologies is an essential requirement for mass personalization of products. Digital technologies provide tools and capabilities for collecting and analyzing vast amounts of data to facilitate product customization. Another great advantage of digital technologies is the possibility of data-driven decision-making for optimizing the process and improving its efficiency and cost-effectiveness. Using smart tools such as machine learning algorithms can greatly aid electropolishing facilities in processing significant amounts of data from long-term monitoring of polishing bath properties, electropolishing procedures, final surface characteristics, and specific process observations. With the insight from previous data, machine learning algorithms can predict the "optimum" process parameters required to obtain various surface qualities.

A study of the literature indicates that in some electrochemical processes, researchers have tried to employ data-driven approaches, especially machine learning to benefit from experience. For example, by combining grey relational analysis (GRA) with an artificial neural network (ANN) model, Asokan et al.<sup>90</sup> found the optimal level of electrochemical machining (ECM) process parameters such as current, voltage, and flow to achieve favorable cutting performance in terms of metal removal rate and subsequent surface roughness of the workpiece. Li et al.<sup>91</sup> used a backpropagation (BP) neural network model to find the optimum machining parameter combinations that can fully meet the manufacturing specifications for aero-engine blades while assuring ECM process stability. BP neural networks were also utilized in the electroforming process to optimize the microhardness and tensile strength of the electroformed copper layer<sup>92</sup>, as well as the physical quality of electroformed metal shells<sup>93</sup>. Goulart et al.<sup>94</sup> were able to

autonomously manage the pH of a mathematically simulated electroplating bath using a machine learning model that maintained the pH value at a predetermined set point by adjusting the neutralizer input flow rate. In other works, to ensure a steady plating process Ellis et al.<sup>95</sup> and Yoon et al.<sup>96</sup> employed artificial neural network algorithms to determine the concentration of various additives in copper deposition electrolytes.

Given their significant potential for mass personalization, one may argue that surprisingly little work has been done on applying data-driven approaches to enhance electropolishing procedures. In fact, to the best of the author's knowledge, no other research has tried to paint a comprehensive picture to demonstrate the effect of variations in bath properties and polishing parameters on the final surface characteristics of polished parts.

## 3. Methodology

### 3.1. Introduction

The goal of this study is to develop a prediction tool based on a machine learning model to predict the electropolishing process parameters required for obtaining a target surface finish at a given polishing bath condition. The first step in constructing the prediction tool is building a sufficiently large dataset that encompasses diverse electropolishing outcomes achieved under varying process parameters and bath conditions. Once a sizable dataset is assembled, a series of data analysis procedures is undertaken to formulate the predictive tool. Ultimately, the tool's performance is assessed in terms of its predictive value and its expandability to scenarios beyond the dataset's original scope.

### 3.2. Experimental set-up and procedure

#### 3.2.1. Workpiece and bath preparation

Various electrolytes have been proposed over the years for the electropolishing of different metals. Given that examining every combination of metals and polishing solutions requires a significant amount of time, the scope of this project was limited to a common metal and electrolyte in the hopes that the results would be more useful for future applications. Thus, the project's focus is on the aging of the phosphoric acid-sulfuric acid-DI water bath commonly used for electropolishing stainless steel parts.

Stainless steel 316 bars of size 70mm × 20mm × 1mm from McMaster-Carr were cut and prepared for the electropolishing experiment with the following procedure:

- Degreasing with soap water for 15 minutes in an ultrasonic bath (Branson Model 1510 ultrasonic cleaner).
- Rinsing with DI water to remove the soap.
- Degreasing with acetone for another 15 minutes using ultrasonic vibrations.
- Cleaning with DI water for 5 minutes in the ultrasonic bath.
- Drying with airflow.
- Coating with varnish on one side to limit the exposed area to a 2cm×2cm square.
- Insulating the remaining area of the sample with Teflon tape.

After the polishing tests, the workpieces were thoroughly rinsed with cold water to remove all acid residues. The samples were then air-dried and characterized.

During the accelerated aging tests, which will be discussed later in this chapter, stainless steel 316 bars from McMaster-Carr were cut in 75 mm x 75 mm x 6 mm dimensions and used as the working electrode.

The initial polishing bath was prepared with a mixture of 35% v/v sulfuric acid, 50% v/v phosphoric acid, and 15% v/v DI water. The concentrations of the sulfuric-phosphoric acid used for the electrolyte preparation were 96.8% and 85%, respectively. The composition of this bath was close to the commercial EPS 4000 solution used in industry for electropolishing of stainless steel.

### **3.2.2. Electropolishing**

Electrochemical polishing and accelerated bath aging tests were conducted in a typical electrochemical three-electrode cell with a B&K Precision Model-9117, multi-range programmable DC power supply. The stainless steel bars were used as the working electrodes. A copper sheet was rolled and placed in the cell as the counter-electrode. The shape and positioning of the counter-electrode provided even current densities to the working electrode. All potentials were measured versus a double junction mercury sulfate (MSE) electrode saturated in  $K_2SO_4$  solution. An ABS (Acrylonitrile Butadiene Styrene) electrode holder was designed and fabricated through fused deposition modeling (FDM) in an Ultimaker 2+ printer. The holder was then used to position the workpiece at the center of the cell and 1 cm from the tip of the reference electrode.

Electropolishing treatments were conducted at 40° C under different applied potentials (3, 4, 5, 6, and 7V) for different durations (300, 600, 900, and 1200 s). During the electropolishing tests the fluctuations of the polishing bath temperature were recorded using a digital temperature sensor.

- Accelerated Ageing Test: In order to obtain polishing baths with various usage histories, solutions were subjected to accelerated aging tests where stainless steel 316 bars (75 mm x 75 mm x 6 mm) were electropolished at constant currents for various durations until the desired level of aging was obtained. After each accelerated aging cycle, the bath could cool down to room temperature and then the parameters of bath quality were measured to ensure a significant change in the solution electrical conductivity or viscosity had happened (a jump of at least 10 mS/cm in the solution's conductivity or a change of about 60 mPa.s in viscosity).

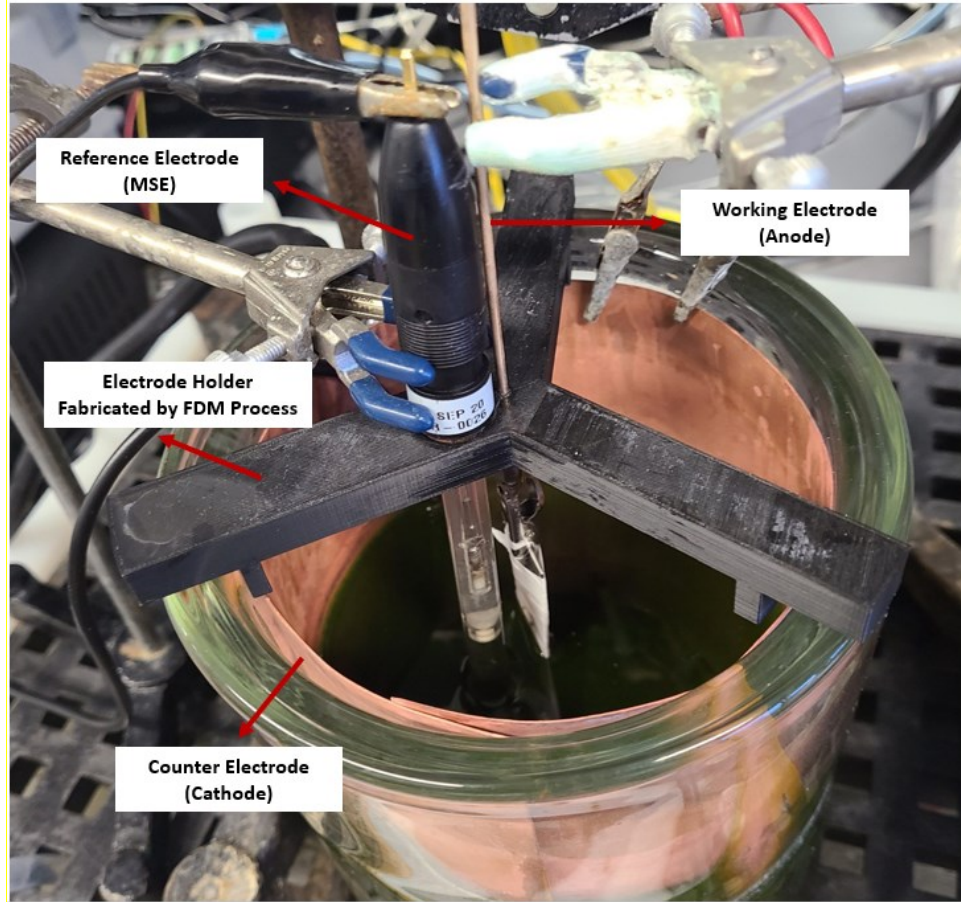


Figure 3.1. A typical electropolishing cell utilized in this study.

### 3.2.3. Bath characterization

Based on their proven relevance and their measurement simplicity, the specific gravity, viscosity, and electrical conductivity of the electrolyte were chosen to evaluate the state of the polishing bath.

Before each polishing process, the specific gravity, electrical conductivity, and viscosity of different polishing baths were measured at room temperature using the METTLER TOLEDO™ handheld density meter, Thermo Scientific Orion benchtop conductivity meter, and SNB-2 rotational viscometer, respectively.

The dissolved metal content of the polishing baths was measured by Inductively Coupled Plasma-Mass Spectroscopy (Agilent-7500ce ICP-MS). Samples of different polishing baths were diluted 20 times with DI water and subsequently filtered with PTFE 0.22- $\mu$  filters before submission for ICP-MS analysis.

The sulfuric acid-phosphoric acid ratio of the polishing baths was measured by acid-base titration end point detection method using methyl orange and phenolphthalein indicators, respectively.

### 3.2.4. Sample characterization

#### Weight measurement

Before and after each electropolishing experiment, the samples were cleaned according to the steps mentioned in 3.2.1 and weighed using a OHAUS PIONEER® precision balance.

#### Surface roughness tests

The surface roughness of the samples was measured before and after each experiment using a Mitutoyo Surftest SJ-210 Series-178, contact-type portable profilometer. The surface roughness measurements were repeated at least on 10 random points of the exposed area. The cut-off length was carefully selected (in function of the measured roughness) for each measurement to ensure correct results.

For each surface roughness measurement three parameters, namely, Ra, Rq, and Rz were measured. The user's manual of the surface roughness tester defines these parameters as follows<sup>97</sup>:

- Ra (Arithmetic Average Roughness) is the arithmetic average of the absolute values of the deviations of profile heights from the mean line within the measurement length.
- Rq (Root Mean Square Roughness) is the square root of the arithmetic mean of the squares of profile height deviations over the measuring length.
- Rz (Maximum Height Roughness), is the maximum peak-to-valley height within a sampling length on the surface profile.

#### Surface gloss tests

A Miza Trigloss Meter was used to evaluate the gloss value of the exposed surface of the bars before and after electropolishing. This device determines the surface gloss by projecting a beam of light at a fixed intensity and angle onto the surface and measuring the amount of reflected light at an equal but opposite angle. It is known that on a smooth surface, the projected beam of light is reflected opposite to the angle at which it arrives, which is referred to as 'specular' reflection. On a rough surface, however, light is reflected at all angles (scattered), and a relatively small amount of light reflects at the specular angle (Figure 3.2).



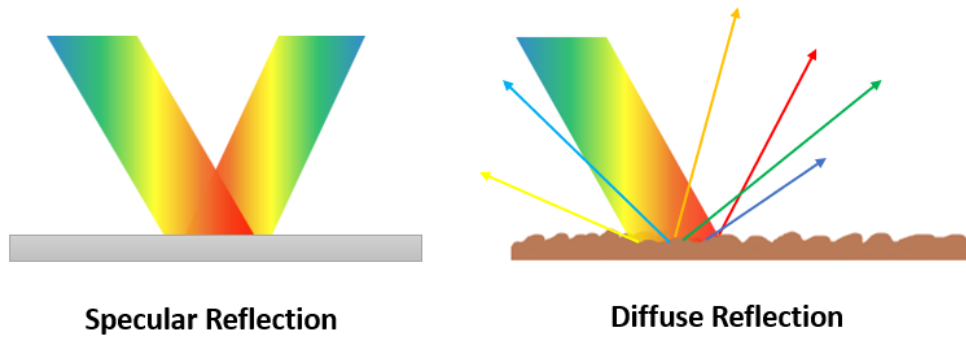


Figure 3.2. Specular and diffuse reflection.

All specular gloss values are based on a primary reference standard, which is a highly polished black glass with an assigned specular gloss value of 100. The ratio of reflected to incident light for the specimen, compared to the ratio for the gloss standard, is recorded as gloss units (GU).

The Miza Trigloss Meter device used in this study enables gloss finish measurements at angles of 20°, 60°, and 85° (Figure 3.3). It is generally recommended by gloss meter manufacturers that the 20° angle gloss should be used for evaluating high gloss finishes, whereas the 60° and 85° angle glosses should be used for assessing medium and low gloss surfaces, respectively.

As a rule of thumb, the incident angle used to describe the brightness of a surface is determined from the gloss measurement at the 60° angle. If the measured surface gloss is less than 70, the surface is considered low gloss and should be investigated with an 85° incident angle. However, if the measured surface gloss is larger than 70, the surface is high gloss and must be studied using the 20° angle gloss.

Considering the relatively bright surface of the as-received samples, only the 20° and 60° angle glosses were measured in this study. Similar to surface roughness readings, gloss measurements were repeated on at least 10 random points of the exposed surface.

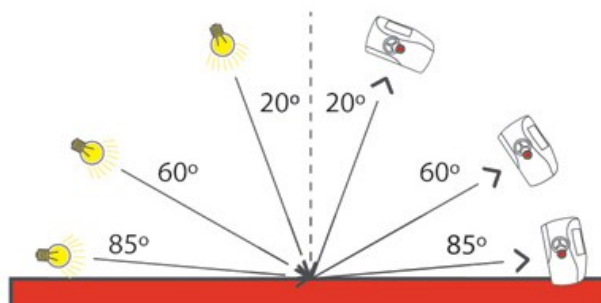


Figure 3.3. Surface gloss measurement angles.

The measurement errors for surface roughness parameters Ra, Rq, and Rz are estimated to be about 0.01, 0.01, and 0.06  $\mu\text{m}$ , respectively. Additionally, the errors in surface gloss measurements are 16 GU for the H20 index and 5 GU for the H60 index (for justifications and details see 5).

### **Surface morphology investigations**

The surface morphology of the electropolished samples was characterized using a Hitachi S3400N scanning electron microscope (SEM).

### **3.3. Model development**

Figure 3.4 provides an overview of the steps taken to develop a machine learning model. This section discusses some of the tools and libraries used in this study for conducting data analysis and developing machine learning models to represent and analyze the dataset.

First, a dataset is built with raw process data coming from experimental results and sensors that record various process parameters. In the case of this study, the building blocks of the dataset are the results of electropolishing experiments under different polishing conditions at various bath states, as well as the variations of the polishing bath temperature and polishing current during the experiments.

Subsequently, the analysis of this dataset is conducted within the framework of Jupyter Notebook—an open-source, interactive web application widely used in data science for data exploration, visualization, and documentation. In the data ingestion step, the Pandas library <sup>98</sup> is used to import the raw data to the Jupyter Notebook in the form of DataFrames and Series. These data structures enable efficient data exploration, cleaning, pre-processing, and transformation. After transforming the dataset into a usable format, its most informative features are identified using different feature selection methods, as well as the existing knowledge of the process (details provided in section 5.6.2). In the next step, various regression algorithms are implemented using the Scikit-Learn machine learning library <sup>99</sup>, and their performance in representing the dataset is compared. Finally, the prediction value of the tool is investigated through a series of experiments in new polishing baths with different preparation and usage histories than those studied in the dataset. During the process, other open-source Python libraries such as Matplotlib <sup>100</sup> and NumPy <sup>101</sup> are also used for data visualization and execution of mathematical and statistical operations on the dataset, respectively. The details of the machine learning model development will be thoroughly discussed in 5.

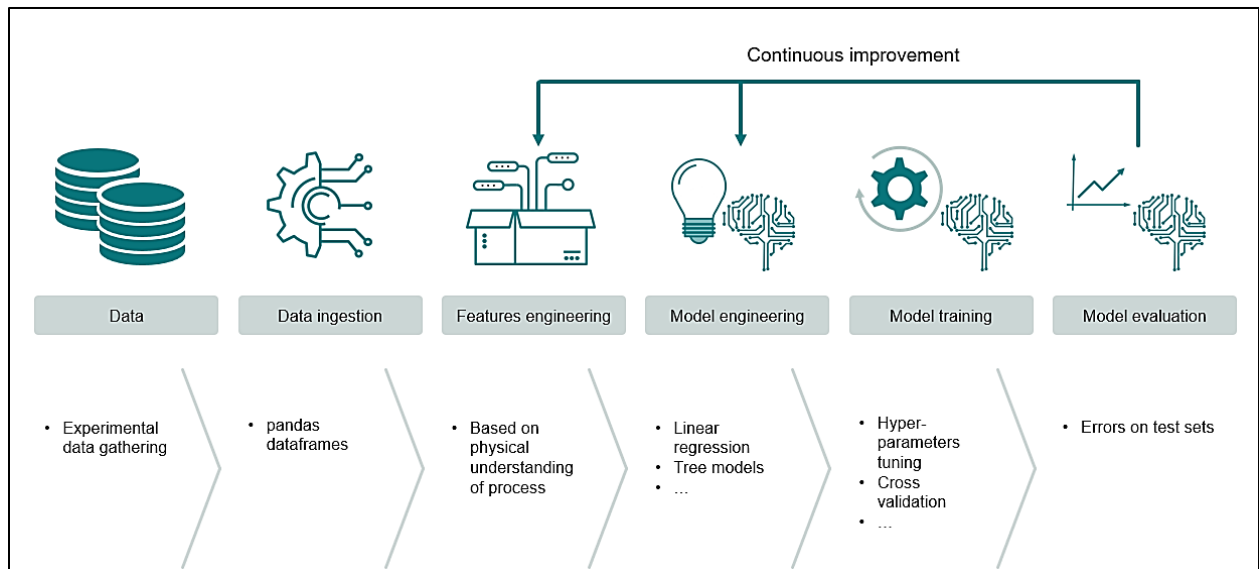


Figure 3.4. Model development steps.

## 4. Polishing Bath History

### 4.1. Introduction

As stated in the literature review section, despite the substantial contribution of electrolyte "aging" to the outcomes and cost of the electropolishing process, there is insufficient information available on the subject in the open literature. The electropolishing industry has devised in-house countermeasures to avoid the consequences of bath aging. However, they are not publicly available and are considered knowledge to be protected due to the risk of losing their competitive advantage.

Among the open questions regarding the effect of bath degradation on the surface quality of the electropolished parts, three are of particular interest to our work. Firstly, there is the issue of defining the state of bath aging. As will be discussed later, the "age" of a polishing bath is not properly the most suitable term to employ for discussing the variation of a bath upon extensive usage. Instead, the "state" of the bath is a more appropriate notion for reflecting the complicated process history it experiences. Consequently, our second question revolves around the assessment of bath state. To be more specific, we aim to determine which physicochemical properties of the bath are relevant, and whether it is possible to characterize the state of the bath using only the properties that are readily available for in-line, real-time measurements. The third question we aim to explore involves the possibility of using such physicochemical properties to make necessary adjustments to the polishing process parameters, such as voltage and time, in order to maintain consistent surface properties (i.e., roughness and appearance) of the workpiece.

To investigate the impact of electrolyte degradation on the electropolishing process, this chapter explores three different polishing bath states: one being relatively new, and the other two having undergone extensive use, but with different process history. Subsequently, an assessment of the resultant surface quality of the samples polished in these baths is carried out, utilizing measurements of surface roughness and brightness, as well as conducting morphological studies using SEM imaging. Finally, potential interpretations and insights are presented to elucidate the influence of the electrolyte's usage history on the ultimate quality of the components.

### 4.2. Bath analysis

Identifying the state of the polishing bath prior to the electropolishing process is a crucial step in building the dataset which will subsequently be utilized to predict the adequate polishing parameters. It must be mentioned, however, that from the author's view, terms like "electrolyte aging" or "aged bath" lack clear and well-defined definitions. When working with polishing electrolytes, it is essential to consider that characterizing a bath based on the number of polished parts or the accumulated ampere-hours of polishing treatment does not necessarily yield a meaningful or accurate understanding of its condition. This is particularly true in industrial electropolishing facilities where the electrolyte is often used continuously with regular additions

or adjustments to maintain the desired composition and performance. It can be, thus, difficult to accurately estimate the state of the electrolyte, given its continuous usage and replenishment. However, given the fact that a bath's usage history and replenishment frequency can significantly affect the electropolishing results, this study aims to study the effect of bath "state" rather than its age. The polishing bath may be characterized meaningfully by physicochemical properties such as its specific gravity, electric conductivity, and viscosity that can be simply and rapidly measured on-line in industrial facilities without sophisticated equipment or extensively trained operators. These electrolyte properties were, therefore, used in this study to demonstrate the state of the polishing baths. In addition, to give a thorough understanding of the various states of the polishing bath, a more time-consuming analysis, to be conducted off-line, of electrolyte composition and metallic ion content is presented in this chapter.

Three solutions were taken from baths with different usage histories, solution 1 being closest to a fresh bath, and solutions 2 and 3 selected from two artificially aged baths. The physicochemical properties to be investigated were selected based on the literature review of 2. In addition to specific gravity, electric conductivity, and viscosity, the bath composition (volume percent of sulfuric acid and phosphoric acid) was evaluated using multiple-point titration, and ICP-MS (Inductively Coupled Plasma Mass Spectrometry) analysis was used to determine the concentration of dissolved metals in the baths. Table 4-1 and Table 4-2 present the results of bath characterization for these three bath states.

Table 4-1. Measured properties for different bath states.

<b>Solution</b>	<b>Electric Conductivity</b> Error: $\pm 0.4$ mS/cm	<b>Viscosity</b> Error: $\pm 0.1$ mPa.s	<b>Specific Gravity</b> Error: $\pm 0.001$ g/L	<b>Composition</b> %(v/v)
1	144.5	23.4	1.673	H <sub>2</sub> SO <sub>4</sub> : 31 H <sub>3</sub> PO <sub>4</sub> : 45
2	38.1	224.5	1.855	H <sub>2</sub> SO <sub>4</sub> : 27 H <sub>3</sub> PO <sub>4</sub> : 52
3	28.6	339.5	1.887	H <sub>2</sub> SO <sub>4</sub> : 34 H <sub>3</sub> PO <sub>4</sub> : 68

Table 4-2. Concentration of dissolved metals measured by ICP-MS analysis.

<b>Sample</b>	<b>Concentration (g/L)</b>				
	<b>Cr</b>	<b>Mn</b>	<b>Fe</b>	<b>Ni</b>	<b>Mo</b>
Fresh Solution	1.19	0.21	6.95	2.45	1.34 E-04
1	7.91	0.43	25.82	1.99	0.95
2	23.04	1.48	85.7	6.29	2.67
3	25.56	1.50	90.36	4.85	2.84

According to Table 4-1, the specific gravity of solutions 2 and 3 is higher than that of the close-to-fresh bath (solution 1) which is evidently due to the higher concentration of dissolved metals from electropolishing reactions. It can also be noted that the electric conductivity and viscosity of baths 2 and 3 are significantly different from those of bath 1. This difference can be explained by the fact that the increased polishing bath viscosity caused by extensive metal dissolution decreases the mobility of charge-carrying species, thereby reducing the electric conductivity of the solution. In addition to the observed changes in the physical properties of the polishing baths, variation of the electrolyte composition upon usage is also known to affect the outcome of the electropolishing treatment. As can be seen in Table 4-2, the concentration of dissolved metals in solutions 2 and 3 is considerably higher than that of the close-to-fresh solution. The higher concentration of dissolved metals in solution 3 may suggest that this bath was operated for a longer time. It can also very well mean that solution 2 was operated longer but replenished more often. This indicates that different usage histories can result in different levels of contamination in the solutions and highlights once more the importance to consider the state of the bath, rather than its “age” or usage history.

In industrial settings, access to the ICP-MS results is challenging for at least two reasons. Firstly, it is a costly process and secondly, and most importantly, since ICP-MS is not accessible within the production facility, it necessitates outsourcing, making it impossible to obtain real-time data on the production line. An important question we attempt to answer within our work is, to know if the state of the bath can be characterized accurately enough using readily available in-line measurements, such as the ones presented in Table 4-1.

### **4.3. Sample analysis**

#### **4.3.1. Surface roughness and brightness characterization**

To demonstrate the effect of bath state, resulting from a certain usage history, on the surface quality of the electropolished parts, three samples were polished with similar process parameters (polishing voltage: 5 V, polishing duration: 300 s) in electrolytes 1, 2, and 3. Electropolished samples were then characterized with regard to their surface roughness, surface brightness, and weight loss. In addition, SEM images were taken to study the effect of the bath state on the surface microstructure of the samples. Figure 4.1 demonstrates the visual difference between the electropolished samples and an untreated sample. It is evident that the sample treated in the near-fresh solution 1 (Figure 4.1(b)) has a bright and mirror-like surface, whereas the surface of the other two samples does not differ considerably from that of the untreated sample. Table 4-3 indicates the results of surface characterization for these samples.

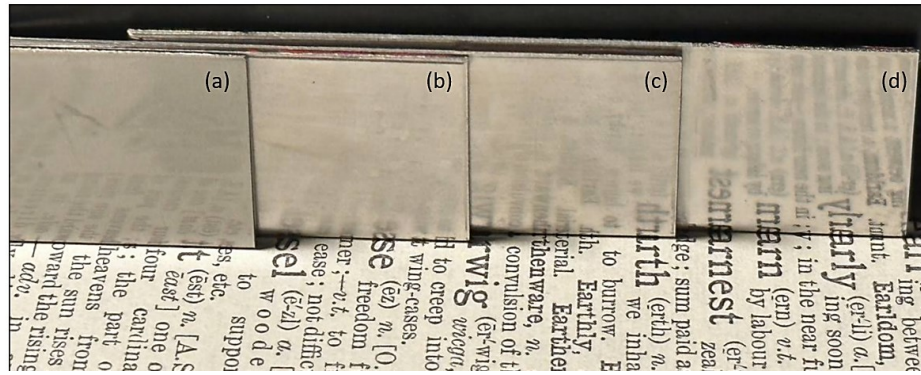


Figure 4.1. (a) Untreated sample and samples electropolished under 5 V, 300 s in (b) solution 3, (c) solution 2, and (d) solution 1.

Table 4-3. Surface characterization and weight loss measurements for three samples electropolished under the same process parameters (5 V, 300 s) in solutions 1, 2, and 3.

Electrolyte	Surface Roughness ( $\mu\text{m}$ )		Surface Brightness (GU)		Weight Loss (g)
	before	after	before	after	
1	<b>Ra</b>	0.1	0.05		0.1515
	<b>Rq</b>	0.15	0.06	<b>20:</b> 138 <b>60:</b> 137	
	<b>Rz</b>	1.09	0.28	<b>20:</b> 925 <b>60:</b> 603	
2	<b>Ra</b>	0.08	0.11		0.0075
	<b>Rq</b>	0.1	0.14	<b>20:</b> 164 <b>60:</b> 225	
	<b>Rz</b>	0.55	0.83	<b>20:</b> 114 <b>60:</b> 261	
3	<b>Ra</b>	0.08	0.13		0.005
	<b>Rq</b>	0.1	0.17	<b>20:</b> 145 <b>60:</b> 175	
	<b>Rz</b>	0.55	1.1	<b>20:</b> 49 <b>60:</b> 127	

According to Table 4-3, compared to the results obtained by baths 2 and 3, electropolishing in the close-to-fresh solution results in a significant reduction of surface roughness and an increase in surface brightness. These results were expected given that the performance of the electropolishing bath generally deteriorates upon usage. Solution 2 does not deliver significant changes in surface roughness or brightness, indicating inadequate polishing action. Solution 3, on the other hand, demonstrates a considerable increase in surface roughness and reduction of surface brightness which indicates that this solution has the weakest polishing performance among the three baths. This conclusion is also supported by the results of the weight loss measurements which show that an effective polishing action in the near-fresh bath causes a considerable decrease in the weight of

the sample, whereas in bath 2 and 3 significantly less weight loss occurs due to insufficient metal dissolution.

### 4.3.2. Scanning Electron Microscopy

SEM images of the samples were captured to investigate the effect of electrolyte degradation on the microstructure of the electropolished surfaces (Figure 4.2). The SEM micrographs of the samples clearly show the substantial impact of bath properties on the surface topography of the polished parts. The SEM image of the untreated part in Figure 4.2 (a) shows a rough surface with deep cracks and scratches. It is clear from the images that the surface polished in the freshest solution (bath 1) is homogeneous and smooth with visible bulk structure, that is, distinct grain boundaries displaying different crystallographic orientations<sup>54,102</sup>. The surface of the part treated with bath 2 is relatively smooth with slightly visible grains, although there is a noticeable amount of surface waviness. Bath 3 delivers the poorest results in terms of surface morphology. As can be seen in Figure 4.2 (d), the surface of the electropolished part appears rough, uneven, and quite similar to the untreated part, which can be suggestive of insufficient polishing.

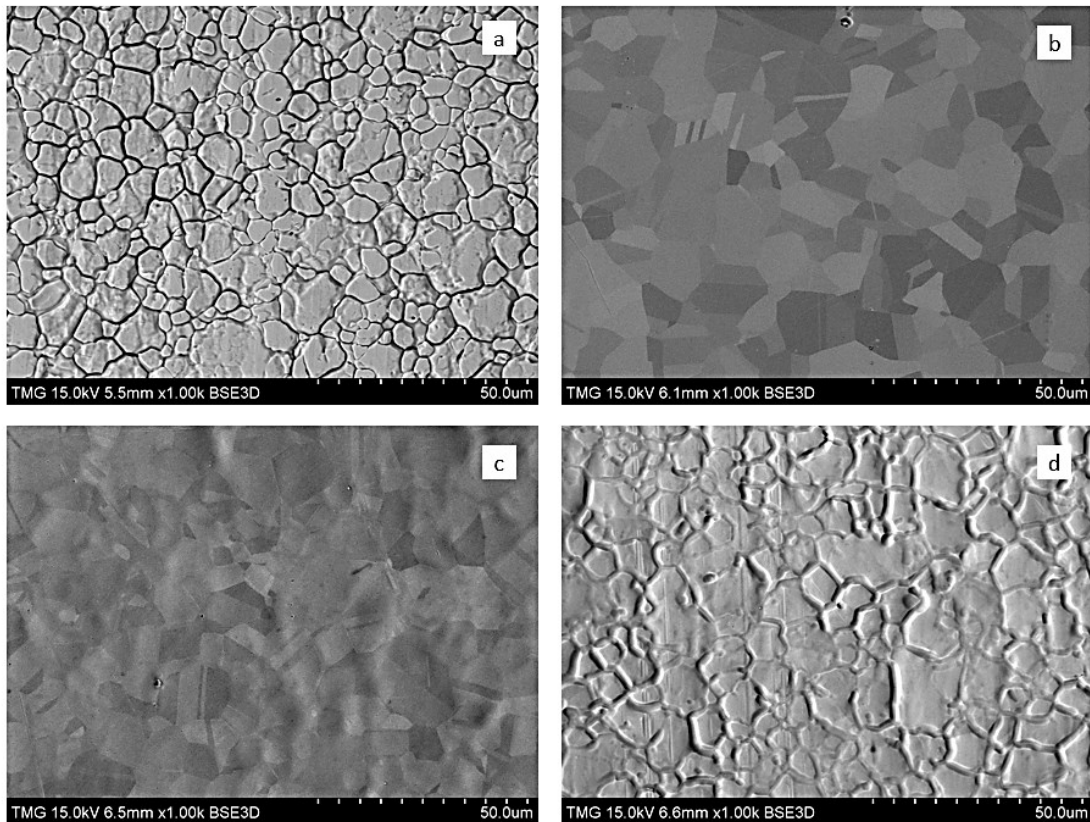


Figure 4.2. SEM images of a) untreated sample and samples electropolished in (b) solution 1, (c) solution 2, and (d) solution 3 under similar polishing parameters (5 V, 300 s).



#### 4.4. Analysis of the results

The observed difference in the polishing results can be attributed to several factors including:

##### a) The increased ohmic drop across the polishing bath

The ohmic drop within an electrochemical cell refers to the resistance encountered by the current as it passes the cell's medium, and it depends on the conductivity of the electrolyte and the geometry of the cell. The ohmic drop's contribution to the potential of the electrochemical cell is given by <sup>103</sup>:

$$U = U_0 + \sum |\eta| + R_0 I \quad (4.1)$$

where  $U$  is the terminal voltage of the electrochemical cell,  $U_0$  is the cell potential at equilibrium (where no current flows) given by the sum of equilibrium potentials at anode and cathode,  $\sum |\eta|$  is the sum of all electrode overpotentials, and the term  $R_0 I$  is the ohmic drop.

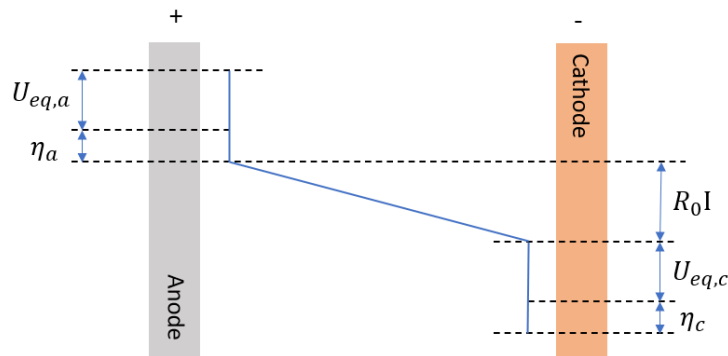


Figure 1.6. Schematic potential distribution in an electrochemical cell.

An external power supply provides the driving force for the electropolishing process. The applied voltage must supply the overpotential needed to drive and sustain the electrochemical reactions that occur during electropolishing. According to equation 4.1, the applied potential must also overcome the voltage drop caused by the internal resistance of the cell, which includes electrolyte resistance, electrode resistance, and any additional resistance in the circuit. In an electrolyte with low electric conductivity, the higher voltage drop across the cell reduces the potential available to the electrodes and, therefore, the effective current density, resulting in slower material removal rates and less efficient electropolishing.

It is known that the electrolyte usage history can have a significant effect on its electrical resistance. Over time, impurities can build up in the polishing bath from different sources, including dissolved metals from the workpiece, reaction by-products, or environmental contaminants. In addition, gradual degradation of the electrolyte due to chemical reactions, exposure to air and moisture, or thermal effects can alter its composition and, ultimately, electric conductivity. For instance, electrolyte evaporation upon prolonged usage can result in more concentrated and aggressive baths that, in turn, can lead to higher concentrations of dissolved metals. All of these factors can increase the electrolyte's electrical resistance, leading to a higher ohmic drop (IR drop) during the polishing process.

In addition to a slower material removal rate, a higher IR drop can cause non-uniform current distribution across the workpiece surface, leading to uneven material removal and poor overall polishing quality. Further, when the IR drop increases, more electrical energy is converted into heat rather than electrochemical reactions. Excessive electrolyte heating can further alter its composition and potentially damage the workpiece surface.

According to Table 4-1, the electric conductivity of the close-to-fresh solution is  $144.5 \pm 0.4$  mS/cm which is significantly higher than those of more-used solutions ( $38.1 \pm 0.4$  mS/cm for solution 2 and  $28.6 \pm 0.4$  mS/cm for solution 3). The electrical resistance of the solutions can be estimated from these data using the following formula:

$$R = \rho \frac{l}{A} \quad (4.2)$$

where  $\rho$  is the electric resistivity of the solution in  $\Omega \cdot \text{m}$  and equal to the reciprocal of electric conductivity,  $l$  is the distance between the working and the reference electrodes (1 cm), and  $A$  is the area of the exposed surface ( $4 \text{ cm}^2$ ). Given the measured values for electric conductivity of the solutions, their electric resistances are roughly estimated as 1.7  $\Omega$ , 6.6  $\Omega$ , and 8.7  $\Omega$  for solutions 1, 2, and 3, respectively. For a current of 0.5 A (which is a typical value of the current observed during electropolishing at 5 V), a voltage drop of 0.9 V, 3.3 V, and 4.3 V can be expected in solutions 1, 2, and 3, respectively. It can be hence concluded that the three samples electropolished in these solutions with similar process parameters (5 V, 300 s) were in fact subjected to different polishing potentials.

For samples electropolished in solutions 2 and 3, the actual available voltage was 1.7 V and 0.7 V, which indicates insufficient electropolishing as one of the main reasons for lower surface qualities. It could, therefore, be expected that if the workpiece is treated with a higher applied voltage to compensate for the estimated ohmic drop of the bath, more favorable results could be obtained. However, polishing experiments at higher polishing voltages (6 V and 7 V) indicated that this approach is not as straightforward as it seems.

Figure 4.3 illustrates the effect of increasing the polishing voltage on final surface roughness of samples electropolished in solutions 1, 2, and 3 for the same duration (300 s). Considering the difference in the initial roughness of the samples ( $R_a$  before), these values are also included in the

plot for a more meaningful comparison of the results. As can be noted in the plot, for the given polishing duration (300 s), the surface roughness of the samples treated in solution 1 are decreased after electropolishing. However, increasing the applied polishing voltage does not yield a substantial improvement in the polishing outcomes. On the other hand, in the case of the samples treated for 300 s in solutions 2 and 3, the surface roughness is increased by the polishing process. It can also be noted that for this polishing duration, increasing the polishing voltage in solutions 2 and 3 does not necessarily enhance the final surface roughness of the samples.

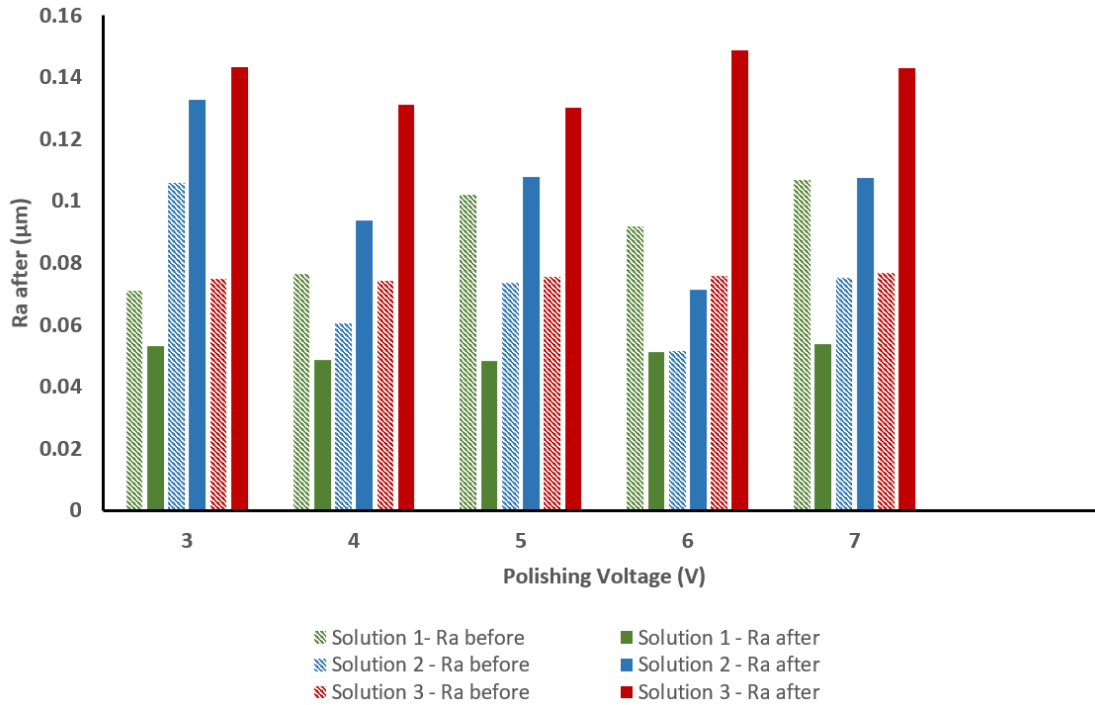


Figure 4.3. The change observed in the surface roughness (Ra) of samples electropolished in solutions 1, 2, and 3 under different polishing voltages for 300 s.

It was also observed during the electropolishing experiments that increasing the polishing voltage up to 7 V resulted in significant bubble formation and heating of the electrolyte, especially in extensively-used baths. In addition, shortly after applying potentials higher than 7 V, the current decreased rapidly, and the polishing stopped. These observations can be explained by the substantial alteration in the electrochemical behavior of the part when subjected to higher polishing voltages, primarily due to the pronounced generation of bubbles. To better illustrate this point, the I-V graphs of samples electropolished at six different bath states are presented in Figure 4.4. These plots indicate that as the electric conductivity of the polishing bath decreases, the current-voltage behavior of the workpiece is further changed, and applying higher voltages results in a less significant increase in polishing current. This behavior is, in fact, observed generally on gas-

evolving electrodes under high potentials. An instance of this voltage-current behavior is exhibited by the water electrolysis process, as shown in Figure 4.5.

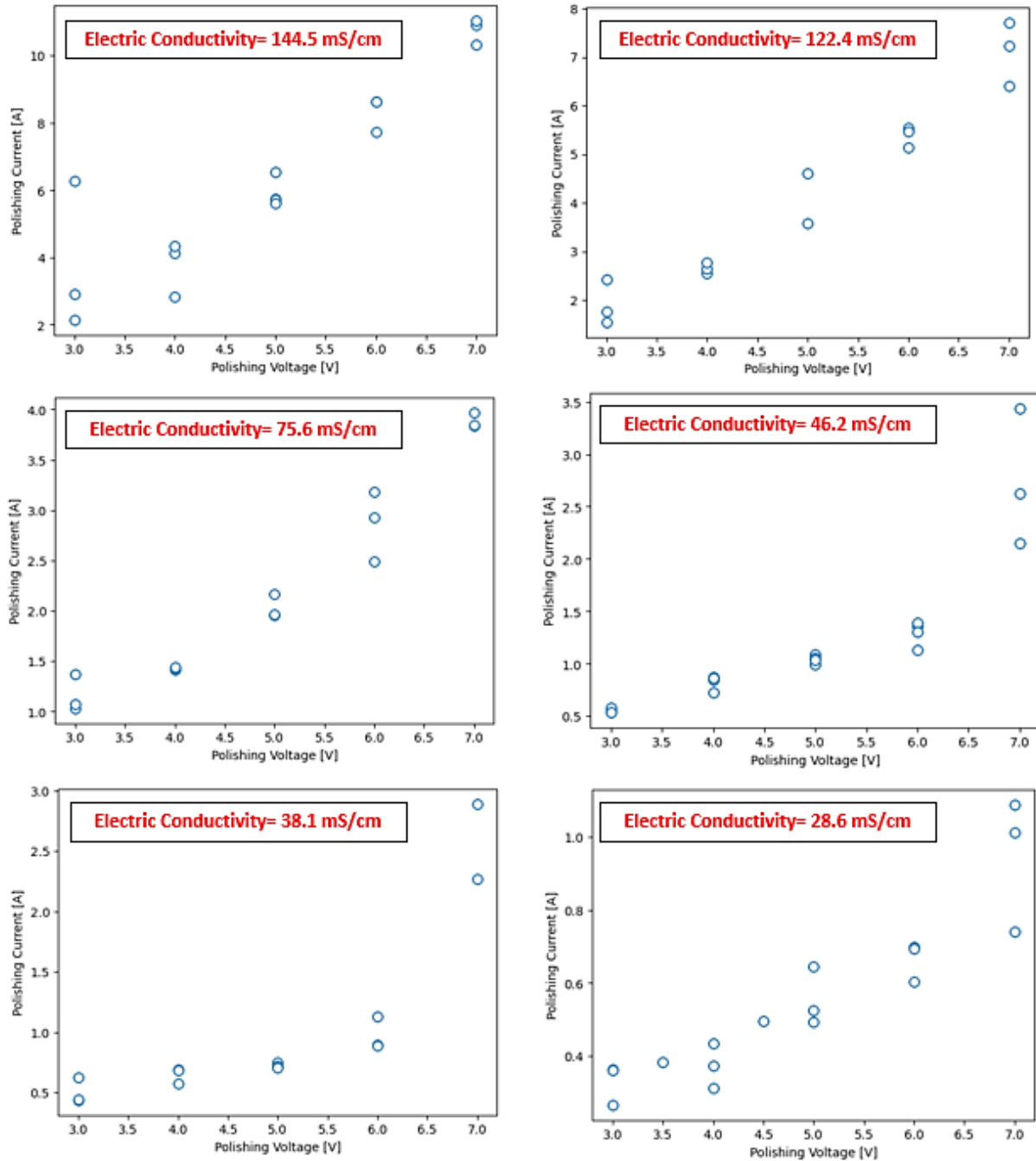


Figure 4.4. Variation of the I-V behavior of the workpiece with electric conductivity of the bath. The polishing current shown in the plots is the average measured current over different durations of the polishing experiments (300 s, 600 s, and 900 s).

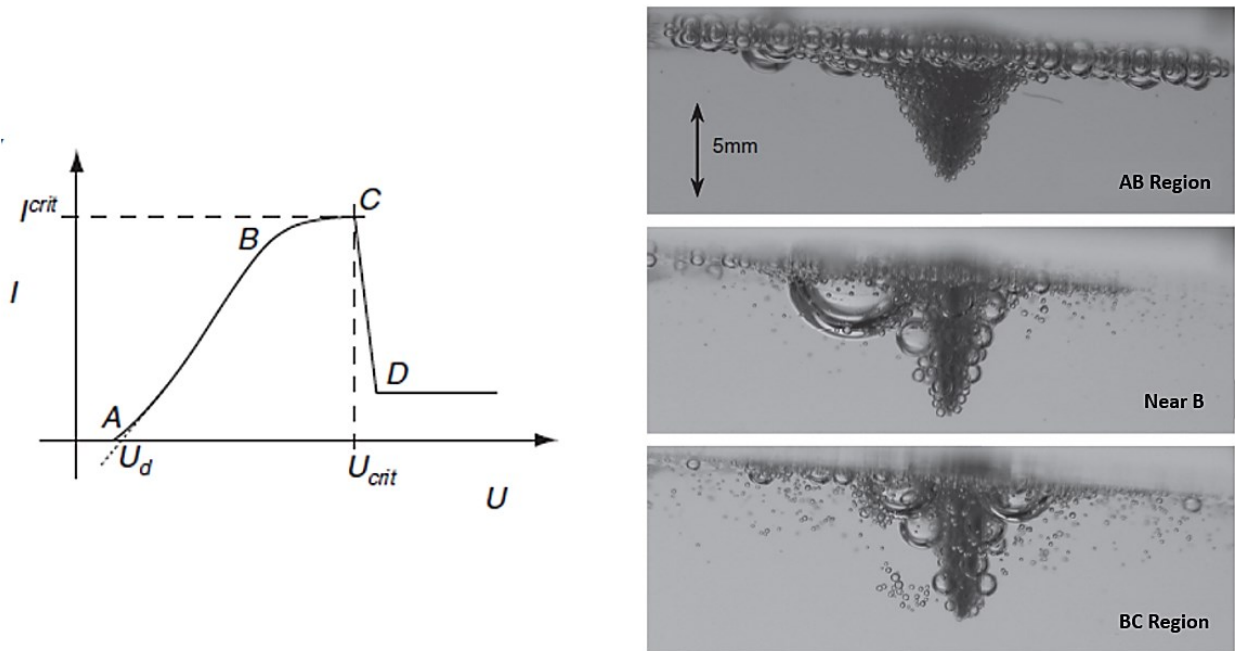


Figure 4.5. (left) Current-voltage plot for water electrolysis process on a gas-evolving electrode, (right) bubble diffusion layers around a cylindrical electrode at various voltages <sup>103</sup>.

As can be seen in Figure 4.5, in the initial region of the I-V curve (AB) the current increases nearly linearly with the polishing voltage. At this stage, a compact bubble layer is forming over the electrode surface from the evolving bubbles. The current continues to increase in the next region (BC) until it reaches a limiting value at which the bubbles start to coalesce. From this point, the current-voltage relationship is no longer controlled by equation 4.1, and the electrolysis process is limited by the ability of the bubbles to detach from the electrode. According to Wuthrich et al. <sup>103</sup>, depending on their size, the electrochemically formed bubbles may or may not be able to leave the electrode surface and significantly influence the interelectrode resistance. Figure 4.6 illustrates the percolation model of the nucleation sites that can be used to describe the bubble size distribution of the formed gas bubbles on the electrode.

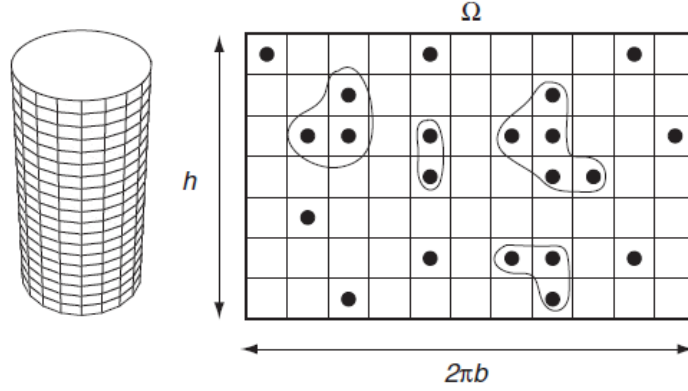


Figure 4.6. Percolation model of the bubble nucleation sites on the lateral surface of an electrode <sup>103</sup>.

In this model, the lateral surface  $\Omega$  of an electrode is subdivided into a lattice of size  $L$ , where each lattice site represents a nucleation site on the electrode surface. The bubbles on a nucleation site grow through coalescence with bubbles from the neighboring occupied sites and form a new larger bubble. If we assume that only bubbles of size smaller than  $S^{\max}$  (a function of the electrode geometry, surface roughness, and wettability) can leave the electrode surface, then the evolution of the surface fraction covered by bubbles ( $\theta$ ) is as follows <sup>103</sup>:

$$\frac{d\theta}{dt} = \frac{\beta j_{local}}{\xi d_n} (1 - \theta) - \frac{1}{\Delta t_b} \sum_{s=0}^{s^{max}} s n_s(\theta) \quad (4.3)$$

where  $\beta$  is the coefficient of faradic gas generation,  $j_{local}$  is the local current density,  $\xi d_n$  is the bubble height written as the product of  $d_n$  (the mean distance between two nucleation sites) and  $\xi$  (the parameter describing the degree of bubble flatness),  $\Delta t_b$  is the bubble detachment time, and  $\sum_{s=0}^{s^{max}} s n_s(\theta)$  is the fraction of nucleation sites the surface covered on by the growing gas bubbles that are able to leave the electrode.

The characteristic I-V curve of the gas-evolving electrode presented in Figure 4.5 can be obtained by solving the differential equation 4.3. In this plot, the limiting current region (BC) ends at a critical current  $I^{crit}$  and voltage  $U^{crit}$  after which the current decreases rapidly with a further increase of the voltage. In the last part of the curve, the current is very small because a gas film is formed on the electrode, completely isolating it from the electrolyte.

In light of the described I-V behaviour on gas-evolving electrodes, the results observed in different polishing bath states may also be interpreted. It has been observed that during the electropolishing process, the electrolyte's resistivity controls the current-voltage relationship in the first region of the curve (AB). Starting from point B, however, other factors must be taken into account. It is known that during the electropolishing process, hydrogen evolution occurs on the cathode surface while oxygen is generated on the metal surface. After gas bubbles are formed, they start to grow

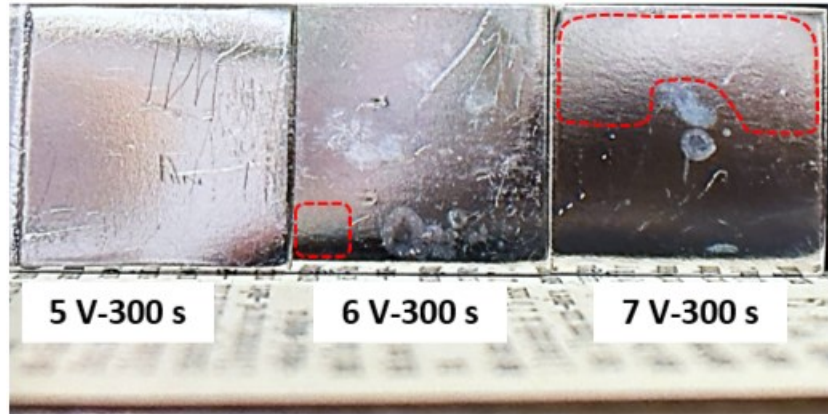
and coalesce with nearby bubbles until they finally detach from the surface and diffuse through the electrolyte. Increasing the polishing voltage in this region has been reported to cause substantial gas evolution to a point where further progress of the electropolishing process is limited by the size, shape, and detachment time of the bubbles generated on the surface. According to equation 4.3, the rate of bubbles' growth and subsequent detachment depend on several electrolyte properties, including viscosity and wettability<sup>103</sup>. Given that a highly viscous electrolyte would resist the detachment and diffusion of the generated bubbles, the application of higher polishing voltages in heavily-used baths can only partly compensate for the increased ohmic drop. At this point, further fine-tuning of the process parameters or the operator's know-how proves insignificant, and the polishing bath must be refreshed or replaced.

Understanding the evolution process of gas bubbles on the polished workpiece can also provide valuable insights into the origins of common defects frequently encountered in industrial electropolishing processes. Figure 4.7 indicates the surface of samples treated with polishing voltages of 5, 6, and 7 V for the same duration (300 s) in solutions 1, 2, and 3. The surfaces of the samples polished in solution 1 exhibit a common defect encountered in the electropolishing industry called the orange peel effect (highlighted on the figure by red dashed lines). The term "orange peel" is used because of the micro pitting pattern on the surface that resembles the dimpled texture of an orange peel<sup>104-106</sup>. In the case of samples electropolished in solutions 2 and 3, it can be noted that with the application of higher voltages, the brightness of the surface is only marginally improved, and flow marks in the form of white stripes appear on the surface (highlighted on the figure by green dashed lines). Also known as "gassing streaks", these flow marks are another common defect observed in electropolishing<sup>107-109</sup>.

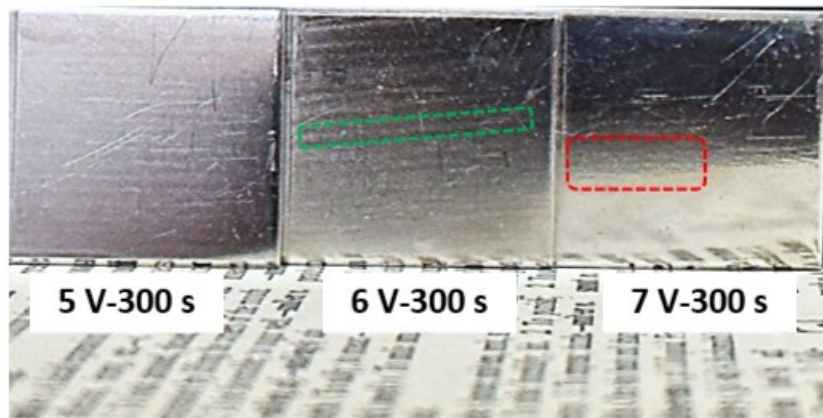
In the electropolishing industry, these defects are generally attributed to intensive bubble generation near the metal surface due to excessive applied polishing potential/current, high solution viscosity, and lack of proper agitation to remove the evolved oxygen gas away from the workpiece<sup>29,104,110,111</sup>. However, a review of the literature indicates that the reason for the appearance of such defects and potential corrective actions is still subject to speculation. In particular, there are no objective criteria currently available that would enable predicting the emergence of such defects in a given bath for a specific set of polishing parameters.

Such surface defects significantly affect the visual quality and functionality of electropolished parts and render them unacceptable or less appealing to customers. Considering the lack of adequate information on the origin of such defects, a closer examination of their evolution process is necessary. Figure 4.8 indicates the obtained surface finishes along with their corresponding I-V graphs for samples treated in solutions 1, 2, and 3 at different polishing potentials for the same duration (300 s).

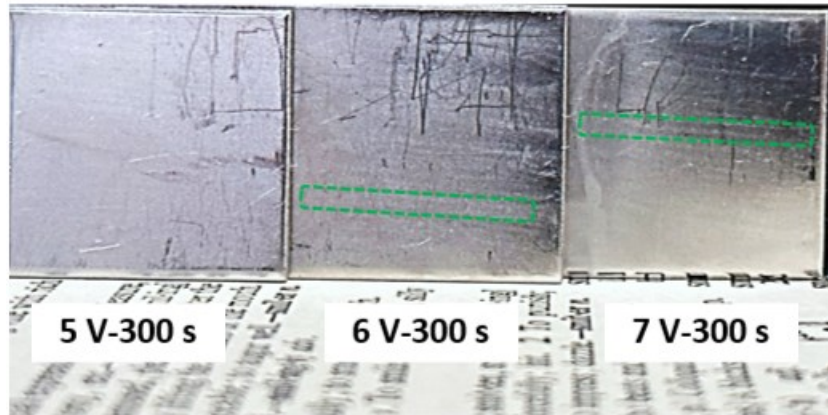




**Solution 1**



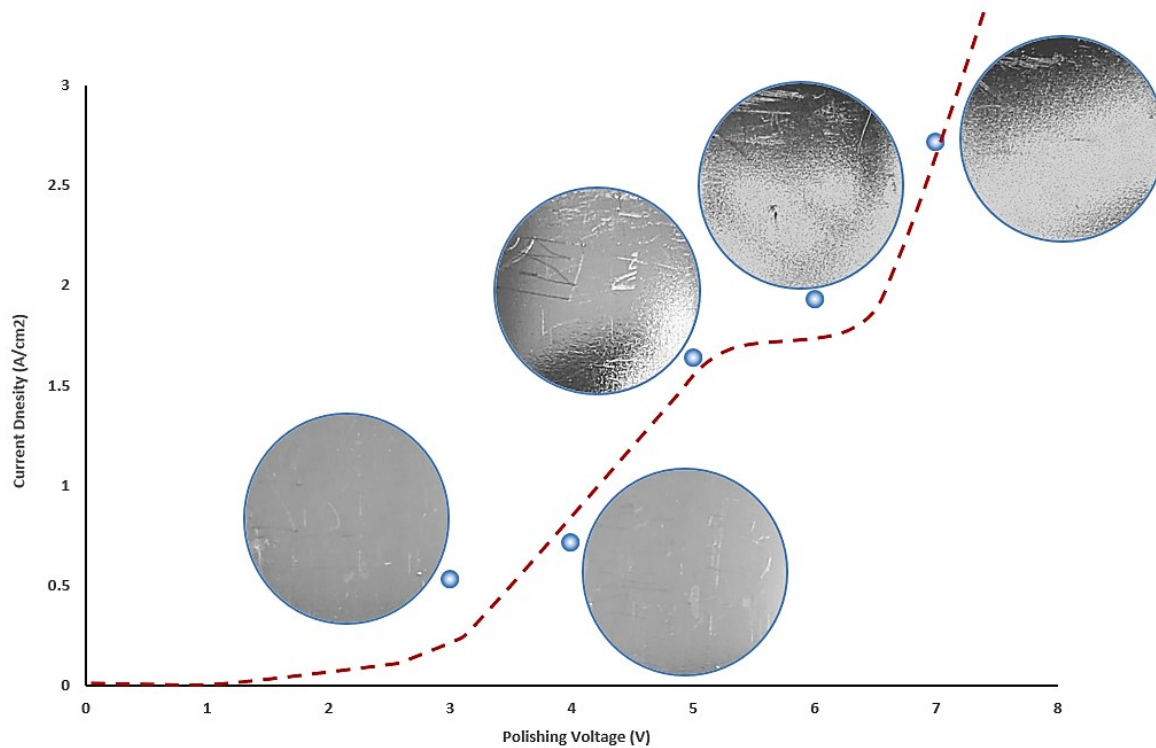
**Solution 2**



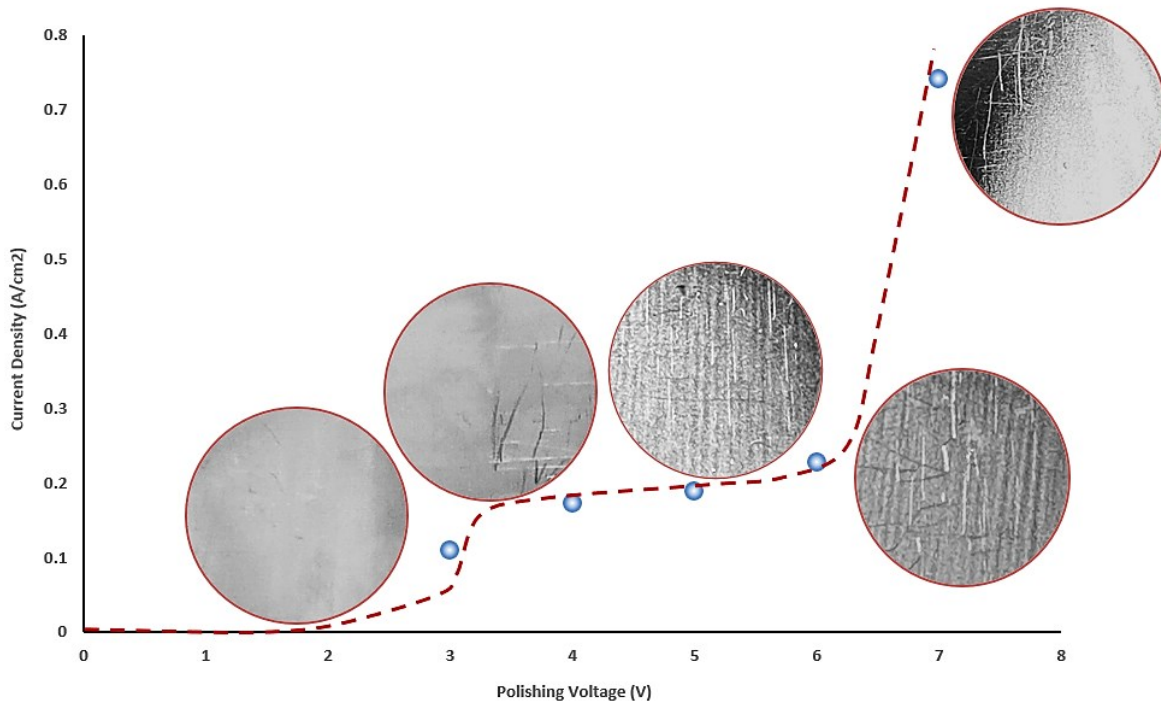
**Solution 3**

Figure 4.7. The surface finishes obtained after electropolishing under increasing potentials (5, 6, and 7 V) for 300 s in solutions 1, 2, and 3. The orange peel effect and the gassing streaks are shown by red and green dashed lines, respectively. Note: the mechanical scratches (defects not highlighted with dashed lines) are due to the manipulation of the samples.

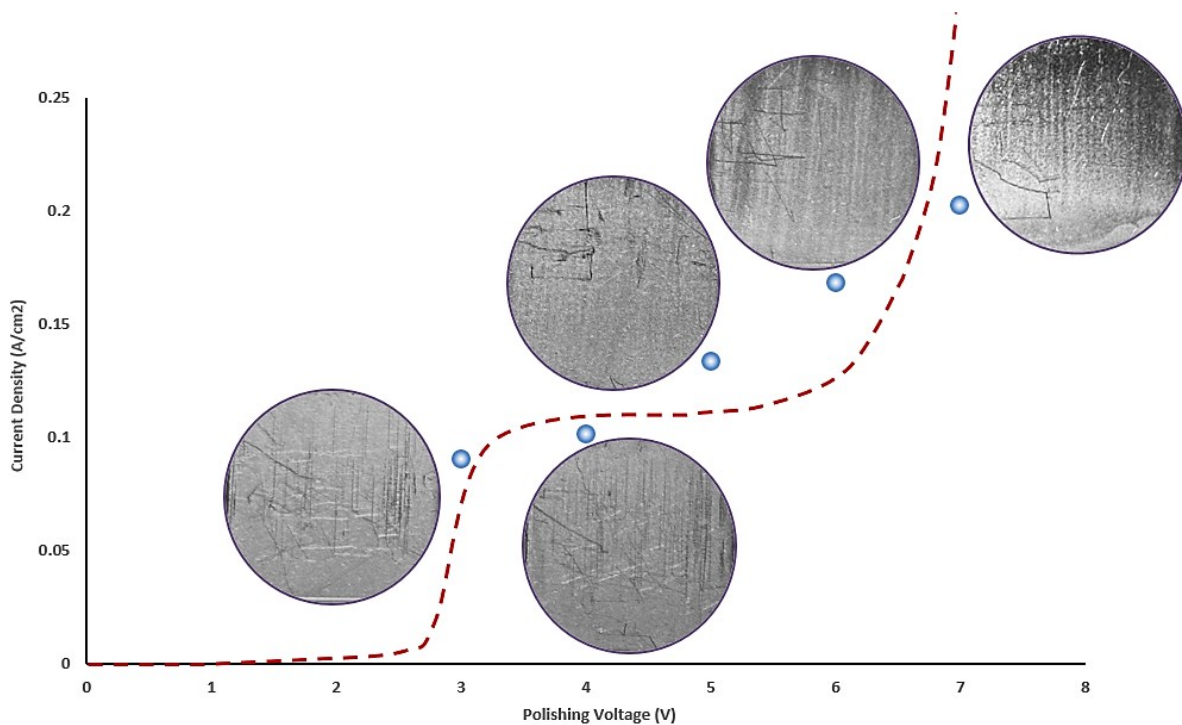




(a)



(b)



(c)

Figure 4.8. Surface finishes obtained at different regions of the current-voltage plot for samples electropolished in (a) solution 1, (b) solution 2, and (c) solution 3 (note: the mechanical scratches on the surface are due to manipulation and handling of the samples.)

The gradual emergences of the previously mentioned defects with increasing the polishing voltage can be noted in Figure 4.8. As can be seen, the orange peel effect (for samples treated in solution 1 and 2) and white stripes (for samples treated in solutions 2 and 3) started to appear when the polishing potential reached approximately 5 V, aligning with the BC region on the current-voltage plot for gas-evolving electrodes as depicted in Figure 4.5. It may be concluded that at this potential bubble generation reaches a level of intensity to significantly impact the surface of the stainless steel workpiece. It can also be noted that in a close-to-fresh solution (solution 1), a bright surface can be achieved at a polishing voltage of 5 V, whereas in more used solutions, higher potentials are required to obtain a slightly bright finish. This can be justified by the higher viscosity of the heavily-used baths that inhibits the diffusion of the gas bubbles towards the bulk of the solution, which may, in turn, lead to pronounced bubble formation, significantly affecting the workpiece surface<sup>111</sup>. In addition, the increased specific gravity of heavily-exploited polishing baths can lead to local overheating and, as a result, to the intensification of emerging defects<sup>112,113</sup>.

The current-voltage graphs depicted in Figure 4.8 can serve as a valuable tool for predicting the likelihood and possible coordinates of surface defects emergence at different polishing bath conditions. For instance, for a given bath condition, test samples can undergo electropolishing at

various polishing voltages for a fixed duration, and the resulting polishing currents can be recorded to generate I-V plots that depict their current-voltage behavior. By analyzing these plots, it becomes feasible to pinpoint the voltages at which the previously mentioned defects are most likely to occur on the workpiece (voltages corresponding to the BC region of the I-V plot shown in Figure 4.5). This way the operator will be able to maintain the polishing consistency of the surfaces through modification of process parameters or implementing corrective measures, such as agitating the electrolyte or replenishing the polishing bath.

#### **b) Variation of the electrolyte base composition**

Another factor contributing to the different polishing behavior of the investigated solutions can be the variation in their compositions due to different usage histories. The results of titration experiments provided in Table 4-1 indicates that the volume percentages of sulfuric acid and phosphoric acid are different among the investigated solutions. These variations can be attributed to different factors, including the consumption of electrolyte components in chemical reactions, the accumulation of dissolved metals and reaction by-products, exposure to environmental contamination, splashing, and evaporation.

Several works have explored the role of different components of the polishing solution used in this study on the final surface quality of electropolished samples. For instance, during the electropolishing of Fe-24Cr parts with a rotating disk electrode setup in a concentrated sulfuric acid solution (in the absence of phosphoric acid), Ponto et al.<sup>114</sup> observed a small limiting current independent of the rotation rate with no polishing effect. It was concluded that sulfuric acid forms a rather stable anodic film on the surface of the workpiece, inhibiting the electropolishing process. Datta et al.<sup>115</sup> also reported that metal dissolution is inhibited in concentrated sulfuric acid baths due to secondary passivation at high anode potentials. It was suggested that concentrated sulfuric acid is not favorable for stainless steel from an electropolishing point of view. On the other hand, Nazneen et al.<sup>116</sup> observed that in concentrated phosphoric acid solution (in the absence of sulfuric acid), the passive oxide film was not formed on the surface, leading to high anodic currents and damaged surfaces, whereas the addition of sulfuric acid to the electrolyte helped improve the surface smoothness in some parts of the sample. Similar observations are reported by Abouzeid et al.<sup>117</sup> for electropolishing aluminum parts in a phosphoric acid-sulfuric acid mixture where an extreme increase of acids ratio in any direction resulted in the disappearance of the limiting current plateau from the polarization curve. These observations suggest that the presence of both acids is necessary for achieving a desirable surface finish.

Nonetheless, mixed, and sometimes even contradictory, results have been reported for the effect of moderate changes in the electrolyte composition on the surface finish of electropolished parts. For example, Ponto et al.<sup>114</sup> reported that at a constant water content in the polishing bath, the polarization behavior of Fe-24Cr parts in phosphoric acid-sulfuric acid solution is relatively insensitive to moderate sulfuric/phosphoric acid ratio variations. Chen et al.<sup>118</sup> and Huang et al.<sup>119</sup> on the other hand, observed an increase in the limiting current density with increasing the phosphoric acid content of the electrolyte and designated  $\text{H}_2\text{PO}_4^-$ ,  $\text{PO}_4^{3-}$  or their complexes as the diffusion-limiting species. In another study, Hwang et al.<sup>120</sup> observed that increasing the sulfuric

acid concentration resulted in damaging the surface of stainless steel parts. The authors proposed that increasing the sulfuric acid content of the electrolyte reduces the thickness of the diffusion layer formed on the surface, which promotes metal dissolution and eventually results in an aggressive attack on the surface.

In addition to the acids mixing ratio, the acid-water ratio of the polishing bath also plays an important role in the electropolishing process. In low-water-content baths, the acid concentration is too high, which can result in increased viscosity of the solution, excessive material removal, and eventually a rough surface finish. Conversely, in baths with high water concentration, the acid content becomes too small, leading to inadequate electrolyte viscosity, insufficient material removal rate, and uneven or incomplete polishing. Magaino et al.<sup>121</sup> reported that the brightness of electropolished stainless steel samples decreased with increasing water concentration and concluded that polishing is not attained in electrolytes with higher water contents. This indicates that a certain water concentration is required to achieve optimal polishing results. Not only the presence of water can help regulate the viscosity of the electrolyte, but it can also affect its conductivity by improving ion mobility and hydration.

Analysis of the existing literature on the effect of electrolyte composition on the outcome of the electropolishing process also shows that the studies do not provide a well-defined range of electrolyte compositions that ensure consistently acceptable polishing results. This might be due to the fact that a universally good or bad electrolyte composition cannot be defined as the electropolishing results also rely heavily on the employed process parameters. However, despite the occasionally conflicting theories proposed for the effect of variations in the electrolyte composition on electropolishing results, it can be confidently stated that a balance should exist between different components of the bath in order to achieve a favorable polishing effect. While it is evident that changes in the electrolyte composition can have a substantial impact on the outcome of the electropolishing process, it's essential to recognize that it's not the sole determining factor in achieving the desired surface finish. Therefore, we hypothesize that restoring the original composition of a heavily-used polishing bath by introducing suitable electrolyte components would not be enough for improving the surface of the parts and ensuring consistent quality.

This important statement was proved through a set of electropolishing experiments in three polishing baths (A, B, and C) with identical constituents (sulfuric acid, phosphoric acid, and DI water) but different compositions. Table 4-4 presents the surface characterization and weight loss results for three samples electropolished in baths A, B, and C using the same polishing parameters (5 V, 300 s) as the samples treated with solutions 1,2, and 3. Comparing the results of Table 4-1 and Table 4-4 indicates that achieving a bright and smooth electropolished surface is not just a question of the mixing ratio of the acids. Other factors, such as the electric conductivity and viscosity of the bath, could be much more effective in determining the final surface finish of the electropolished samples. It can be noted that the viscosity and conductivity of the fresh solutions are generally in the same range, and they are all potentially capable of yielding smooth and bright surfaces. This is evident in the similarity between the results obtained in solution 1 (close-to-fresh) and solutions A, B, and C. The electric conductivity and viscosity of solutions 2 and 3, however, are far from those of the fresh solution, mostly due to the accumulation of metal dissolution

products that lower the polishing performance. Therefore, it can be argued that the sole action of resetting the electrolyte composition should not be expected to yield considerable improvement in the electropolishing results.

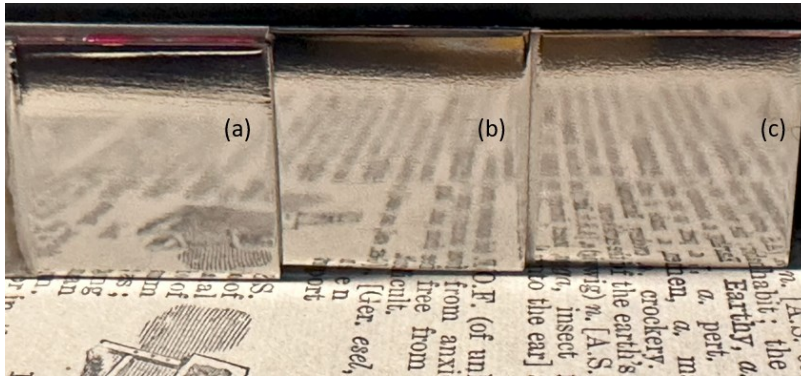


Figure 4.9. Samples electropolished under 5 V, 300 s in (a) solution A, (b) solution B, and (c) solution C.

Table 4-4. Electropolishing results for samples treated in polishing baths with different compositions.

Electrolyte	Composition %(v/v)		Surface Roughness ( $\mu\text{m}$ )		Surface Brightness (GU)		Weight Loss (g)
			before	after	before	after	
A	H <sub>2</sub> SO <sub>4</sub> : 25 H <sub>3</sub> PO <sub>4</sub> : 50	<b>Ra</b>	0.11	0.05	H20: 135	H20: 829	0.1043
		<b>Rq</b>	0.14	0.06	H60: 135	H60: 586	
		<b>Rz</b>	1.02	0.3			
B	H <sub>2</sub> SO <sub>4</sub> : 30 H <sub>3</sub> PO <sub>4</sub> : 50	<b>Ra</b>	0.11	0.04	H20: 164	H20: 1029	0.1823
		<b>Rq</b>	0.14	0.05	H60: 178	H60: 598	
		<b>Rz</b>	1.01	0.24			
C	H <sub>2</sub> SO <sub>4</sub> : 40 H <sub>3</sub> PO <sub>4</sub> : 50	<b>Ra</b>	0.07	0.02	H20: 138	H20: 1119	0.1894
		<b>Rq</b>	0.1	0.02	H60: 142	H60: 596	
		<b>Rz</b>	0.6	0.1			

### c) Increased viscosity of the solution

The viscosity of the solutions could also contribute to their different polishing behavior. Considering that solutions 2 and 3 are more extensively used than the close-to-fresh solution 1, their significantly higher viscosity seems reasonable. The viscosity of a heavily used polishing bath increases due to a variety of factors, including the accumulation of dissolved metals, solution by-products, precipitates, and environmental contamination, as well as the evaporation of volatile components, particularly water, due to high temperatures and exposure to air.

For instance, Table 4-1 indicates that the specific gravity of solutions 2 and 3 is higher than that of solution 1, which can be due to the increased concentration of dissolved metals upon usage. According to the ICP-MS results presented in Table 4-2, the concentration of heavy metals such as Fe, Cr, Ni, and Mn in solutions 2 and 3 are much more than those of the close-to-fresh solution 1. Another explanation for increased bath viscosity upon usage comes from the titration results in Table 4-1, showing a significant loss of water content for solution 3, compared to solutions 1 and 2. This could be attributed to the considerable heating of solution 3 during the electropolishing process as a result of its lower electric conductivity. Decreased water content of a polishing bath can increase the concentration of other components, such as acids and dissolved particles that can cause greater intermolecular interactions and hinder fluid flow, thereby increasing the bath viscosity.

As previously discussed in Chapter 2, although viscous acidic solutions are commonly employed for electropolishing treatment, excessive solution viscosity can damage the final surface finish of the parts in multiple ways<sup>122</sup>. A more viscous solution opposes the free flow of the charge carriers, thereby increasing the electrical resistance and ohmic drop in the solution. As a result, the available effective current density is reduced, leading to a lower material removal rate and insufficient polishing action<sup>123,124</sup>. This effect was most evident in the SEM images of the sample polished in solution 3 (exhibiting the highest viscosity) that suffered from inadequate polishing. The lower polishing current and material removal rate for low-conductivity (high-viscosity) solutions were also evident in the current-voltage curves presented in Figure 4.4.

Another consequence of the increased viscosity of the solution is the slower movement of bubbles generated during the polishing process. It has been established that excessive bubble generation can result in the orange peel effect or the appearance of strikes on the surface of the workpiece<sup>29,110,111</sup>. In fact, one of the justifications for the pulse-electropolishing process is providing sufficient off-time for refreshing the electrolyte in the inter-electrode gap and removing generated bubbles and polishing by-products away from the workpiece surface<sup>125</sup>.

Finally, it was also proposed that increased viscosity of the polishing bath can decrease the diffusion coefficient of mass-transport limiting species (equation 2.1), thereby slowing the electropolishing process and lowering the polishing current<sup>126</sup>.

#### **d) Increased level of contamination in the polishing bath**

The buildup of dissolved metals, precipitates, and other reaction by-products can also degrade the polishing bath quality and affect the surface finish of the parts in different ways. Their presence in the electrolyte between the inter-electrode gap can interfere with electropolishing reactions and result in non-uniform material removal. In addition, they can hinder the formation of a smooth and uniform oxide layer on the workpiece during electropolishing, resulting in an uneven or rough surface finish. It is also possible that dissolved metals re-deposit onto the workpiece surface, leading to the formation of micro-defects, such as nodules or rough patches. Different contaminants coming from the solution can also stick to the metal surface and result in a dull or tarnished finish by absorbing light. A study by Aguilar-Sierra et al.<sup>127</sup> indicated that the brightness of electropolished aluminum parts was affected by the presence of impurities on their surface.

In addition to its direct influence on the surface appearance of the parts, solution contamination can also affect the electropolishing process indirectly. Lower saturation solubility of dissolved metals in highly contaminated electrolytes decreases the polishing current density by hindering further metal dissolution. Longer polishing times are, therefore, required, which, in turn, can exacerbate the bath contamination issue. In addition, higher concentrations of dissolved metals and polishing product precipitates increase the electrolyte density, viscosity, and electric resistance, which can have different consequences, including inadequate polishing, solution overheating, the appearance of pitting, and streak marks on the surface as discussed previously in this chapter.

#### **4.5. Concluding remarks**

The results of bath and sample characterizations in this chapter indicated that the samples electropolished in heavily-used baths suffered from insufficient or inadequate polishing action. Several sources were discussed for this behavior:

- *Increased IR drop:* As a polishing bath undergoes prolonged use, the buildup of dissolution products and environmental contaminants diminishes the bath's electrical conductivity. Consequently, a higher voltage drop occurs across the cell, reducing the available potential for efficient electropolishing on the workpiece.
- *Variation of electrolyte base composition:* It has been reported that extreme deviations from the base composition of the electrolyte (for example the absence or significant depletion of one of the acids) can significantly impact the polishing results. Minor changes in the electrolyte composition (volume percent of the acids), however, cannot account alone for the decline in surface quality observed in extensively-used electrolytes.
- *Increased viscosity:* The viscosity of extensively-used electrolytes increases as a result of impurity accumulation and the evaporation of volatile elements. Higher bath viscosity can decrease the polishing rate by impeding the movement of charge carriers, consequently reducing electrical conductivity, and obstructing the diffusion of species

that limit mass transport. Moreover, the increased viscosity hinders the dispersion of gas bubbles generated during the process, exacerbating the occurrence of defects on the workpiece surface.

- *Increased electrolyte contamination:* In addition to the possibility of a non-uniform or defected surface caused by the impurities on the workpiece surface interfering with the polishing process, the accumulation of these impurities in the polishing bath has been demonstrated to elevate the electrolyte's specific gravity, viscosity, and electrical resistance. These changes can collectively lead to a reduction in polishing current and an insufficient polishing effect.

The three questions mentioned in 4.1 can be addressed with several key observations presented in this chapter:

- It was demonstrated that the variations in the properties and performance of the polishing bath depend on its usage and replenishment history. Consequently, when considering factors that influence the quality and consistency of electropolishing outcomes, the condition of the bath before the electropolishing process holds greater significance than either the number of treated parts or the total ampere-hours of polishing treatment carried out in the bath.
- It was also shown that physicochemical properties such as the specific gravity, electric conductivity, and viscosity of the polishing bath serve as robust indicators of its condition and significantly affect its performance. Notably, these properties not only offer valuable insight into the varying performance of the bath at different states but can also be easily and rapidly measured on-line within industrial settings, without the need for complex equipment or highly trained personnel.
- In addressing the question of whether consistent electropolishing results can be achieved through adjustments to polishing process parameters guided by the relevant physicochemical properties of the bath, our experimental findings revealed that such bath properties are not the only factors that contribute to the outcome of the electropolishing process, and as such, seemingly straightforward actions such as modifying the applied potential or re-adjusting the electrolyte composition cannot guarantee consistent polishing outcomes under the same set of polishing parameters. For instance, it was observed that raising the applied polishing potential to compensate for the increased IR drop in extensively-used electrolytes resulted in pronounced bubble formation and the emergence of pit marks and white streaks on the surface. It was also shown that merely altering the bath composition may not be sufficient for restoring its performance. It was therefore concluded that at a given bath condition, knowledge of the relevant physicochemical properties of the bath must be accompanied by application of correct process parameters to achieve consistent electropolishing outcomes.
- The current-voltage plots obtained from electropolishing test samples at various voltages for a fixed duration have shown significant promise as a predictive tool for identifying the voltage threshold at which surface defects, such as the orange peel effect and gassing



streaks, may occur at a given bath state. These voltages align with a specific section in the I-V plot of gas-evolving electrodes, where bubble generation reaches an intensity level significant enough to affect the surface of the workpiece. When selecting the necessary process parameters to achieve a desired surface finish, this tool can be invaluable in preventing the occurrence of surface defects.

The substantial impact of process parameters on the surface quality of electropolished parts highlights the necessity for an intelligent approach to finding the correct process parameters. Using previous production experience, such an approach determines suitable polishing parameters tailored to the unique characteristics of the part, polishing bath, and intended application.

## 5. Open Dataset for Stainless Steel Electropolishing

### 5.1 Introduction

The result of Chapter 4 highlighted the profound impact of usage history on the state of a polishing bath, which, in turn, significantly influences the outcomes of the electropolishing process. One of the most important changes observed in a bath upon extensive use is the decline in the electric conductivity, leading to a substantial IR drop across the polishing cell and a considerable reduction in the available polishing potential. Moreover, Chapter 4 revealed that due to the multitude of factors influencing the final surface finish of parts, simple measures like correcting the ohmic drop or readjusting the polishing bath composition do not necessarily result in repeatable polishing outcomes. This indicates the necessity for an intelligent approach to maintain the consistency of the electropolishing results despite the dynamic nature of the polishing bath. This approach would have the capability to determine the process parameters required to achieve a desired surface finish based on the part and bath parameters as well as the intended application.

As previously mentioned, one of the objectives of this study is to create a substantial dataset comprising electropolishing outcomes achieved under various process parameters and bath conditions. This dataset would serve as the foundation for developing a predictive tool that can determine the necessary process parameters to achieve a specific surface finish under given bath conditions. Throughout the experimental phase of this study, a multitude of polishing experiments were conducted, yielding a significant volume of data points of the polishing process parameter and results.

In this chapter, the constructed dataset is examined from a data analytics perspective. Initially, the details of the dataset construction process, including measurement errors for variables such as electrical conductivity, bath temperature, and surface roughness and brightness of the samples, are discussed. The dataset is then explored, with a focus on investigating the variation trends, statistical distributions, and inter-correlations among different variables, along with justifications for these observations. Subsequently, various aspects of the model development process, including feature selection and hyperparameter tuning for the investigated machine learning algorithms, are covered. The performance of these algorithms in predicting different target variables is then compared, and the most accurate model for representing the dataset is selected as the basis for the development of our prediction tool.

## 5.2 Determining the correct process parameters in an ever-changing polishing bath

Given the significant effect of the electrolyte condition on the surface finish of electropolished parts, various control methods are used in the industry to maintain or restore the polishing bath quality. However, even in a well-maintained polishing bath, preserving the consistency of the polishing results is challenging. In a mass production paradigm, where the polishing process is always carried out for the same type of alloy coming from the same supplier, the type and amount of contaminants entering the bath can be known and controlled. This is also true if the electropolishing treatment is conducted in the same facility as one of the steps of a well-known and controlled manufacturing process. However, most electropolishing facilities only perform the polishing treatment and accept the parts from different customers with significantly different manufacturing histories.

Depending on the production process of the parts, different kinds of oil, dirt, and contaminants are introduced into the solution, considerably affecting the consistency of the results. The situation becomes even more challenging with the new mass personalization trend. Even with an optimized process, inconsistent results would be obtained if parts of slightly different alloys (such as different grades of stainless steel) or parts with different shapes (for instance, having difficult-to-reach corners) were to be electropolished. Determination of the required process parameters in such challenging conditions is not only reliant on the experience and know-how of the operator but also requires time and resource-consuming trial-and-error experiments. As already stated, the overarching goal of this study is to develop a data-driven approach for determining the optimum process parameters for achieving a desired surface finish at a given bath state.

One important aspect of this goal is the modification of electropolishing process parameters to obtain different surface qualities. Our previous study on titanium (grade 5) electropolishing in 0.9 M NaCl- ethylene glycol solution indicated that it is possible to achieve a range of electropolished surface finishes by tuning the polishing process parameters<sup>128</sup>. Figure 5.1 displays the titanium samples treated with different combinations of polishing potential and duration at the solution temperature of 20 °C. As can be noticed in the obtained surface finishes, 10 V was the lower limit of the applicable potentials that yielded an insufficient polishing effect for the effective removal of the surface oxide layer. It was also noted that applying a potential beyond 25 V would lead to intensive bubble generation and sudden stopping of the test. In addition, electropolishing at the same solution temperature and with the same applied polishing potential of 20 V for different durations (10, 20, 30, and 40 minutes) yielded a range of diverse surfaces.

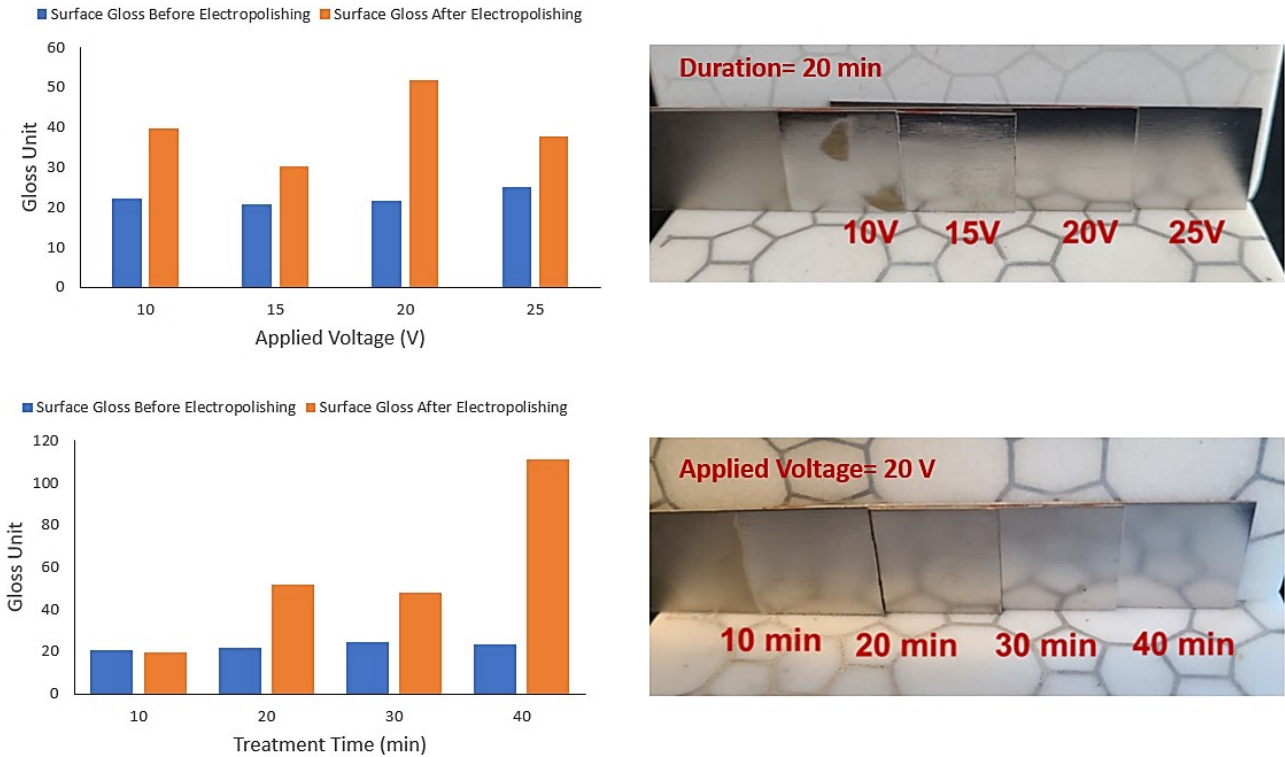


Figure 5.1. Up: Surface finishes obtained for titanium samples for (top) 20 minutes polishing duration and different polishing voltages (10, 15, 20, and 25V) and (bottom) 20 V polishing potential and different polishing durations (10, 20, 30, and 40 min) <sup>128</sup>.

The ability to achieve a wide range of surface qualities could be highly appealing for a variety of decorative purposes, including architectural finishes, home appliances, automobile parts, consumer electronics, and luxury goods. Since decorative applications place a high value on the visual aesthetics of the products, acquiring different surface finishes gives them greater design flexibility and the ability to create visually striking products that stand out in the market. The transition of electropolishing treatments towards mass personalization manufacturing can potentially accommodate different industries' needs for a broader range of electropolished surface finishes. However, for most electropolishing facilities, determining the proper polishing conditions for achieving a target surface finish is neither simple nor affordable. Depending on the operator's level of expertise, the process might require rounds of trial-and-error experiments (potentially inconclusive or imprecise), considerable waste of materials and energy, and significant delays in the production schedule.

Given the considerable costs of stopping the main production line, one possible solution would be establishing a small pilot plant on the side to find the required process parameters through trial-and-error experiments. However, not only this pilot bath would have a different history from the main polishing bath, but its properties may also undergo changes during the experiments due to its smaller volume in comparison to the main bath. Therefore, the only way to find the "correct" process parameters is to stop the production by conducting trial and error in the main bath, which

is very costly. The profitable incorporation of a mass personalization paradigm in an industrial electropolishing facility calls for rapid process-tuning approaches to justify the production of small batches financially. This is another aspect of this study's goal, developing an approach to promptly determine the required process parameters for obtaining a desired surface quality.

Driven by the findings of our prior work on titanium samples, in this project, a variety of surface finishes were obtained for stainless steel 316 parts by modifying electropolishing voltage and time. Figure 5.2 presents the various surface finishes obtained on stainless steel samples with their corresponding surface gloss measured before and after the electropolishing process and different polishing parameters. The electrolyte used for these experiments was solution 1 from Chapter 4 (close-to-fresh solution).

The results of these experiments indicate that obtaining a better surface finish (in this case, a higher surface gloss) by modifying the process parameters is not as straightforward as one might expect. There appears to be a trade-off between the electropolishing process parameters and final surface results. For instance, it can be noted that the use of a higher polishing voltage or longer polishing duration does not necessarily yield a better surface finish, as illustrated on Figure 5.2, where sample 6, treated with 3 V for 600 seconds, shows a higher surface gloss than samples 7 and 8, which were treated for the same duration with 4 and 5 V, respectively. Another example is sample 13, polished with 5 V for 900 seconds, which has a higher brightness compared to samples 11, 14, and 16, treated for the same duration with 3, 6, and 7 V, respectively. Sample 6 itself (3 V, 600 s) is brighter than sample 13 (5 V, 900 s) even though, as previously stated, one might expect that employing higher voltages or longer polishing times would result in higher surface gloss.

Such observations further indicate that a right balance must be reached between achieving the desired surface finish and maintaining other essential factors such as material removal rate and cost efficiency. These results also indicate the importance of employing the correct process parameters for obtaining the target results and accentuate the operator's critical role in estimating the optimum process conditions.

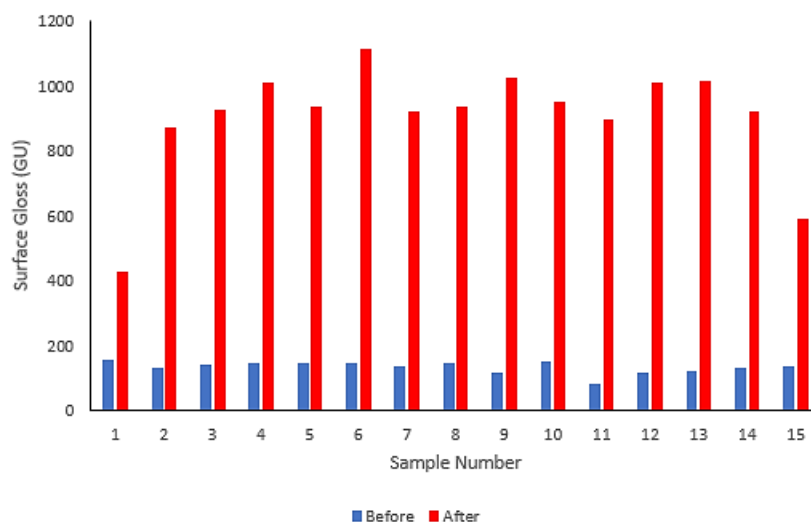
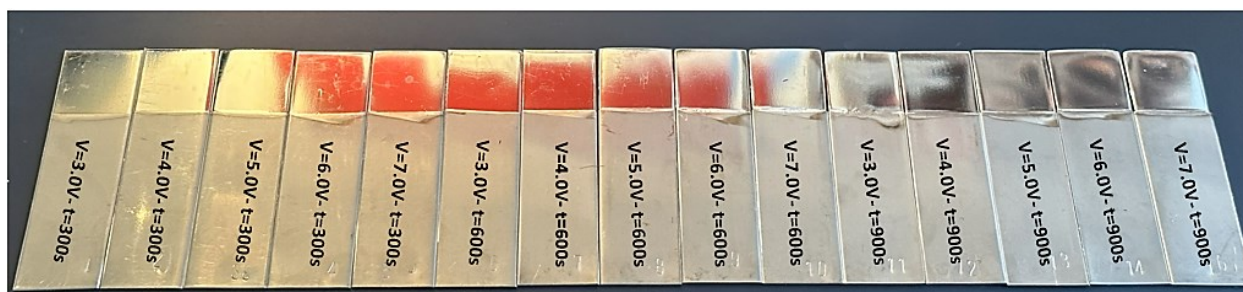


Figure 5.2. (top): Range of surface finishes obtained for stainless steel 316 samples by changing the electro polishing voltage and duration in solution 1, (bottom): variation of the corresponding surface gloss (the samples are organized in order of applied polishing voltage and polishing duration).

However, determining the correct process parameters with a constantly varying bath is an exceedingly difficult task, even for a skillful operator with several years of experience, because it requires repeated trial-and-error experiments. Modification of process parameters at different bath states indicated that the obtained surface finishes also vary from one electrolyte to another due to the different usage histories. Figure 5.3 shows the surface appearance and corresponding surface gloss of the samples polished in solution 3 from Chapter 4. The significant deterioration of electro polishing results is evident in this picture.

Compared to the relatively “fresh” solution 1 that yielded almost only bright surfaces (albeit with different levels of surface gloss), the more “used” bath is only able to deliver bright surfaces under certain conditions. Figure 5.3 also shows that despite the deterioration of the polishing bath quality due to extensive usage, it is still possible to attain acceptable surface finishes by employing the “correct” polishing parameters. These observations demonstrate another focus point of this study, the polishing bath history. The ideal approach for rapid determination of the process parameters for obtaining a desired surface quality must also take into account the dynamic nature of the polishing electrolyte, and ideally, compensate it.

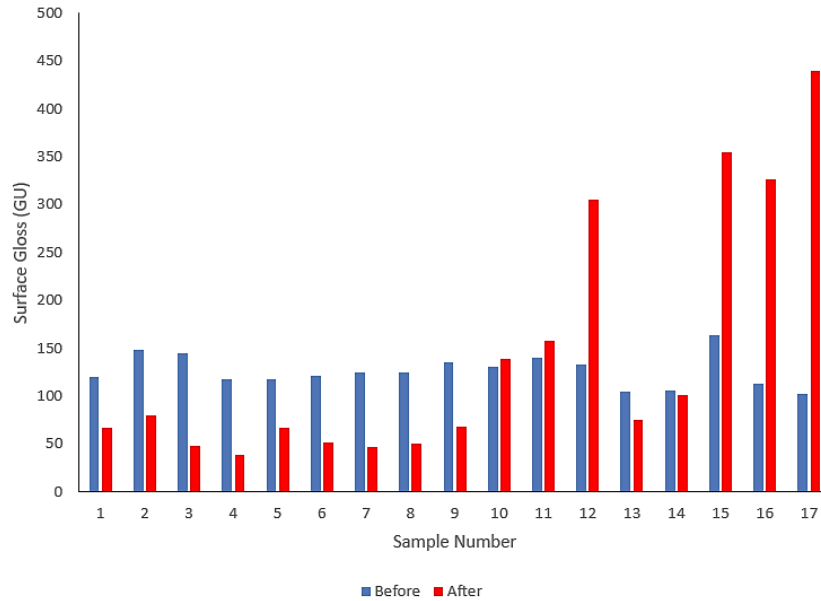
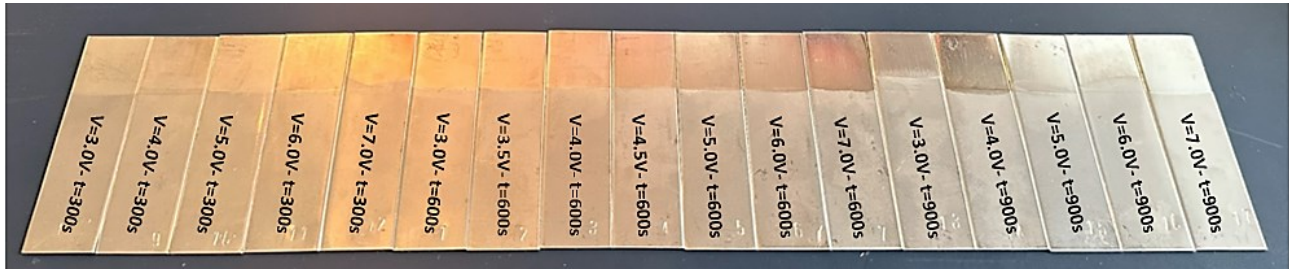


Figure 5.3. (top): Range of surface finishes obtained for stainless steel 316 samples by changing the electro polishing voltage and duration in solution 3, (bottom): variation of the corresponding surface gloss (the samples are organized in order of applied polishing voltage and polishing duration).

The main idea of this study is to build a comprehensive dataset of various polishing parameters and resulting surface finishes for a wide range of solutions with different usage histories. Models will then be applied to the dataset, and their precision in representing the dataset will be evaluated from a purely mathematical perspective. Finally, the model providing the most accurate presentation of the dataset shall be used to develop a prediction tool for determining the process parameters required for achieving a target finish.

### 5.3 Dataset construction

The dataset was built with the goal of obtaining polishing baths representative of those observed in the industry. Therefore, to have a broad range of polishing bath conditions, the accelerated aging

process was conducted between experiments to simulate a “heavily contaminated” polishing bath. The solutions were also gradually refreshed by mixing with fresh electrolytes.

Overall, 17 polishing baths with different usage histories were studied, going from the “standard fresh state” to a “heavily used” state. For each solution, the specific gravity, viscosity, and electric conductivity were measured multiple times. The precision of the devices used for measuring specific gravity and viscosity were  $0.001 \text{ g/cm}^3$  and  $0.1 \text{ mPa}\cdot\text{s}$ , respectively. The measurement of electric conductivity, however, is known to be more intricate from an electrical point of view and therefore, was repeated 20 times before each polishing experiment. To estimate the precision of the measurements, the average ( $0.4 \text{ mS/cm}$ ) of the distribution of all measurement standard deviations of the dataset was used (Figure 5.4).

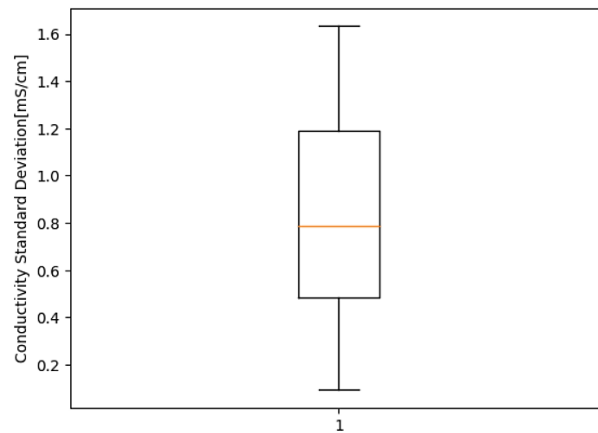


Figure 5.4. Boxplot of the standard deviation in conductivity measurements for different solutions (340 samples).

On average, between 10 to 20 samples were electropolished in each solution with different polishing parameters (polishing voltage and polishing duration). Table 5-1 presents the polishing parameters used for the construction of this dataset. Despite efforts to maintain the temperature of the polishing bath constant, factors, including the ambient temperature, equipment malfunction, and intense polishing reactions, resulted in occasional bath temperature fluctuations during the electropolishing process. Figure 5.5 displays the distribution of the bath temperature over the conducted experiments. It was also observed that the standard deviation of the bath temperature increased with the duration of the electropolishing process, which could be attributed to intensive polishing reactions and gas bubble generation.



Table 5-1. Electropolishing process parameters used for the construction of the dataset.

<b>Polishing Potential</b>	3, 4, 5, 6, and 7 V
<b>Polishing Duration</b>	300, 600, 900, and 1200 s
<b>Polishing Solution Temperature</b>	40 °C

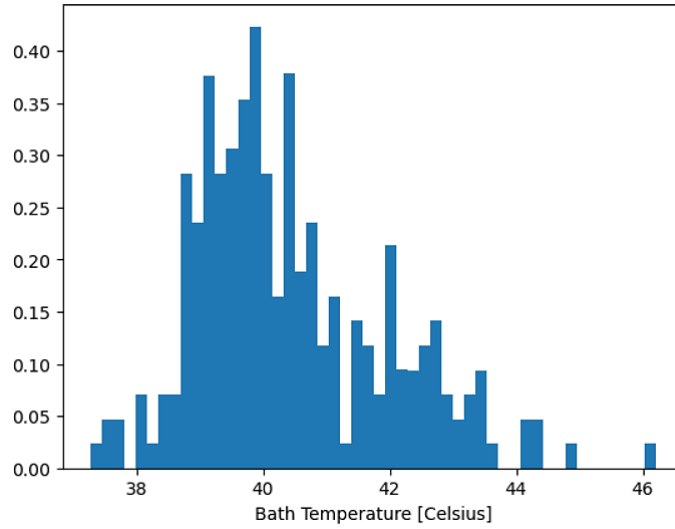


Figure 5.5. Distribution of bath temperature in conducted experiments (249 samples).

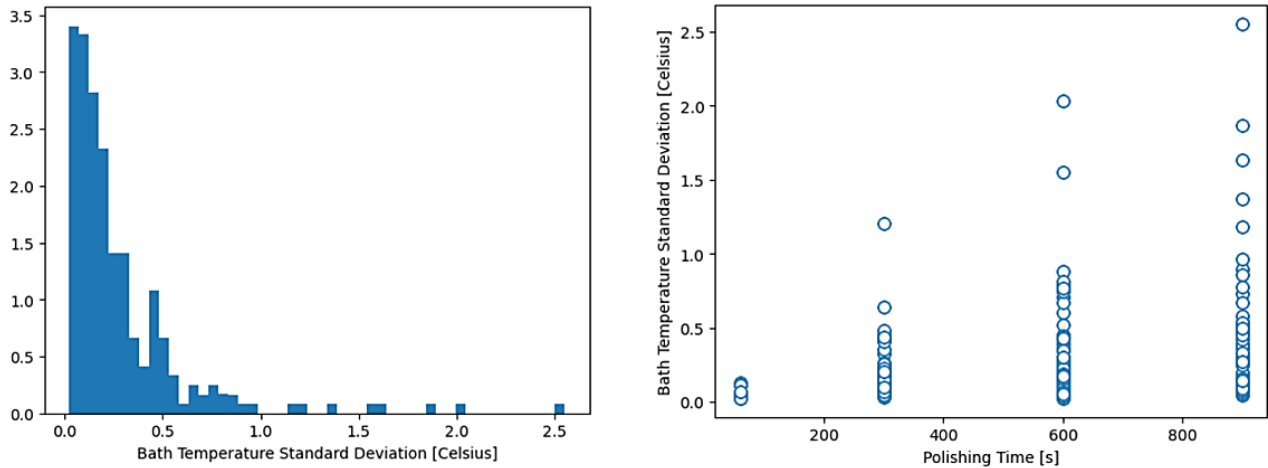


Figure 5.6. (left) Distribution of the standard deviation in bath temperatures, (right) effect of polishing duration on bath temperature standard deviation (249 sample).

The surface roughness and surface gloss of the samples were measured 10 times before and after each electropolishing experiment to ensure accuracy. Figure 5.7 and Figure 5.8 present the standard deviation in measurements of the various surface roughness and surface gloss indexes before and after each polishing treatment. The standard deviations of measured roughness and brightness values exhibit a lognormal distribution as expected for a normal distributed random variable.

The average of the distributions of standard deviation indicates a precision of 0.01, 0.01, and 0.06  $\mu\text{m}$  for Ra, Rq, and Rz measurements, respectively. Similar calculations for surface gloss give a precision of 16 and 5 GU for the measurements of the H20 and H60 indexes, respectively.

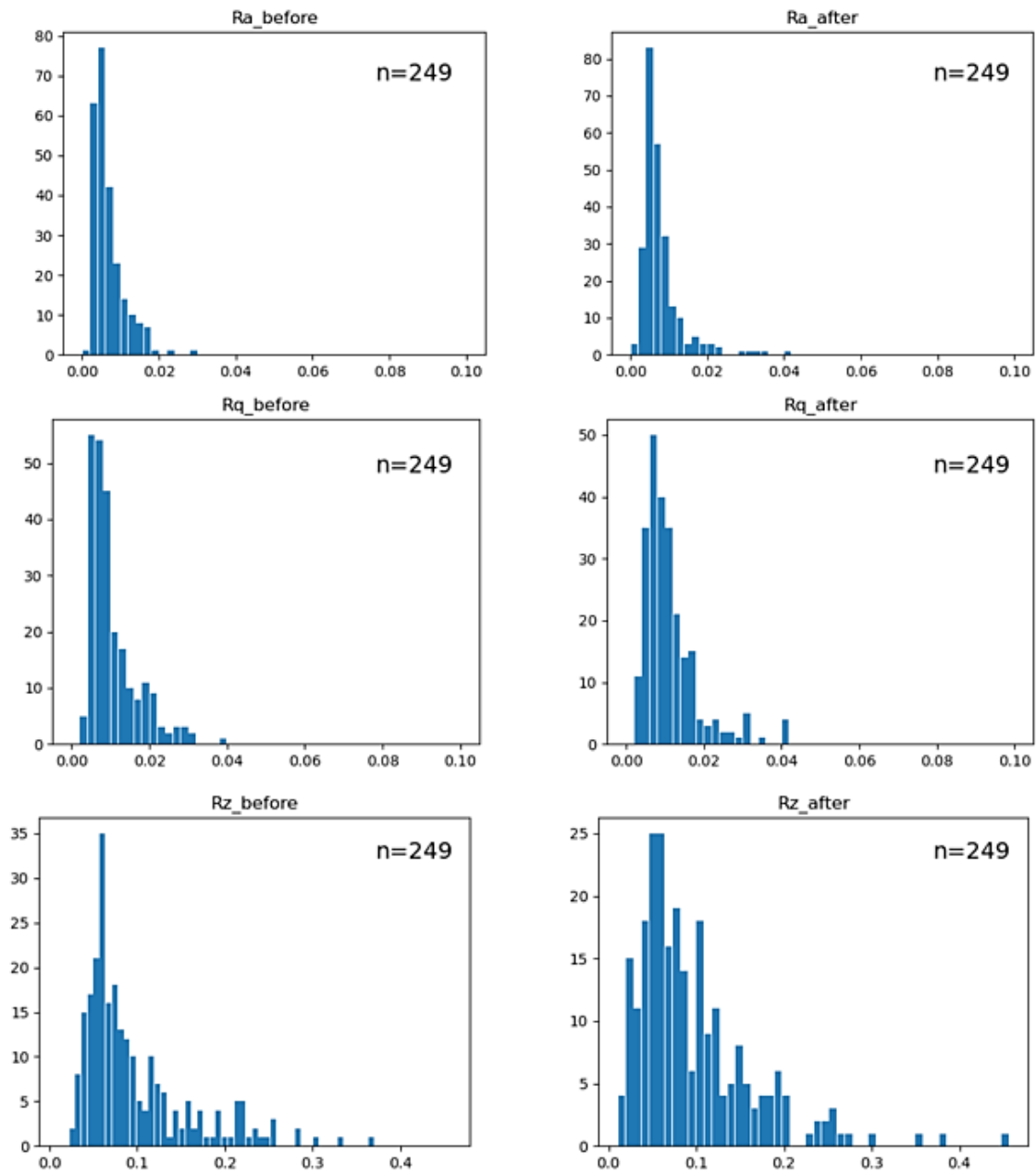


Figure 5.7. Standard deviation of surface roughness indexes before and after electropolishing treatment (249 samples).

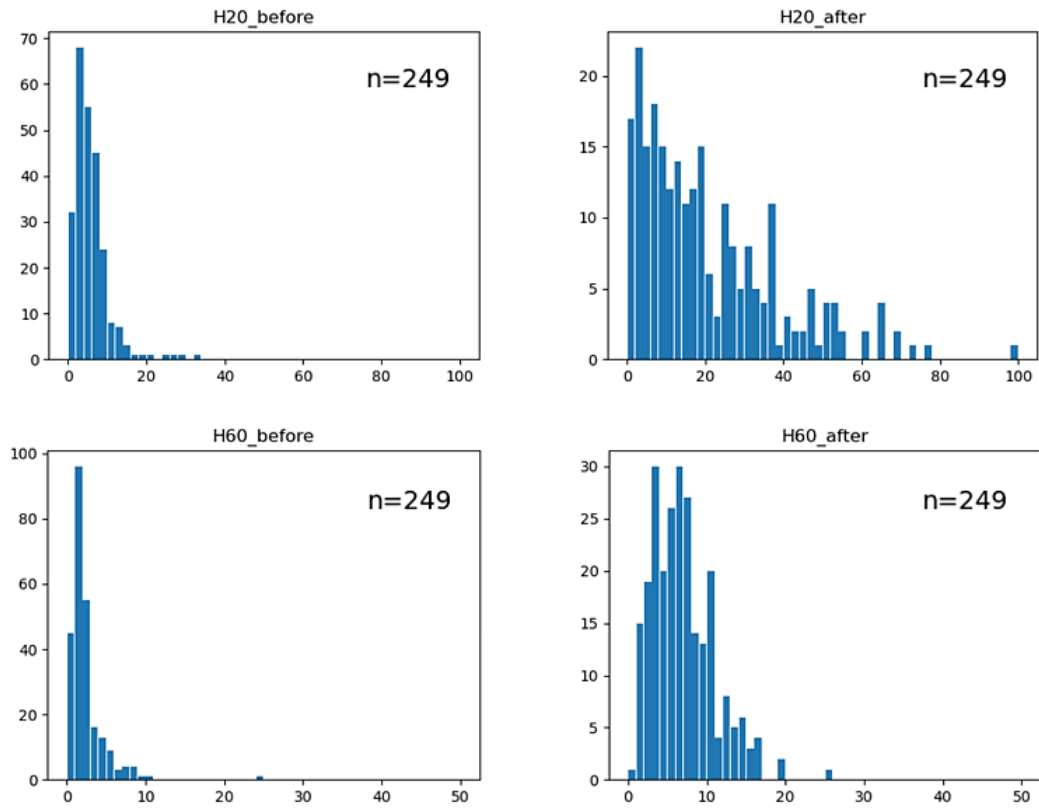


Figure 5.8. Standard deviation of surface gloss measurements before and after electropolishing (249 samples).

The weight loss of the samples was also measured before and after each polishing treatment. In addition, during the electropolishing experiments, different process parameters, including the polishing voltage and current, as well as the solution temperature, were recorded. Table 5-2 indicates the average number of measurements conducted for the construction of the dataset.

Table 5-2. Average number of measurements conducted for dataset construction.

<b>Number of solutions</b>	17
<b>Total number of conductivity/viscosity/density measurements</b>	340
<b>Typical number of samples polished per solution</b>	10-20
<b>Total number of samples</b>	249
<b>Total number of Ra/brightness measurements</b>	2492
<b>Total number of weight measurements</b>	249

## 5.4 Dataset exploration

The constructed database allows for the meaningful illustration of the variation patterns of different parameters in the investigated polishing system. Figure 5.9 displays the distributions of the viscosity and conductivity values of the investigated polishing baths together with their cumulative percentage. As can be noted in the plots, the dataset is distributed in a way that there are not noticeably more instances of one bath state than others. This shows that the built dataset is not skewed, meaning that the distribution of conductivity and viscosity values is balanced and representative. Indeed, it was intended during the dataset construction step to include a sufficient number of sample solutions for different bath states (fresh, medium-used, and heavily-used) to avoid over-representing any particular bath state compared with others. This is crucial as a balanced dataset prevents the machine learning model from making biased predictions due to imbalanced class distributions.

Figure 5.10 indicates the variation of electric conductivity and viscosity of the polishing baths as they go from a “fresh” state to a “heavily-used” condition. It is evident that as the polishing bath becomes more viscous, a significant drop occurs in its electric conductivity. This can be explained by the reduced mobility of electric charge carriers in highly viscous solutions.

It is worth noting that, despite the correlation between solution viscosity and electric conductivity, it has been observed that both properties are required to determine the state of a polishing bath. As can be seen in Figure 5.10, for low-viscosity solutions, a slight change in the viscosity results in a considerable change in electric conductivity. Similarly, for highly viscous solutions, a small variation in the electric conductivity is accompanied by a large difference in viscosity. Therefore, given that a small measurement error in one property can lead to a considerable misestimation of the other, both properties should be measured to determine the polishing bath state.

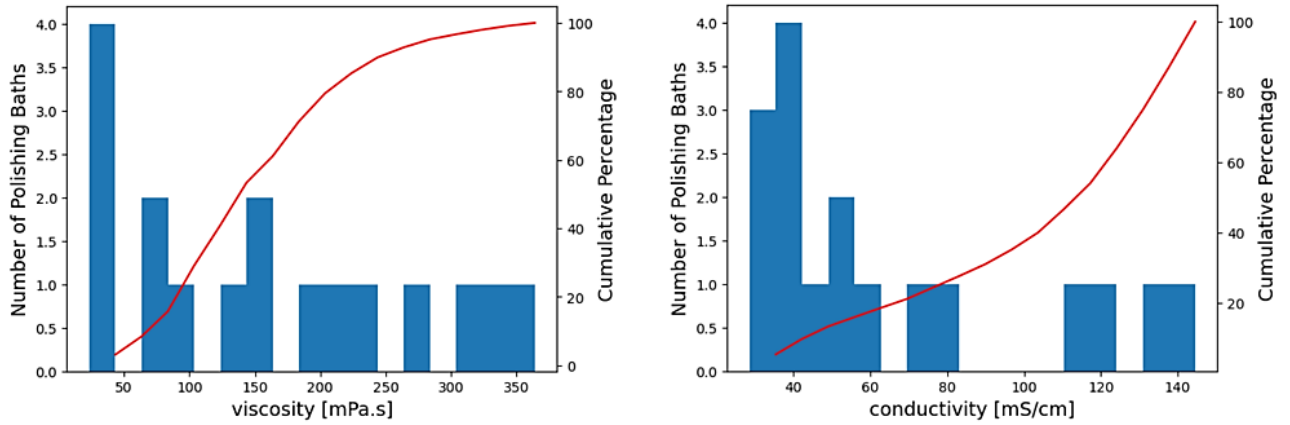


Figure 5.9. Cumulative distributions of viscosity and conductivity for the investigated solutions.

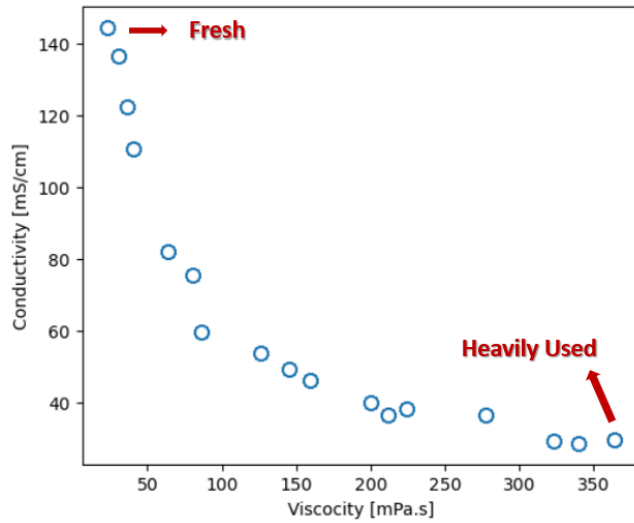


Figure 5.10. Variation of the electric conductivity and viscosity among the studied electrolytes.

Figure 5.11 presents the distribution of the initial and final surface roughness of the studied samples. The samples utilized for this study were cut from four different stainless steel 316 sheets. The histograms of the initial surface roughness indexes indicate two distinct populations of values, which could suggest that two of the utilized sheets must have had a similar surface roughness. It can also be noted that, in general, two populations of samples were achieved upon the electropolishing, which is probably a result of the polishing bath history, and it will be explored later in more detail.

Figure 5.12 illustrates the distribution of surface gloss values before and after electropolishing treatments. Given that all of the measured values for the H60 index were higher than 70, the H20 index was considered more relevant than the H60 index. Therefore, in the future, we will only

discuss the H20 index for the surface brightness of the samples. The wider distribution of H20 brightness values after the electropolishing treatment (ranging from around 60 to 1000 GU) can be explained by the fact that a broad range of finishes going from matt to semi-bright to mirror-like surfaces could be obtained (Figure 5.2 and Figure 5.3; the reader is as well invited to compare this with Figure 5.12).

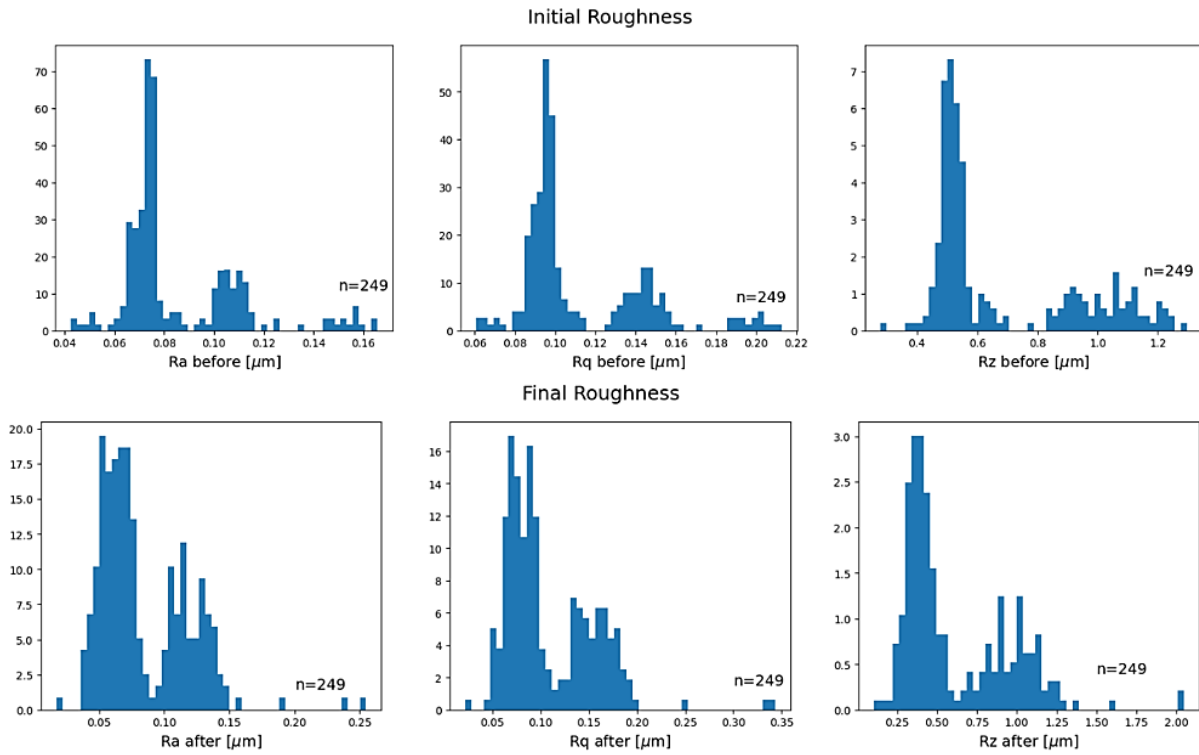


Figure 5.11. Surface roughness distribution of the samples (top) before, and (bottom) after electropolishing treatments (249 samples).

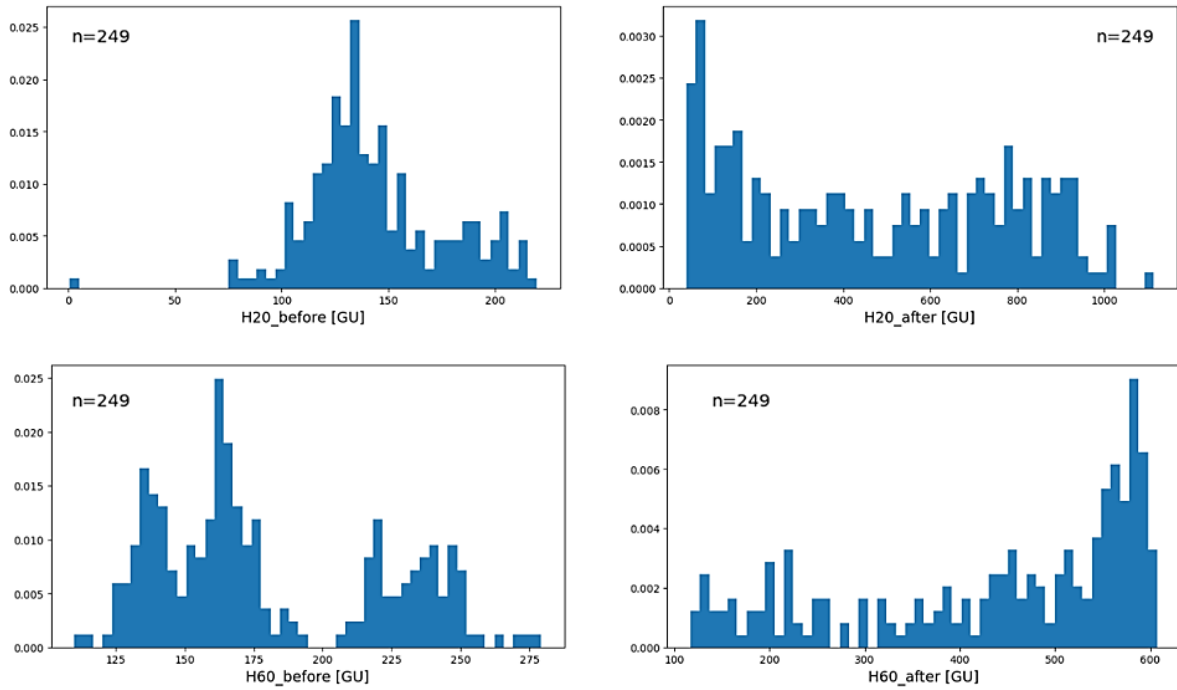


Figure 5.12. Surface brightness distribution of the samples (top) before, and (bottom) after electropolishing treatments (249 samples).

Figure 5.13 represents the correlation matrix constructed to visualize the relationships between different variables in the electropolishing process. Each cell in the matrix represents the correlation coefficient between two variables ranging from 0 to 1. A higher correlation coefficient (closer to 1) indicates that the variables are strongly correlated and that changing one will significantly affect the other. The following conclusions can be made based on the correlation matrix:

1. The initial roughness of the samples is strongly correlated to their initial weight. This can be explained by the fact that the studied samples are generally similar before electropolishing (similar dimensions and nearly similar surface roughness), and no significant change is observed in either of the measured quantities.
2. The final surface roughness and brightness of the samples are highly correlated with each other, as well as with the conductivity and viscosity of the polishing bath. This correlation was expected, given the effect of surface topography on its light-reflecting properties. In addition, it has been established that the electric conductivity and viscosity of the solution can significantly affect the outcome of the electropolishing process.
3. The viscosity of the electrolyte is highly correlated with its electric conductivity. This is expected since, as previously stated, an electrolyte's electric conductivity tends to decrease



as its viscosity increases. This is due to the fact that viscous solutions hinder the movement of charge carriers, making it more challenging for them to carry an electric current.

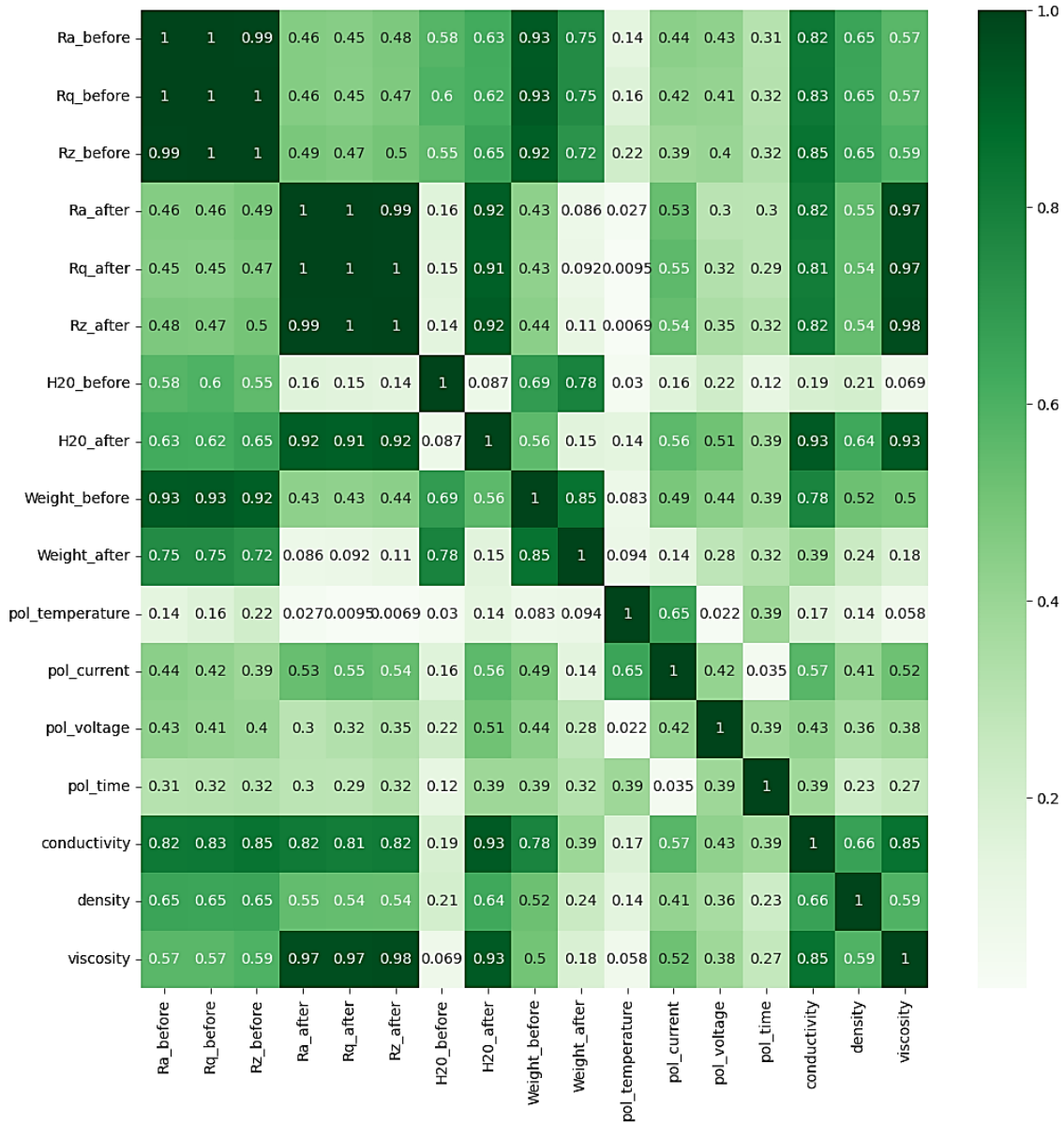


Figure 5.13. Correlation matrix for different variables of the electropolishing process.

The following plots illustrate some of the correlations observed in the correlation matrix between different variables of the electropolishing process. Figure 5.14 indicates that the solution viscosity and electric conductivity have opposite effects on the final surface roughness (Ra) of the samples. Similar trends can also be noted in the effect of solution viscosity and electric conductivity on the

final surface brightness of samples (Figure 5.15). This can be expected given the diminished polishing performance of highly viscose and low-conductivity electrolytes. Figure 5.16 displays the correlation between surface roughness indexes (Ra, Rq, and Rz) and surface gloss. Evidently, as the surface becomes smoother, it has fewer irregularities that can scatter light, therefore, it reflects light more uniformly, resulting in a higher gloss unit.

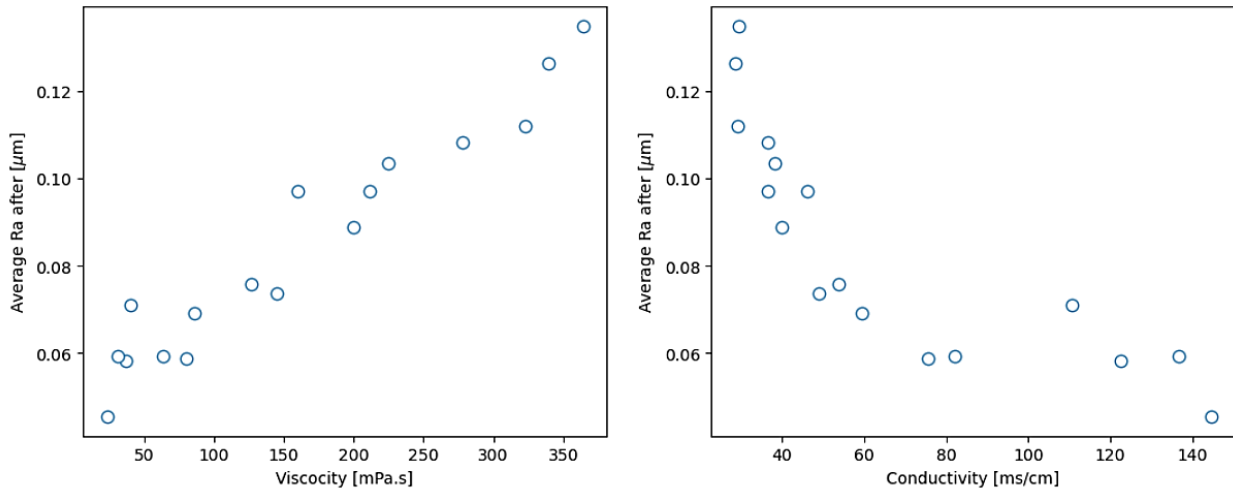


Figure 5.14. Effect of bath viscosity and electric conductivity on the average final roughness (Ra) of the electropolished samples.

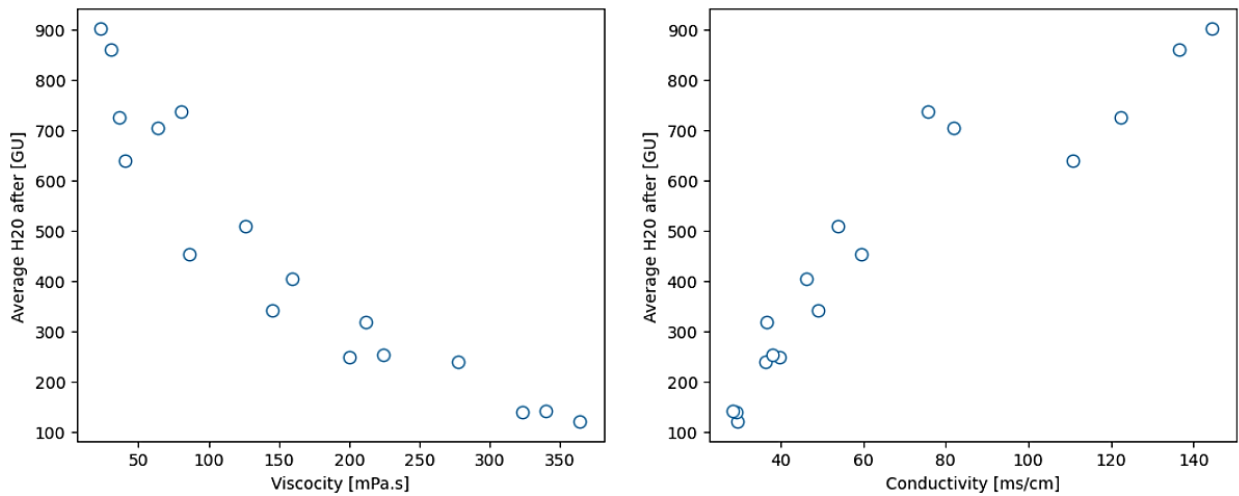


Figure 5.15. Effect of bath viscosity and electric conductivity on the average final roughness (Ra) of the electropolished samples.

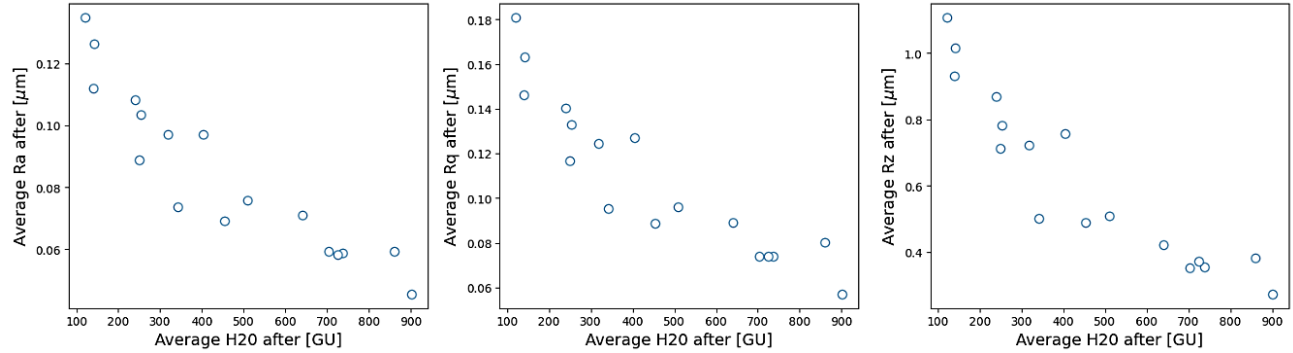


Figure 5.16. Correlation of the average final roughness (Ra) of the electropolished samples with the average surface gloss.

## 5.5 Dataset preprocessing

After dataset construction and exploration, machine learning models can be employed to make decisions or predictions based on the dataset. However, before the raw data can be fed to machine learning models for training and prediction, it must be cleaned and transformed (preprocessed) to a suitable format. In the cleaning and preprocessing step, the outliers and missing values of the dataset are properly handled. In addition, in the cases of datasets that contain numerical features with different scales and units, the features are standardized to ensure their equal contribution to the model. The dataset collected in this study was, henceforth, cleaned, and the occasional missing or outlier values were re-measured to avoid errors or biased results. In the preprocessing step, the dataset was scaled using the standard scaling method, which transforms the data to have a mean of 0 and a standard deviation of 1. In addition, the average surface roughness and brightness values were calculated and utilized for each investigated sample.

## 5.6 Model development

The construction of a comprehensive dataset that covers a wide range of polishing bath states with different usage histories enables us to predict the required process parameters for achieving a desired surface finish in almost any given bath condition in the studied range. In the case of a new bath state, this dataset can be used as a look-up table to find the polishing parameters used in the most similar situations. However, given the size of the dataset and the variety of the studied features, developing an appropriate mathematical model that can clearly describe the dataset can greatly facilitate the polishing parameter tuning process. As already explained, the goal of this study is to develop a model that can predict the final surface finish of the parts using the employed polishing parameters and vice versa. The first step towards this goal is to reduce the dataset complexity by creating simplified mathematical representations that capture the essential information and patterns in the data.

For a better understanding of a model's performance in capturing the essential patterns of a dataset, it is necessary to split the dataset into training and test sets. As can be expected from their names, the training dataset will be used to train the model, while the test dataset will be used to evaluate its performance. Splitting the dataset yields a more realistic estimation of the model's generalization power by assessing its performance on previously unseen data points. The constructed dataset in this study was hence divided into training and test sets with a split ratio of 80%:20%, respectively.

### 5.6.1. Definition of the target variable

After preprocessing, the dataset is ready to be explored and analyzed by the modeling algorithm. The first step in model development is determining the target variable, which is the variable that the model is going to predict. In the case of the electropolishing process, various target variables can be considered, including the post-electropolishing surface roughness and brightness or the ideal polishing voltage or duration for achieving a desired surface finish. In the following examples, various models were compared with regard to their performance in predicting the final surface roughness parameters of the parts ( $Ra\_after$ ,  $Rq\_after$ , and  $Rz\_after$ ).

The target variable could also be the relative surface roughness of the parts calculated as follows:

$$\begin{aligned}
 Ra_{rel} &= \frac{Ra_{after}}{Ra_{before}} \\
 Rq_{rel} &= \frac{Rq_{after}}{Rq_{before}} \\
 Rz_{rel} &= \frac{Rz_{after}}{Rz_{before}}
 \end{aligned}
 \tag{5.1}$$

### 5.6.2. Feature selection


A machine learning algorithm utilizes a set of features (also known as attributes or input variables) to make predictions or decisions based on the dataset. In the case of the dataset used in this problem, different parameters of the electropolishing system, such as pre-electropolishing surface roughness and brightness or the polishing voltage and duration, can be used as the model features. As a critical step in the machine learning model development process, the goal of feature selection is to choose a subset of relevant and informative features from the original set of variables to improve model performance and reduce its complexity. The most informative features of the dataset can be determined using different methods, such as removing low variance features, univariate feature selection, and tree-based feature selection. A deep understanding of the process

can also provide valuable insights into which features are crucial in determining the outcome of the process. The knowledge of an expert can help prioritize and select relevant features even if they might not have the highest correlation with the target variable.

After cleaning and preprocessing the dataset a number of potentially relevant features were studied to identify the most informative features. Three different feature selection methods were employed to find the most relevant features of the current database. The definition and results of each method are presented as follows:

1. **Variance-based feature selection:** This technique is used to identify and remove features with little variation in their values across the dataset. Such features are often considered less informative as they provide no information that allows machine learning models to predict the target variable. Eliminating low-variance features can simplify the model, reduce computation time, and improve generalization performance. Figure 5.17 presents a list of investigated features based on a low-variance feature removal approach. The features are sorted in the order of decreasing variance, going from polishing time to the Ra roughness of the sample before electropolishing. According to this method, a feature presenting a high variance, like the polishing time, is more relevant than a low-variance feature, like the pre-electropolishing surface roughness. The low-variance features of the dataset can be removed using the Variance Threshold method of the Scikit-Learn library, which is a convenient and straightforward way to filter out the features whose variance is below a defined threshold.
2. **Tree-based feature selection:** Feature selection using Random Forests is another technique for identifying the most important features in a dataset. Random Forests is an ensemble learning method combining multiple decision trees to make predictions. This method involves ranking the model features according to their Gini importance, which is a (normalized) measure of how much a feature contributes to the overall predictive power of the model. The Gini importance of a feature is calculated by evaluating how much the feature reduces the impurity (Gini impurity) in the data when making splits in a decision tree. To conduct this method, a Random Forests model is fitted to the training data after the dataset is cleaned, preprocessed, and split into training and test sets. Next, the Feature Importance, which is an attribute of the Random Forests model, can be used to obtain the importance score of each feature in predicting the target variable. Figure 5.17 indicates the investigated features sorted according to their importance scores. For instance, it can be understood from the order of the features that splitting the dataset based on the conductivity and viscosity of the polishing bath is more informative than doing so according to its specific gravity.
3. **Univariate feature selection:** This method selects the best features based on univariate statistical tests between each feature and the target variable. It helps identify the most relevant features by evaluating their relationships with the target variable. The Select K

Best is one of the classes used to perform univariate feature selection in Scikit-Learn. This method selects the first K highest-scoring features. Different scoring functions such as  $f_{\text{regression}}$ ,  $f_{\text{classif}}$ , and  $\chi^2$  are used to evaluate the significance of features concerning the target variable. The investigated features of our dataset were scored using the  $f_{\text{regression}}$  test which computes the F-value and p-value for each feature by performing an analysis of variance (ANOVA) test between the target variable and each feature. As can be seen in Figure 5.17, the viscosity and conductivity of the polishing bath have the highest F scores and are hence, considered most informative by this method.



	Random Forests	Low Variance	Select K Best
Most Informative	Conductivity	Polishing Time	Viscosity
	Viscosity	Viscosity	Conductivity
	H2O_before	Conductivity	Rz_before
	Rz_before	H2O_before	Specific Gravity
	Ra_before	Polishing Voltage	Rq_before
	Rq_before	Bath Temperature	Ra_before
	Polishing Time	Rz_before	Bath Temperature
	Bath Temperature	Specific Gravity	Polishing Voltage
Least Informative	Polishing Voltage	Rq_before	Polishing Time
	Specific Gravity	Ra_before	H2O_before

Figure 5.17. Dataset features in order of their importance in predicting  $Ra_{\text{rel}}$  using various feature selection methods.

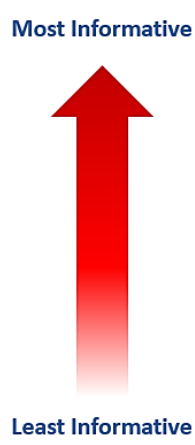
Investigation of the results obtained from the studied methods indicated that the Random Forests and Select K Best methods are more reliable for feature selection than the Low Variance method. Both Random Forests and Select K Best methods take into account the relationship between features and the target variable. The Low Variance method, on the other hand, only considers individual feature variations, which may not be sufficient to assess its relevance in the context of predicting the target variable.

It can be concluded from the results of Random Forests and Select K Best methods that besides the viscosity and conductivity of the polishing bath, the state of the parts' surface before electropolishing is as important as the polishing parameters used. Given their statistical nature, these methods, however, might not be able to capture the importance of some features. For instance, Figure 5.17 indicates that the polishing temperature is not considered highly informative by any of the investigated models. However, our understanding of the process tells us that, on the contrary, the temperature of the polishing bath significantly affects the material removal rate and the outcome of the electropolishing process. The statistical method's wrong assumption that

temperature is insignificant comes from the limitation of the dataset, where only one bath temperature (40°C) was examined due to time constraints. As a result, the effect of temperature is not shown in the raw data.

Upon consideration of the feature selection results and our previous experience with the electropolishing process, the following features were considered most informative and selected to be used with different machine learning algorithms for the prediction of the final surface roughness of the parts: electric conductivity, viscosity, and temperature of the polishing bath, electropolishing voltage and time, as well as the initial surface roughness (Ra, Rq, Rz) of the samples.

The feature selection step was also performed for the gloss value prediction. Figure 5.18 represents the result of the feature selection analysis for predicting H20\_after. It can be noted that compared to the important features for predicting the surface roughness, polishing parameters appear higher in the importance ranking for gloss predictions. It can be concluded that the influence of polishing parameters on optical properties is much more significant than on surface roughness values. Therefore, while tuning the polishing parameters to modify the optical properties appears to be realistically possible, it looks to be more challenging for roughness properties. In addition, even though there was no significant variation in the temperature of the bath during the polishing process, bath temperature seems to have a stronger effect on surface brightness than surface roughness. Based on our knowledge of the process and using the results of feature selection methods, the following dataset features were selected to be used by the models for the prediction of surface brightness after electropolishing: electric conductivity, viscosity, density, and temperature of the bath, polishing voltage and time, Rq\_before, Rz\_before, and H20\_before.



	Random Forests	Low Variance	Select K Best
Most Informative	Viscosity	Polishing Time	Viscosity
	Conductivity	Viscosity	Conductivity
	Polishing Time	Conductivity	Density
	Polishing Voltage	H20_before	Rz_before
	H20_before	Polishing Voltage	Bath Temperature
	Bath Temperature	Bath Temperature	Polishing Voltage
	Density	Rz_before	Ra_before
	Rq_before	Specific Gravity	Rq_before
Least Informative	Ra_before	Rq_before	Polishing Time
	Rz_before	Ra_before	H20_before

Figure 5.18. Dataset features in order of their importance in predicting H20\_after using various feature selection methods.

### 3.3.3. Model training

After determining the most relevant features of the database, a model may be used to learn from the selected features and make accurate predictions. In this step, various statistical learning algorithms can be evaluated and compared regarding their performance on the dataset. Three different models were investigated in this study to predict the designated target variables using the selected features from the dataset: linear regression, k-Nearest Neighbors (KNN), and Random Forests.

Each model was trained on the training dataset set using the selected features. Next, their performance was compared based on their Root Mean Squared Error (RMSE) on the test set. The model with the best performance was then selected to be used for the mathematical representation of the dataset.

### 3.3.4. Hyperparameter tuning

Some of the investigated algorithms, such as KNN or Random Forests require hyperparameter tuning to maximize their predictive value. In this process, the model's performance is scored with a cross-validation strategy for different values of hyperparameters (number of neighbor points in KNN or the number of decision trees in the Random Forests model). The k-fold cross-validation is one of the strategies used for the hyperparameter tuning of models. This method involves dividing the training data into k subsets (folds) and training/evaluating the model k times, each time using a different fold as the validation set. The Repeated K Fold cross-validation strategy utilized in the current study is a variant of the K-fold cross-validation technique that involves repeating the k-fold process multiple times with random data shuffling.

Figure 5.19 presents the results of the Repeated K-fold cross-validation method for hyperparameter tuning of the KNN and Random Forests models for predicting the Ra\_rel. As indicated, for each model, the root mean square error (RMSE) of the k fold training and validation sets are calculated at different values of the hyperparameters until the optimal value (minimum RMSE for the k fold validation set) was reached. It can also be understood from these plots that both models behave as expected. For example, for the KNN model, the RMSE of the training set is very small for fewer number of neighbors, whereas the error of the model shown through the validation set is very high in the beginning and decreases afterward (indeed if  $K=1$ , the prediction on the training set has no error as the algorithm simply reproduces the training set, but will have no generalization power). The Random Forests model, however, behaves differently. Both K fold training and validation sets exhibit high RMSE for a smaller number of trees, and the predictive value of the model increases as the number of trees goes up, as expected. It can also be noted that while the error in the k fold validation set decreases with increasing the number of trees, the error of the k fold training set does not change after a while.



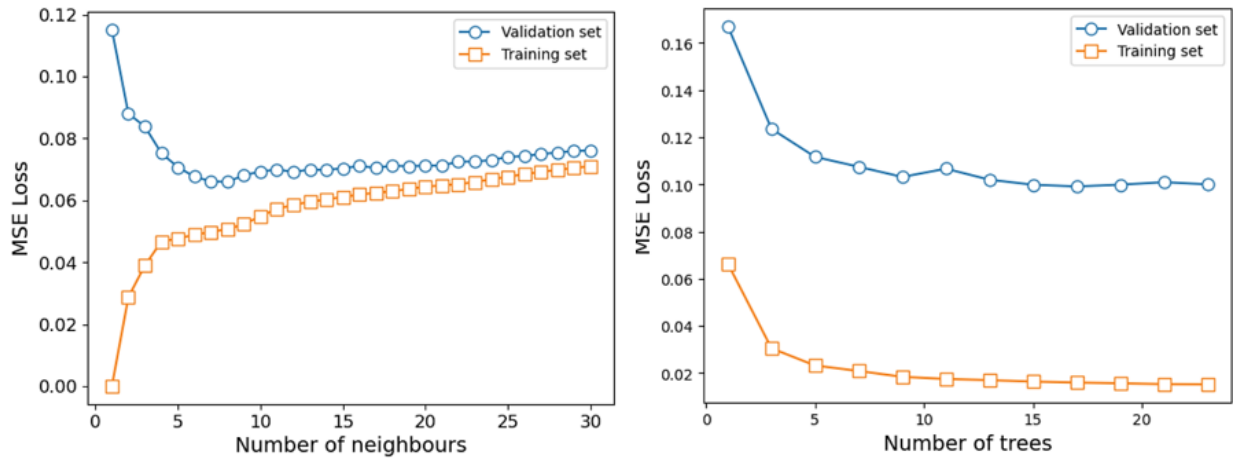


Figure 5.19. Hyperparameter tuning using cross-validation for (left) KNN algorithm and (right) Random Forests algorithm.

## 5.7 Model selection

The following figures present the performance of the studied models with regard to predicting the final surface roughness parameters of the electropolished parts,  $Ra_{after}$ ,  $Rq_{after}$ , and  $Rz_{after}$ . It must be noted that these plots are just one example of model predictions based on one similar train-test-split in the dataset. To investigate whether the solution history affects the model's accuracy, the models' error ( $y - y_{pred}$ ) has been plotted as a function of the solution viscosity.

In addition, a voting ensemble algorithm was used to combine the predictions of the studied models to make a final prediction. Ensemble learning methods may be used to improve model performance, ideally achieving better performance than any single model used in the ensemble. In this study, the voting regressor ensemble was used to average the individual predictions from different models to form a final prediction. Figure 5.23 displays examples of predictions made by the ensemble method.

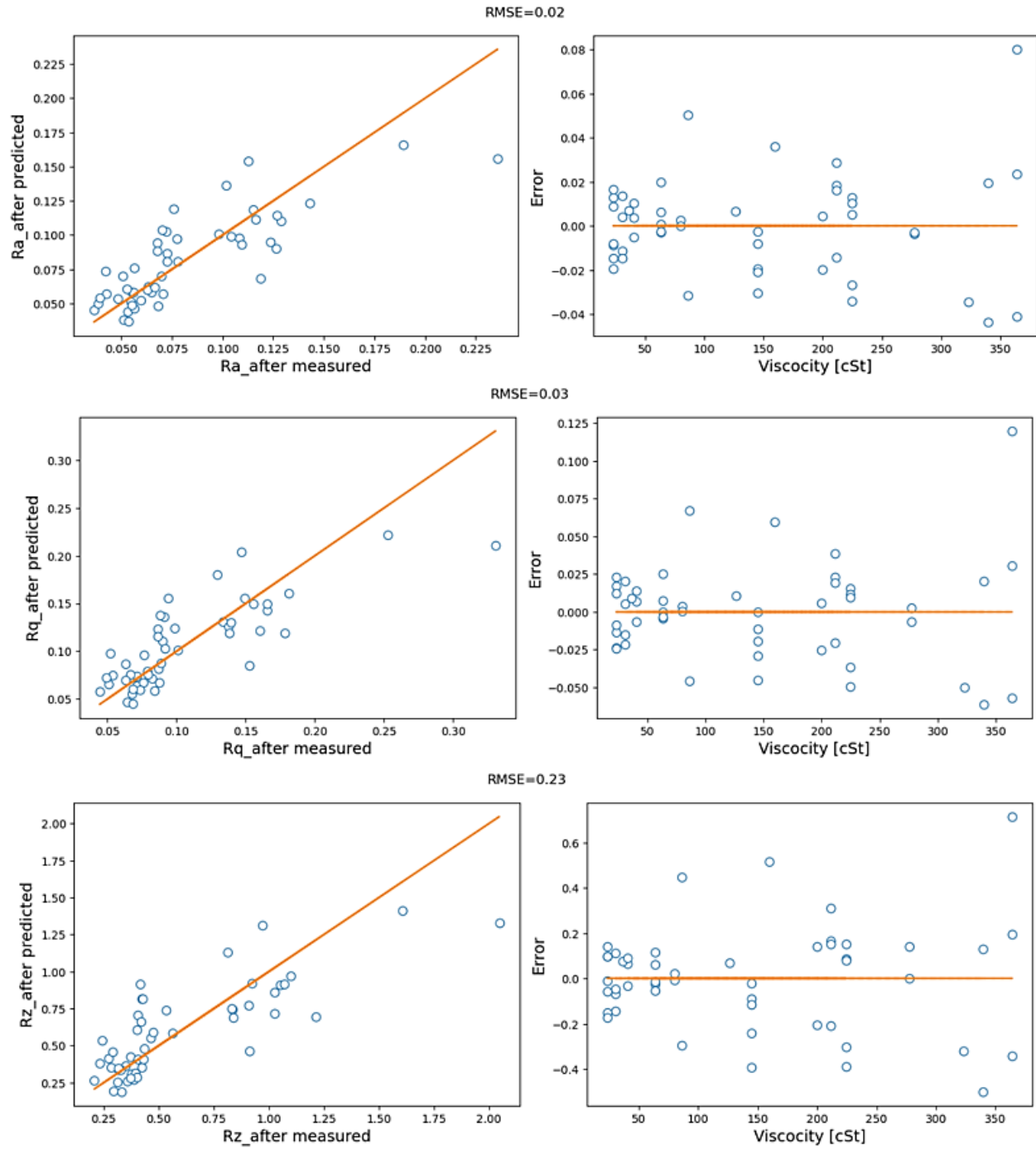


Figure 5.20. The linear regression model used for the prediction of Ra-after, Rq-after, and Rz-after.

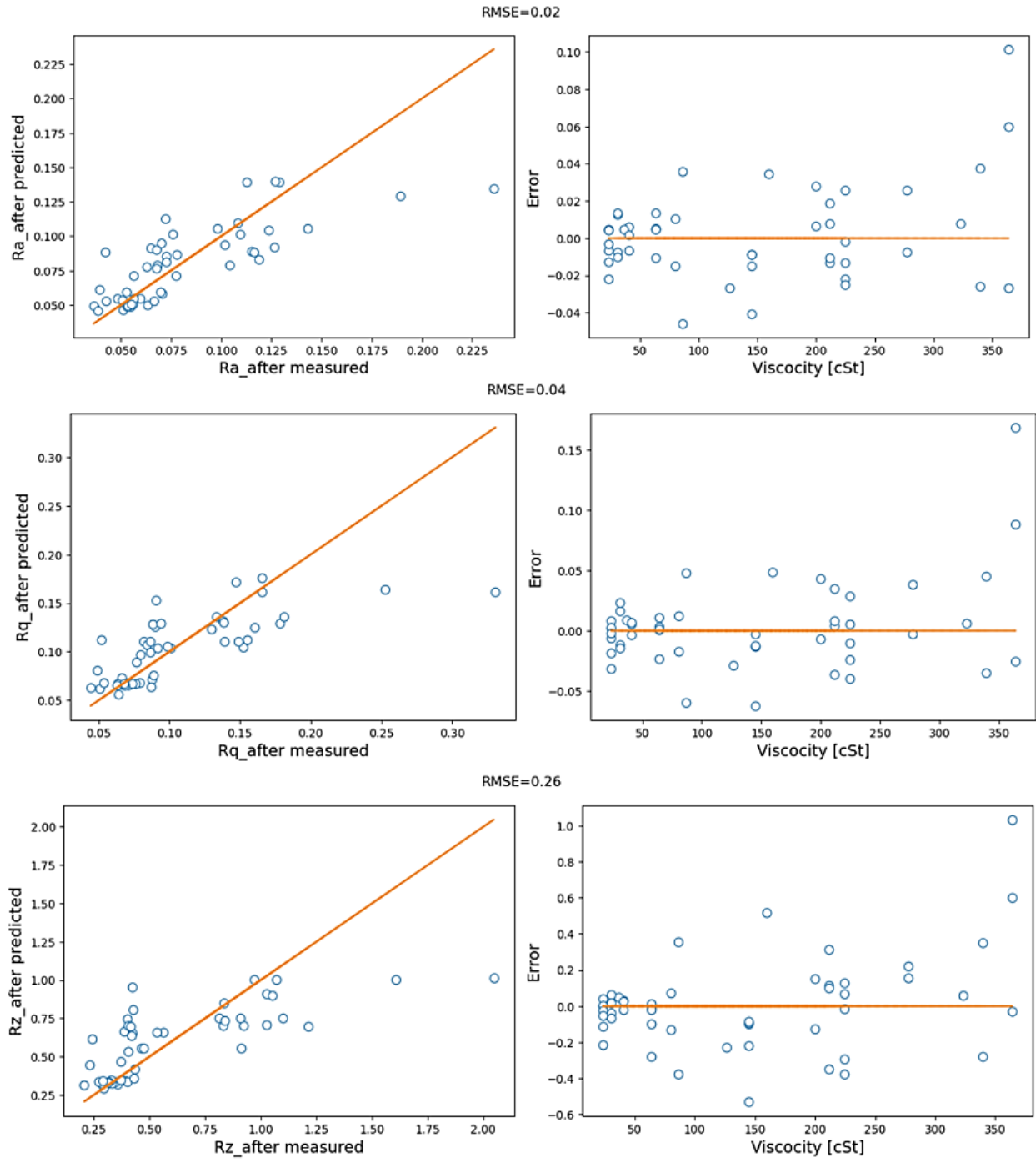


Figure 5.21. The KNN model used for the prediction of Ra-after, Rq-after, and Rz-after.

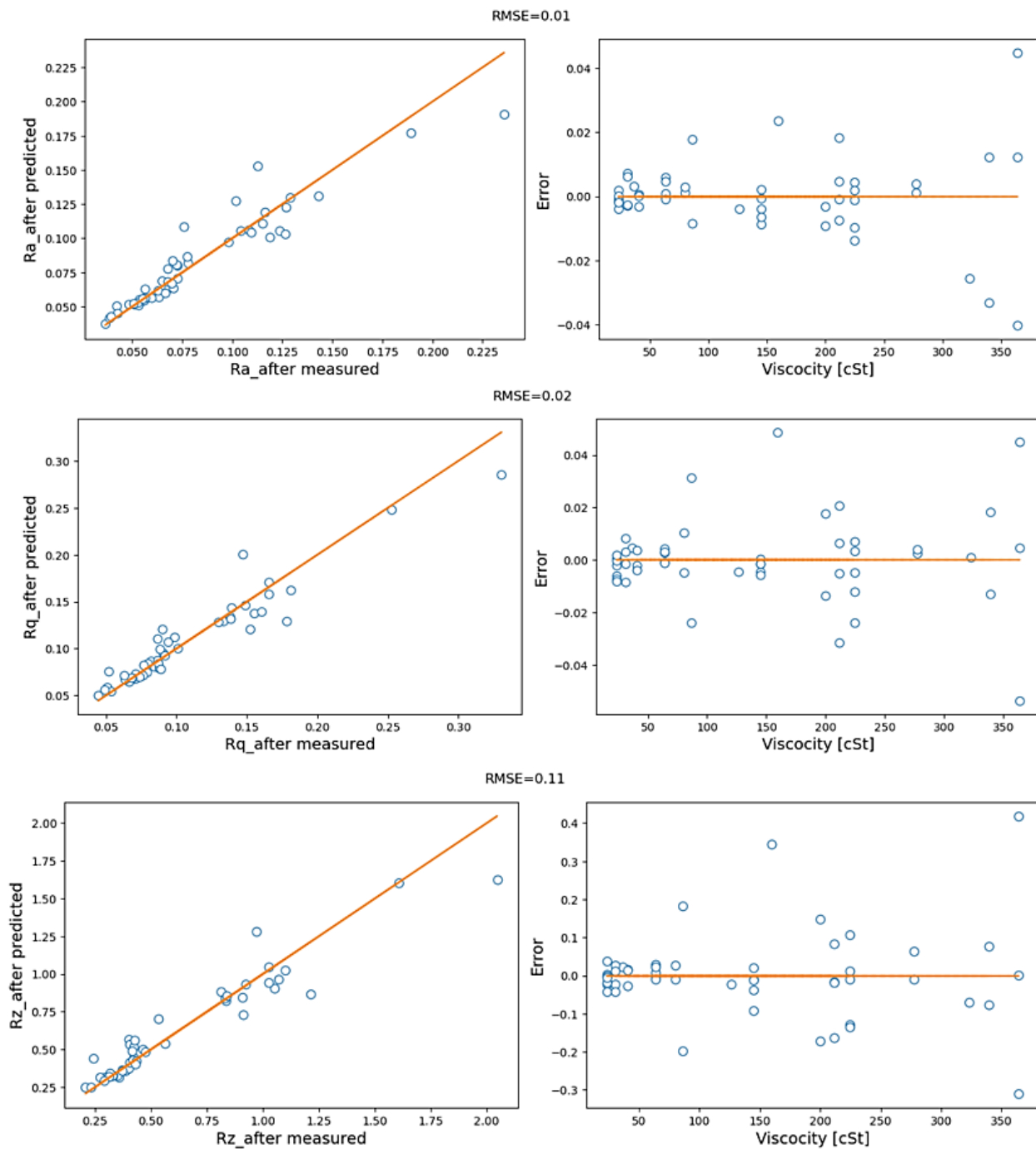


Figure 5.22. The Random Forests model used for the prediction of Ra-after, Rq-after, and Rz-after.

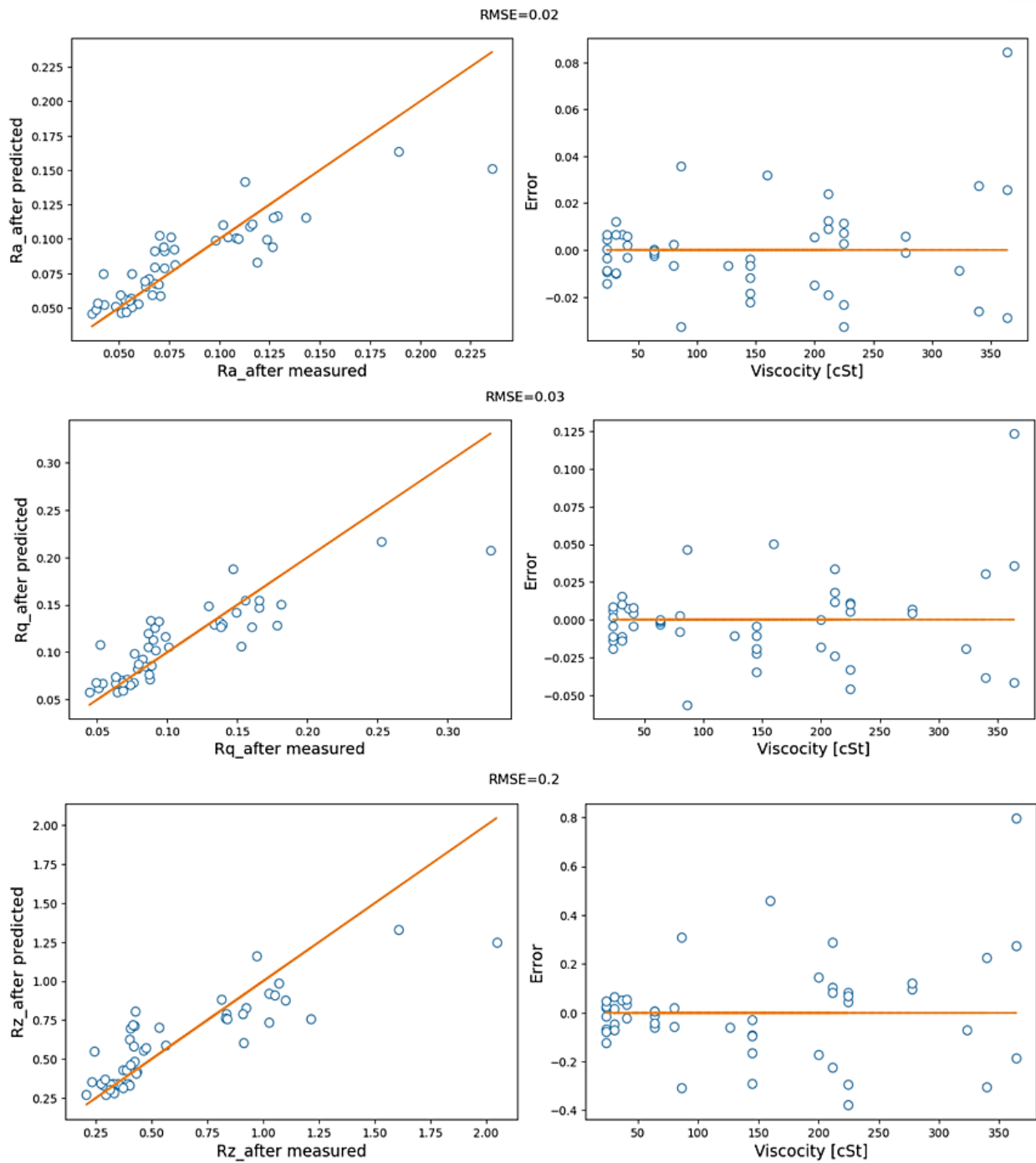


Figure 5.23. The Voting Regressor ensemble used for the prediction of Ra-after, Rq-after, and Rz-after.

To better compare the models' predictive power their root mean squared error (RMSE) distribution in prediction of different target variables based on 100 train-test-splits of the dataset was plotted (Figure 5.24). All predictions were made on the data from the test set.

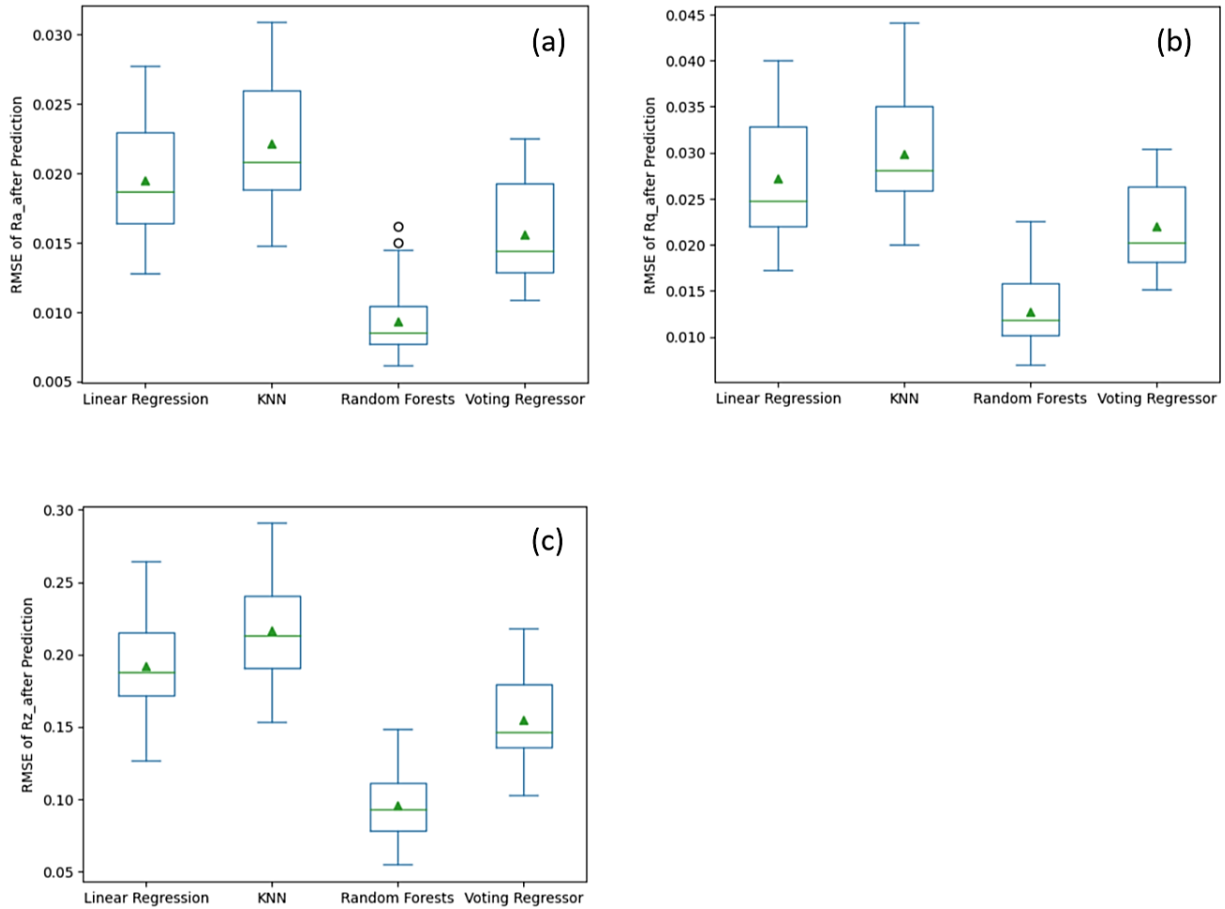


Figure 5.24. RMSE distribution of different models for prediction of Ra-after, Rq-after, and Rz-after on the test set.

The box plots in this figure feature "whiskers" that span from the minimum to the maximum prediction errors of the models. Within each box, the lower and upper boundaries correspond to the 25th and 75th percentiles of the RMSE values, respectively, providing a visual representation of the central 50% of the distribution. The median RMSE, signifying the middle value in the ordered set of prediction errors, is denoted by a green line inside each box. Additionally, the green triangles near the median line represent the mean RMSE value. Any individual data points that fall noticeably outside the whiskers are typically identified as outliers, suggesting the presence of uncommon or extreme values within the dataset.

It can be concluded from the plots that, on average, the Random Forests model provides the most accurate representation of the dataset. Note that the Random Forest algorithm is as well the only model that reproduces the dataset over the full range of roughness data (For instance, the KNN model demonstrates accurate predictions for low roughness values but exhibits significant errors when it comes to high roughness values; see Figure 5.21). The Random Forests algorithm was hence selected to be used for the development of the target prediction tool.

The result of model predictions for the relative surface roughness of the electropolished parts are presented in Chapter 10. These results are in agreement with the observations for the absolute surface roughness values, indicating the Random Forests model as the most accurate algorithm in representing the dataset of this study, both for absolute and relative roughness values.

Similar steps were also taken for the prediction of the surface gloss after electropolishing. Figure 5.25 indicates the root mean squared error (RMSE) distribution of the studied models in prediction of final surface gloss based on 100 train-test-splits of the dataset. All predictions were made on the data from the test set. As can be seen in this figure, the Random Forests model exhibits again the strongest performance in representing the dataset.

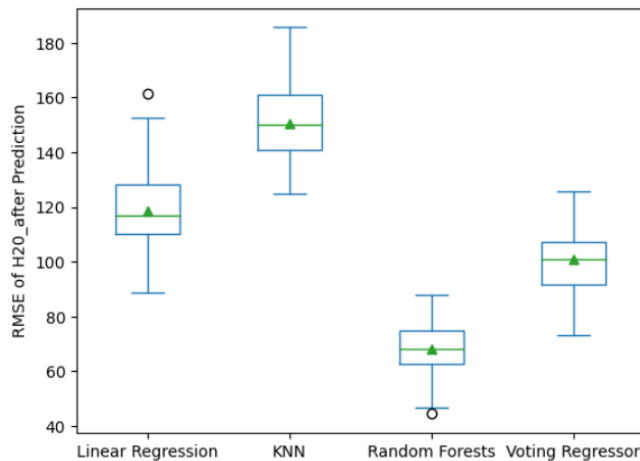


Figure 5.25. RMSE distribution of different models for prediction of final surface gloss on the test set.

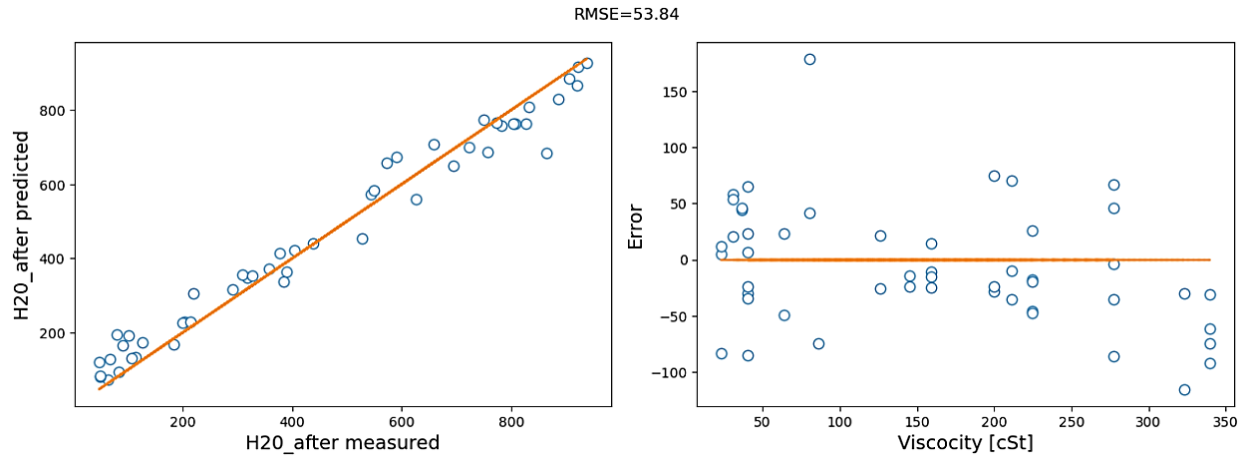


Figure 5.26. Results of Random Forests model in prediction of H2O<sub>after</sub>.

Figure 5.26 indicates the performance of the Random Forests model in predicting the final surface gloss. It must be noted that this plot is just one example of model predictions based on one random train-test-split in the dataset.

As can be noted in Figure 5.22 and Figure 5.26, the RMSE error of the Random Forests model in the prediction of Ra<sub>after</sub> and H2O<sub>after</sub> is 0.01  $\mu\text{m}$  and 53.84 GU, respectively. Earlier in this chapter, the measurement error for the surface roughness (Ra) and gloss (H2O) was estimated at 0.01  $\mu\text{m}$  and 16 GU, respectively. It can be concluded that the constructed dataset has enabled the Random Forests model to reach the surface roughness measurement precision, which is the highest attainable precision for the model. The error of the Random Forests model in prediction of surface gloss is also quite close to our surface gloss measurement precision.

## 5.8 Concluding remarks

- The results of electropolishing experiments indicate the feasibility of achieving a range of surface finishes through the adjustment of polishing process parameters. However, it is essential to find the right balance between obtaining the target surface finish and upholding other critical factors like material removal rate and cost-efficiency.
- Even in an extensively-used polishing bath, satisfactory surface qualities can be attained by using the correct polishing settings.
- The dataset created in this study exhibits a well-balanced distribution of conductivity and viscosity values, ensuring a sufficient representation of various bath states without an undue emphasis on any particular state.
- The final surface roughness and brightness of the samples exhibit a high degree of correlation with each other, as well as with the conductivity and viscosity of the polishing bath.



- All the investigated machine learning algorithms demonstrated an increase in their prediction error as the viscosity of the solution increased.
- The Random Forests model emerged as the most accurate representation of the dataset and was consequently chosen for use in the prediction tool.
- The Root Mean Square Error (RMSE) of the Random Forests model in predicting the final surface roughness of the electropolished samples was found to have reached the level of surface roughness measurement precision, representing the highest achievable precision for a model. The prediction error of the Random Forests model for the final surface gloss of the samples is also quite close to the estimated surface gloss measurement precision.

## 6. Model Prediction of Polishing Parameters for Given Bath States

### 6.1. Introduction

As previously discussed, the target of this study is to develop a prediction tool to be used by electropolishing operators for tuning the polishing process parameters. This tool should predict the required process parameters for achieving a desired surface finish for a given bath state. As discussed in Chapter 5, in the first step towards developing this tool, a representative and balanced dataset was constructed from various electropolishing conditions and results. Next, different machine learning algorithms were used to analyze the dataset. The results of model performance evaluations in Chapter 5 indicated that among the studied models, the Random Forests model had the highest accuracy in representing and summarizing the constructed dataset together with the highest generalization potential. Therefore, this model was selected to be used as the basis of our target prediction tool. In this chapter, first, the development process of the prediction tool from the selected model is explained, and several instances from the dataset are used to showcase the performance of the tool over familiar conditions. The tool's capacity to generalize to unseen conditions, such as polishing baths different from those used in the dataset, is next examined through a series of electropolishing experiments. Finally, the results are interpreted, and potential limitations of the tool are discussed.

### 6.2. Development of the prediction tool

After training and hyperparameter tuning, the Random Forests model was reversed to predict the polishing parameters required for achieving different surface finishes. A linear regression model was further added as output layer to remove the noises and smoothen out the Random Forests model's predictions. The outcome of the linear regression model is the final tool to be used by the operator for estimating the required process parameters. Figure 6.1 illustrates the structure of the prediction tool. Figure 6.2 presents an instance of the prediction tool calculations, where blue circles demonstrate the predictions made by the Random Forests model, and the orange line denotes the linear regression model fitted to the predictions. The input parameters of the tool are the initial surface roughness indexes of the part ( $R_a$ ,  $R_q$ ,  $R_z$ ) and the temperature, electric conductivity, and viscosity of the polishing bath. The tool predicts the process parameters necessary for obtaining various surface qualities for two scenarios: a) Using a polishing voltage of 5 V and variable polishing times, and b) Using a polishing time of 900 s and different polishing voltages.

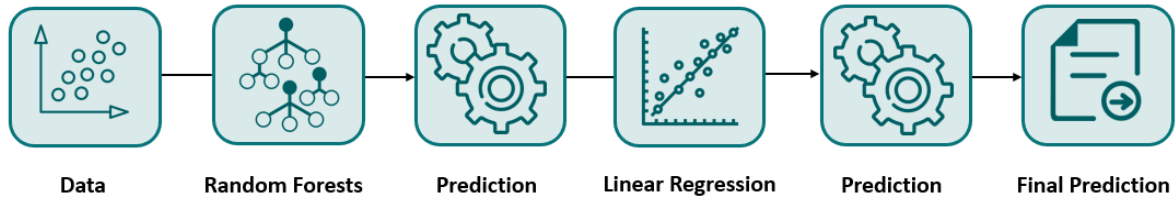


Figure 6.1. Architecture of the prediction tool.

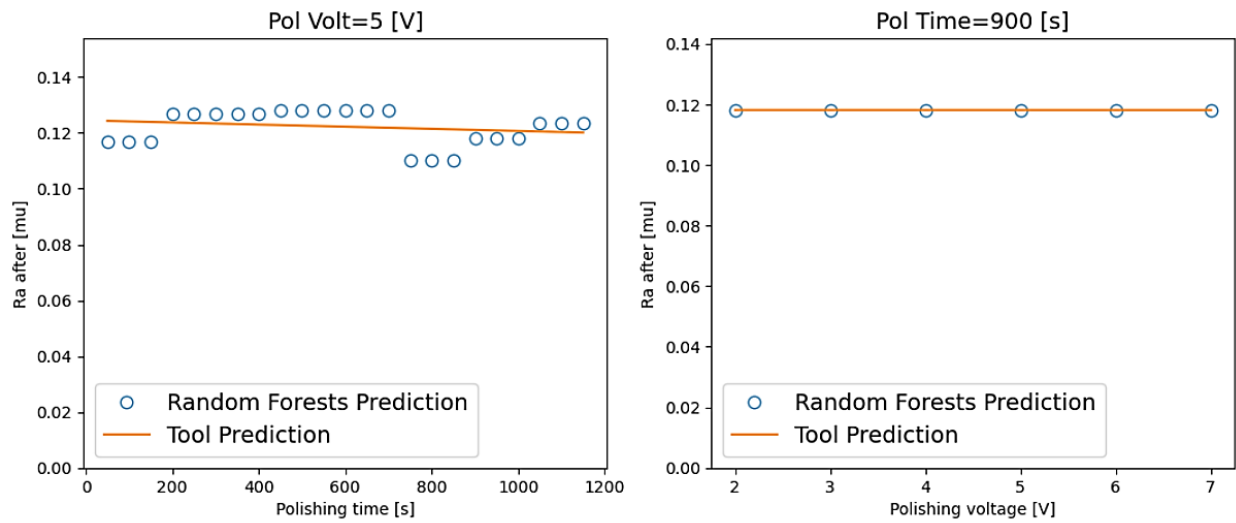


Figure 6.2. Predictions made by the tool outlined in Figure 6.1.

### 6.3. Performance of the prediction tool on previously seen solutions

To compare the tool predictions with actual observations, the tool was first trained on the complete dataset (no train-test-splitting). Next, sample data of the initial surface roughness and bath conditions were extracted from the dataset and fed to the tool. Figure 6.3 presents the tool predictions (blue line) and measured values (orange circle) for the final Ra, Rq, and Rz roughness of the parts electropolished in solutions 1, 2, and 3 of Chapter 4. The error bars shown in the plots demonstrate the Ra, Rq, and Rz measurement errors obtained by calculating the average of the surface roughness standard deviations. It can be understood from these plots that the prediction tool works properly on points from the dataset which was expected as the points are drawn from the dataset used to build the model.

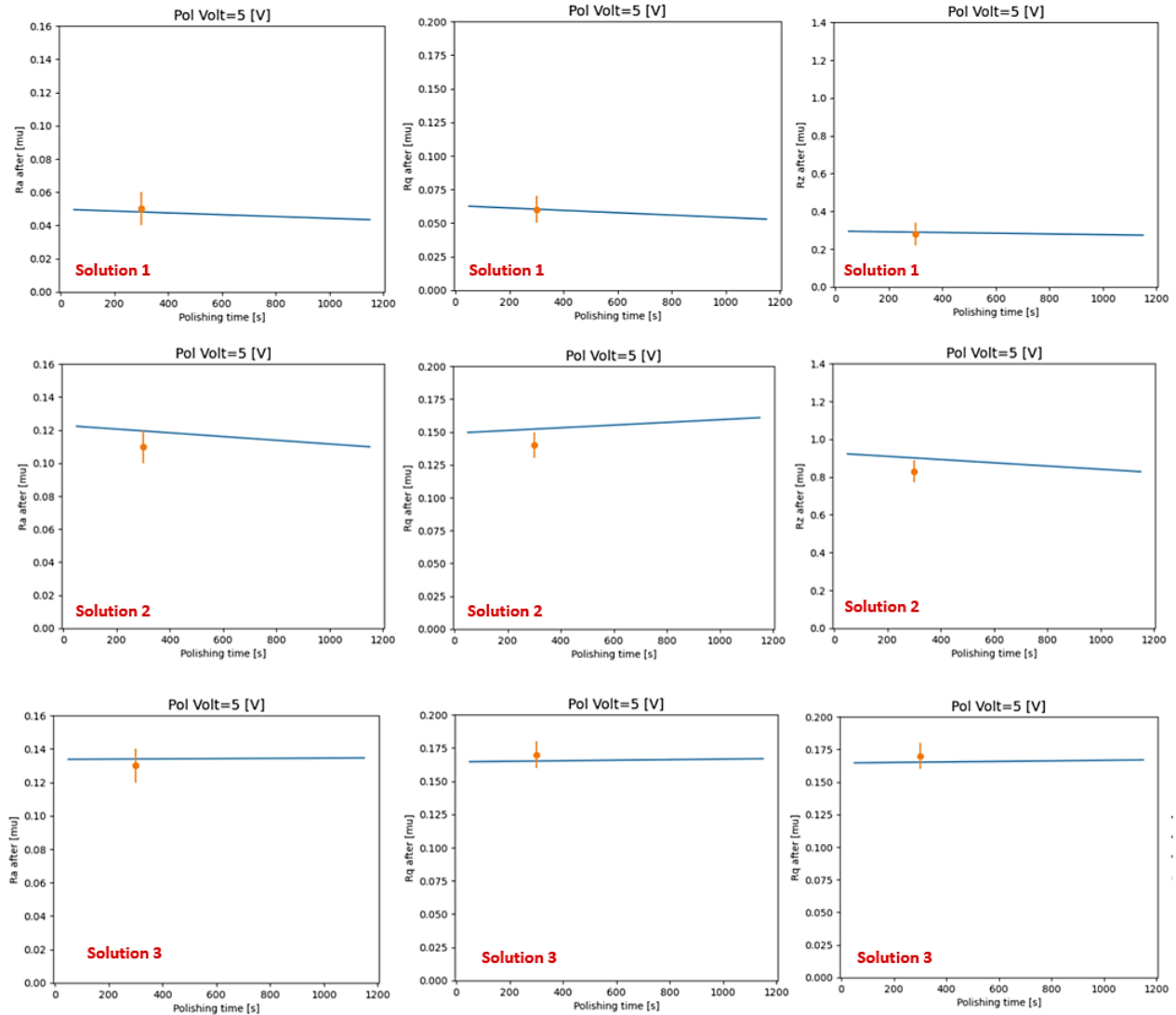


Figure 6.3. Final surface roughness predictions for the for the sample polished in solutions 1, 2, and 3 of Chapter 4, under 5 V for 300 s. The blue line is the prediction tool, while the orange circles demonstrate the measured values.

#### 6.4. Generalization capacity of the prediction tool to unfamiliar polishing baths

As expected, the tool predictions made for initial surface roughness and solution characteristics extracted from the dataset were in agreement with the measured values. The next step is to determine the tool's capability to generalize to new, unseen data. Therefore, the prediction value of the tool is investigated in the case of samples treated in previously unseen polishing baths. In this step, seven solutions were studied that differed from the dataset electrolytes in terms of preparation and usage history, acids mixing ratio, and the type and concentration of impurities. These solutions were prepared to simulate various situations that might arise during the service

life of an industrial polishing bath. Table 6-1 presents the main characteristics of the investigated solutions.

Table 6-1. Characteristics of studied baths.

<b>Bath</b>	<b>Electric Conductivity (mS/cm)</b>	<b>Viscosity (mPa.s)</b>	<b>Major Difference Compared to the Training Dataset</b>
1	171.7	14.3	Acids mixing ratio
2	187.2	13.1	Acids mixing ratio
3	116.5	22	Acids mixing ratio
4	27.2	279.8	Usage history Type and concentration of impurities (Copper ions)
5	45.5	141.3	Usage history Acids mixing ratio
6	33	247.7	Usage history Used for polishing AlSi10Mg parts.
7	91.3	52.9	Acids mixing ratio

The baths presented in the Table 6-1 are numbered in order of decreasing similarity to the original bath studied in the dataset. Baths 1, 2, 3 of the table were prepared by adding fresh electrolytes (sulfuric acid- phosphoric acid- DI water) with different acids-to-water mixing ratios to a moderately-used bath (Table 6-2).

Table 6-2. Composition of the fresh electrolytes used in the preparation of baths 1, 2, and 3.

<b>Fresh solution</b>	<b>Composition %(v/v)</b>		
	<b>Sulfuric Acid</b>	<b>Phosphoric Acid</b>	<b>DI Water</b>
Original	35	50	15
Used in Solution 1	25	50	25
Used in Solution 2	30	50	20
Used in Solution 3	40	50	10

Baths 1, 2, and 3 were used to simulate situations where the original aged bath is replenished with a fresh electrolyte of slightly different composition. Indeed, in industrial electropolishing facilities, bath replenishment is not always conducted correctly. For instance, if the supplier of the original polishing solution is changed, the new fresh electrolyte might not have the same composition as the original bath. Especially since the exact composition of the commercially available electrolytes are usually not disclosed. These solutions are essentially similar to previously investigated baths; yet the effect of their slight compositional difference on the performance of the prediction tool merits consideration.

Baths 5 and 7 were utilized to investigate the performance of the prediction tool in more extreme scenarios of incorrectly formulated fresh electrolytes. In the case of bath 5, a severely-used electrolyte (which was even more aged than the dataset's heavily-used electrolytes) was mixed with a fresh solution of the incorrect composition (sulfuric acid 25% v/v: phosphoric acid 50% v/v: DI water 15% v/v). Bath 7 on the other hand, was prepared by adding pure sulfuric acid to a moderately-used electrolyte.

In industrial electropolishing operations, it is not uncommon for counter electrodes, which are typically made of copper, to fall accidentally into the bath during manipulation. Over time these electrodes dissolve into the solution and release excess copper ions. Bath 4 was used to simulate such cases and investigate the performance of the prediction tool in the presence of other metal impurities in the polishing bath. In order to prepare bath 4, 0.5 mol/L of copper sulfate ( $\text{CuSO}_4$ ) (similar to the amount of Fe ions detected by ICP analysis in solution 1, from 4 (Table 4-2)) was dissolved in the severely-used electrolyte. As mentioned before, to move further away from the previously examined baths, the severely-used electrolyte was aged to a point that is not typically observed in practical production as it would have been long replenished.

Finally, bath 6 was prepared to simulate the situation where the electrolyte is used for polishing metals other than stainless steel 316. This could happen if a polishing facility needs to urgently process a part made from a metal other than the one the polishing bath was intended for. To prepare this bath, the severely-used electrolyte was mixed in a 2:3 ratio with a solution that had been employed for a long time to electropolish an AlSi10Mg part with a 316 stainless steel cathode. Bath 6 is radically different from the solutions studied in the dataset as it contains materials such as aluminum, silicon, and magnesium.

Each bath was then used to electropolish two samples. For easier use of the prediction tool and comparison with previous results, the samples were treated either with an applied polishing voltage of 5 V for 300 s or 3 V for 900 s. The tool was then employed to predict the final surface roughness of the samples in each bath. Although, in reality, the tool could use the complete available dataset for making predictions of new data points, 100 train-test-splits of the dataset were conducted at this step to simulate different cases. The error of the tool was then estimated by plotting the distribution of its root mean squared error (RMSE) in the prediction of different target variables ( $Ra_{\text{after}}$ ,  $Rq_{\text{after}}$ ,  $Rz_{\text{after}}$ ) based on 100 train-test-splits (Figure 6.4).

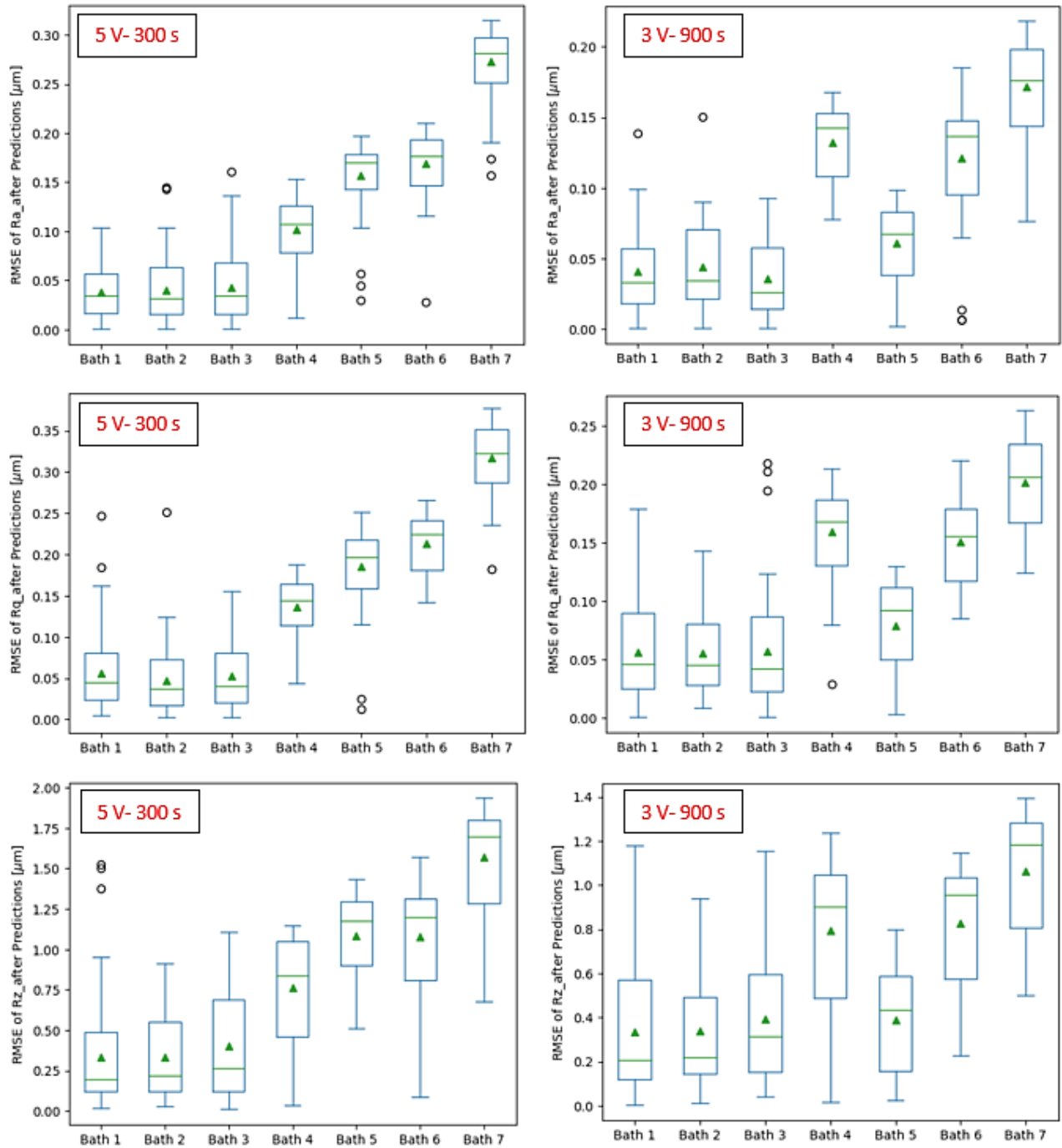


Figure 6.4. Distribution of the tool's RMSE in prediction of Ra, Rq, and Rz for samples electropolished under 5 V for 300 s, and 3 V for 900 s in the studied solutions.

As can be seen in Figure 6.4, the RMSE of the tool predictions for the first 3 solutions with higher conductivities appear to be in the same range and considerably less than the rest of the investigated solutions. Figure 6.5 displays the surface of the samples electropolished with different polishing parameters in the first three baths. As previously discussed in 4, moderate variations in the composition of the polishing bath do not significantly affect the electropolishing results. As can be noted in the picture, all of the electropolished samples appear smooth and bright, which could be attributed to the high electric conductivity and low viscosity of the baths that facilitate the polishing action.

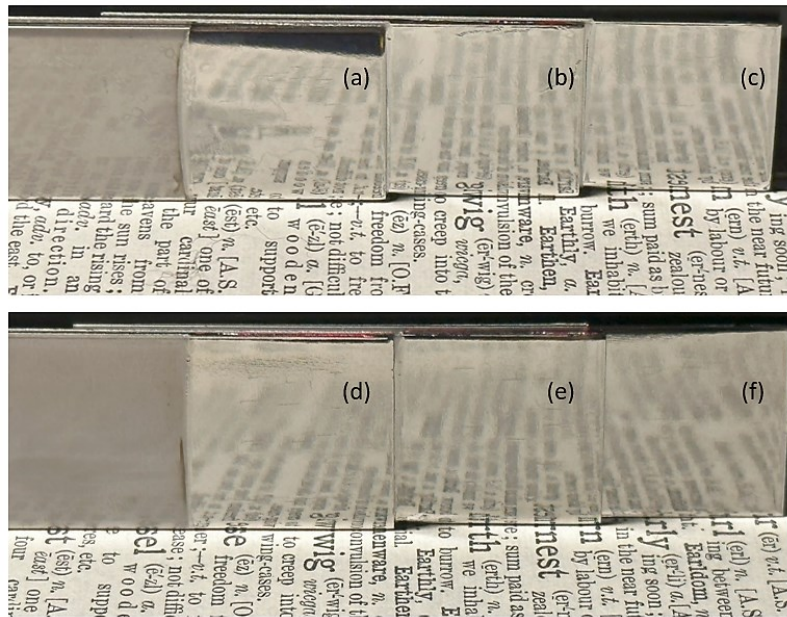


Figure 6.5. Samples electropolished under 5V and 300s in (a) solution 1, (b) solution 2, and (c) solution 3, and under 3V and 900s in (d) solution 1, (e) solution 2, and (f) solution 3.

These results suggest that refreshing the severely used baths with a fresh electrolyte whose composition is slightly different does not undermine the accuracy of the tool predictions. However, as previously stated, achieving favorable polishing results requires a balance between different constituents of the bath. This point was also observed while electropolishing in solution 7, which was prepared by adding pure sulfuric acid to a moderately-used solution. According to Figure 6.4, in bath 7, the RMSE of the tool in the prediction of  $Ra_{after}$ ,  $Rq_{after}$ , and  $Rz_{after}$  is the highest among all studied solutions. These results can be explained by the fact that the polishing bath's composition was radically changed by adding only sulfuric acid. Given that the model was never trained on such scenarios, it is normal that it does not perform well in this example.

Pictures taken from the surface of the samples electropolished in bath 7 (Figure 6.6) further corroborate the results. The surface of both electropolished samples is dull and matt, which is indicative of nonexistent polishing action. It has been pointed out by several studies that both



sulfuric acid and phosphoric acid must be present in the polishing bath to obtain acceptable results. Indeed, it was pointed out by Ponto et al. <sup>1</sup> and Datta et al. <sup>2</sup> that in concentrated sulfuric acid solutions, metal dissolution is inhibited due to the formation of a stable passive film on the surface, and hence, no polishing effect is observed. It can, however, be deduced from Figure 6.4 that the increase in the tool's prediction error is still within a reasonable range, even in a situation as extreme as eliminating one of the acids from the polishing bath.

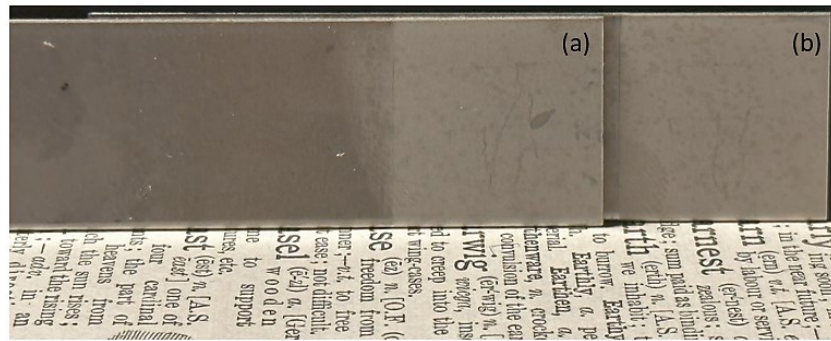


Figure 6.6. Samples electropolished in solution 7 under (a) 5 V and 300 s, and (b) 3 V and 900 s.

It is also evident from Figure 6.4 that in comparison to the first 3 solutions, the RMSE of the prediction tool is higher in solutions 4, 5, and 6. As it was discussed in 5, the error of the Random Forests model increases with the viscosity of the polishing bath. Table 6-2 indicates that solutions 4, 5, and 6 have the highest viscosities among the studied baths. The surface of the samples electropolished in solutions 4, 5, and 6 is shown in Figure 6.7. In addition to their generally matt finish, streak marks can be observed on some surfaces, which as previously discussed in 4, is one of the major downsides of electropolishing in high-viscosity solutions. The defect occurs because highly viscous solutions oppose the movement and diffusion of the generated bubbles away from the workpiece surface.

Figure 6.4 indicates that although the prediction tool does not perform as well for solutions 4, 5, and 6 as it did for the first three solutions, it is still reliable enough to be used as a starting point to quickly estimate proper polishing parameters.

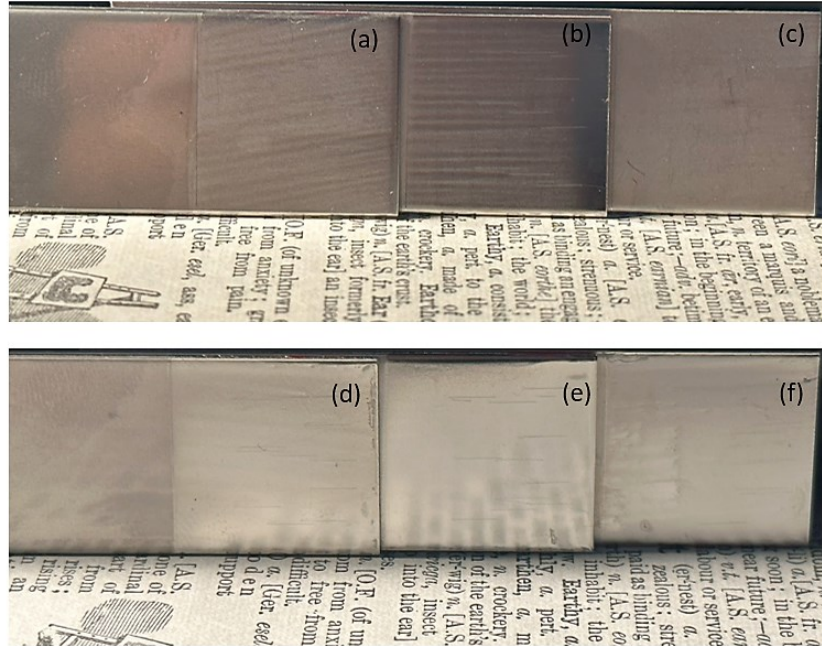


Figure 6.7. Samples electropolished under 5 V and 300 s in (a) solution 4, (b) solution 5, and (c) solution 6 and samples electropolished under 3 V and 900 s in (d) solution 4, (e) solution 5, and (f) solution 6.

Overall, it was shown that the prediction value of the tool decreases with the degradation of the polishing bath and the increase of its viscosity. Naturally, there comes a point in the service life of the polishing bath beyond which the high solution viscosity prevents the tool from delivering acceptable results. Consequently, in real-life applications, industrial electropolishing operations may establish thresholds for the bath viscosity or acceptable prediction error to determine the point of bath replenishment or replacement. The threshold point can be determined based on the application or the customer's required level of surface finish accuracy or quality consistency. For instance, biomedical and food and beverage industries have stringent requirements for surface quality, while decorative applications may be more forgiving.

### 6.5. Concluding remarks

- The prediction tool operates as expected on initial surface roughness and solution parameters collected from the dataset.
- The RMSE error of the prediction tool was at its lowest for baths 1, 2, and 3, owing to their high electrical conductivity and low viscosity. It may be concluded that the accuracy of the tool predictions is not significantly compromised by adding a fresh electrolyte of a slightly different composition to a heavily-used bath.

- The performance of the prediction tool experienced a decline as the polishing baths diverged further from the previously studied electrolytes. It was, however, shown that the RMSE of the prediction tool remained acceptable in previously unexplored scenarios, such as the presence of different types of metal impurities in the bath or the use of the polishing bath on a metal different from the one originally intended for the electrolyte.
- Despite the decrease in the prediction tool's accuracy with the deterioration of the polishing bath and the increase in its viscosity, the tool remains sufficiently reliable to serve as an initial reference point for rapidly estimating appropriate polishing parameters.
- The highest prediction error of the tool was exhibited for the case of refreshing a moderately-used solution with pure sulfuric acid. However, the increase in the tool's prediction error in a situation as extreme as eliminating one of the acids from the polishing bath was still found to be within a reasonable range.
- The most substantial prediction error of the tool was observed in the extreme case of replenishing the polishing bath with only one of the acids. Nevertheless, even for such a radical change in the polishing bath, the increase in the tool's prediction error was still found to be within a reasonable range.
- Despite the promising performance of the prediction tool in anticipating the final surface roughness and brightness of samples electropolished with different parameters across various bath states, it does not predict the appearance of common surface defects encountered in the electropolishing industry, such as the orange peel effect or gassing streaks. As previously shown in Chapter 4, use of I-V plots derived from electropolishing tests conducted at varying voltages for a fixed duration can aid in predicting, at different bath states, the polishing voltages at which these defects may appear. By integrating these two tools, a complete picture of the expected outcomes of the polishing process for different part and bath conditions and process parameters can be attained.

## 7. Outlook

In this chapter some of the potential future research avenues are proposed for wider application of the findings presented in this study.

### 7.1. Extending the scope of the study

The results of this project proved for the first time that it is indeed possible to predict the proper parameters (to achieve a desired outcome) for an electrochemical process based on the current bath state. The prediction tool developed in this project demonstrated excellent precision by matching the precision of Ra surface roughness and H2O brightness measurements (0.01  $\mu\text{m}$  and 12 GU prediction error vs. 0.01  $\mu\text{m}$  and 16 GU measurement error).

Furthermore, as demonstrated in Chapter 6, the prediction tool is highly robust, as seen by its adequate performance even in situations quite far from the dataset. The prediction tool was found to be tolerant of severely contaminated electrolytes or even the electropolishing of other metals in the bath. Given the promising performance of the tool, we can begin to build upon it and unlock its potential for various applications.

Due to time constraints, this project only considered a simple case of one type of polishing bath and metal. It seems, however, quite possible that a similar model be developed for other combinations of metals and polishing baths. Power and water usage for processing and washing each item can also be recorded for cost-per-part estimations. All this data may be combined in a sizable dataset to be used later for finding the best polishing parameters that not only produce the desired surface finish but also guarantee the least amount of energy or water consumption or bath pollution. Of course, training the models takes longer with such large datasets. Alternatively, more time-efficient models can be utilized to build the prediction tool.

### 7.2. Increasing the size of the dataset for better generalization

An important benefit of using a data-driven strategy for personalization and quality control of electropolishing services is the capacity for continuous improvement. As more polishing operations are conducted, additional data is collected from the process, and the machine learning model becomes more capable of detecting the subtle patterns in the dataset that may not have been apparent initially. As a result, the model makes more precise predictions and is better equipped to generalize its learning to new, unseen data.

The prediction tool developed in this study has the capacity to learn from previous experience and improve with size of the dataset. To illustrate this capacity, the tool was trained on increasing portions of the dataset points and its root mean squared error (RMSE) distribution in prediction of

different target variables based on 100 train-test-splits of the dataset was plotted. Figure 7.1 presents the RMSE error of the tool as a function of the dataset size for 3 samples electropolished at 3 different bath states. As can be noted in the plots, the RMSE of the prediction tool decreases as the number of electropolished samples grows. It must however be emphasized that the dataset constructed in this study was large enough to allow the prediction tool to reach the precision of roughness measurements, which is the best possible outcome as the prediction cannot be more accurate than the process itself.

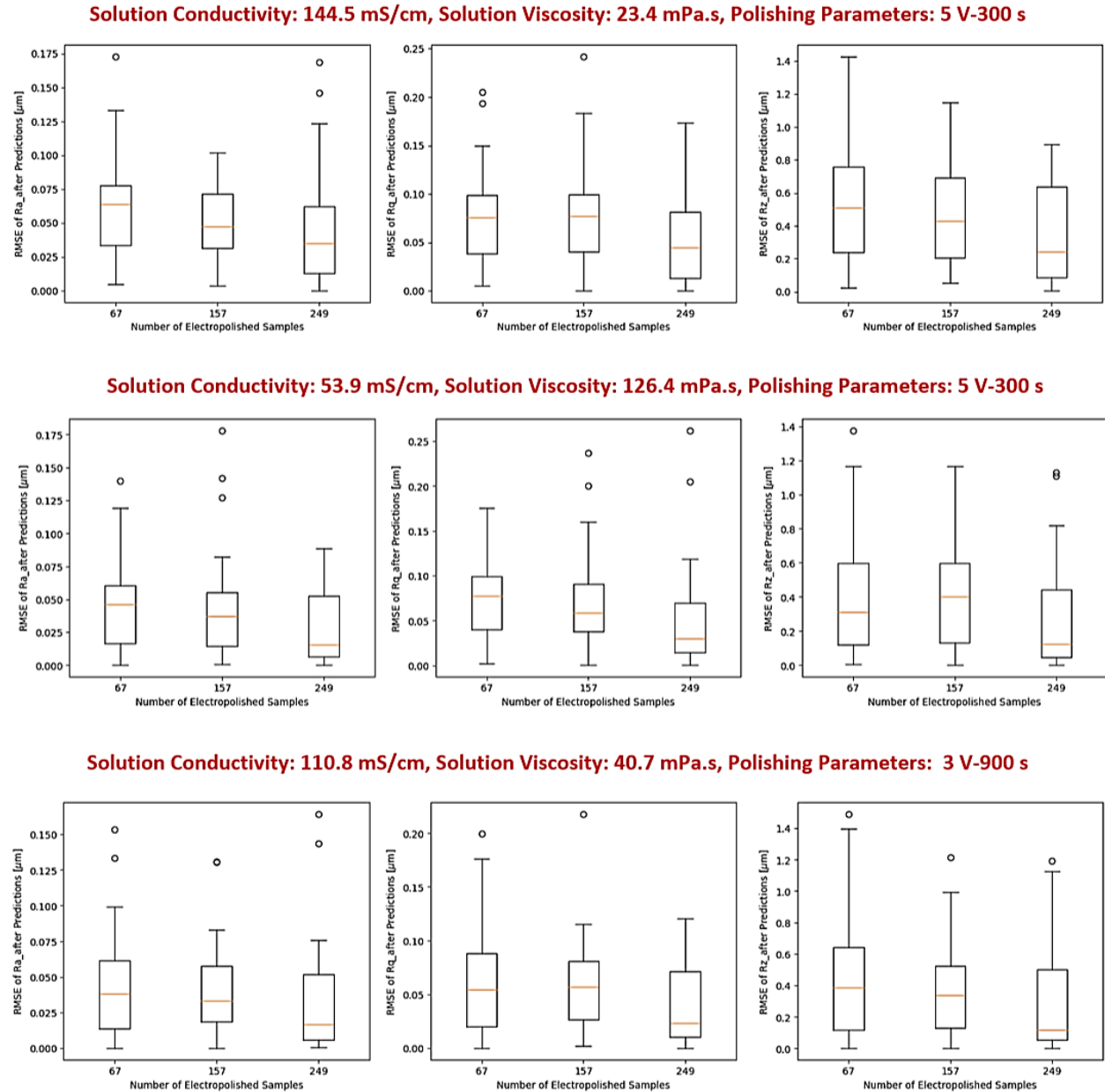


Figure 7.1. Variation of the tool RMSE error in prediction of Ra<sub>after</sub>, Rq<sub>after</sub>, and Rz<sub>after</sub> with increasing the size of the dataset.

### 7.3. Application of the K Nearest Neighbors (KNN) algorithm

Creating a smart electropolishing process necessitates regular monitoring and recording of bath and part parameters. Aside from the ability to improve with a growing dataset, the ideal prediction tool should not require complete retraining when new data points are received. In applications where new data constantly arrives, a model capable of incremental learning can easily adapt to the dynamic changes of the production environment and maintain its performance. Therefore, in the context of smart electropolishing operations where new data is continuously collected from various sources such as roughness measurements or bath temperature sensors, incremental learning can help the prediction tool adjust to the changing bath conditions and preserve the consistency of the surface quality. This ongoing learning process can lead to better decision-making and prediction accuracy.

During the training phase, "eager" machine learning algorithms (also known as model-based algorithms) build a specific model that summarizes the correlations and patterns in the dataset to make predictions on new, unseen data. A "lazy" or instance-based machine learning algorithm, in contrast, doesn't learn a specific function or make generalizations while training on the dataset. Instead, it stores the entire training dataset in memory and makes predictions by comparing new data points to the existing training examples <sup>1</sup>. Since lazy learning algorithms can easily incorporate new data without the need to rebuild the entire model, they are well suited for continuous data streaming applications.

As a model-based learning algorithm, Random Forests actively builds and trains decision trees during the training phase and then combines the predictions of these trees to make more accurate and robust predictions for new data. Therefore, the Random Forests model has to be continually retrained as the dataset evolves. The k-Nearest Neighbors (KNN) algorithm, on the other hand, as the most common lazy learning algorithm, determines the k nearest data points from the training dataset based on a similarity metric (Euclidean distance) to predict a new data point. This approach is thus especially useful in scenarios where new data points are constantly added to the dataset since it does not need to be completely retrained to make predictions on these new points. This approach may also be further improved by optimizing the similarity metric used by the KNN model. For example, rather than relying on the Euclidean distance (as we have done in 5), a distance-weighted strategy may be implemented. In this approach, higher weights are assigned to the nearest neighbors and lower weights to the more distant neighbors <sup>129</sup>. This ensures that the influence of closer neighbors on the final prediction or decision is more pronounced, while still allowing for some consideration of information from more distant neighbors.

Retraining the Random Forests model is not an issue for the dataset constructed in this study, but larger datasets might require employing more efficient models. Although the KNN model proved

---

<sup>1</sup> If the dataset becomes so large it can no longer fit into the memory, tools from the field of Big-Data will have to be used (e.g. distributed data processing systems such as Apache Sparks)

less precise than the Random Forests model, it can nevertheless facilitate incremental learning for the smart electropolishing process. Figure 7.2 displays the RMSE error of the KNN algorithm as a function of the dataset size for the 3 samples discussed in Figure 7.1. Compared to the Random Forests model, the KNN algorithm is easier to employ with a growing dataset. It is only necessary to confirm that the algorithm's  $k$  value is still acceptable when additional data points are received. However, after the dataset has grown large enough, we expect the  $k$  value remains constant.

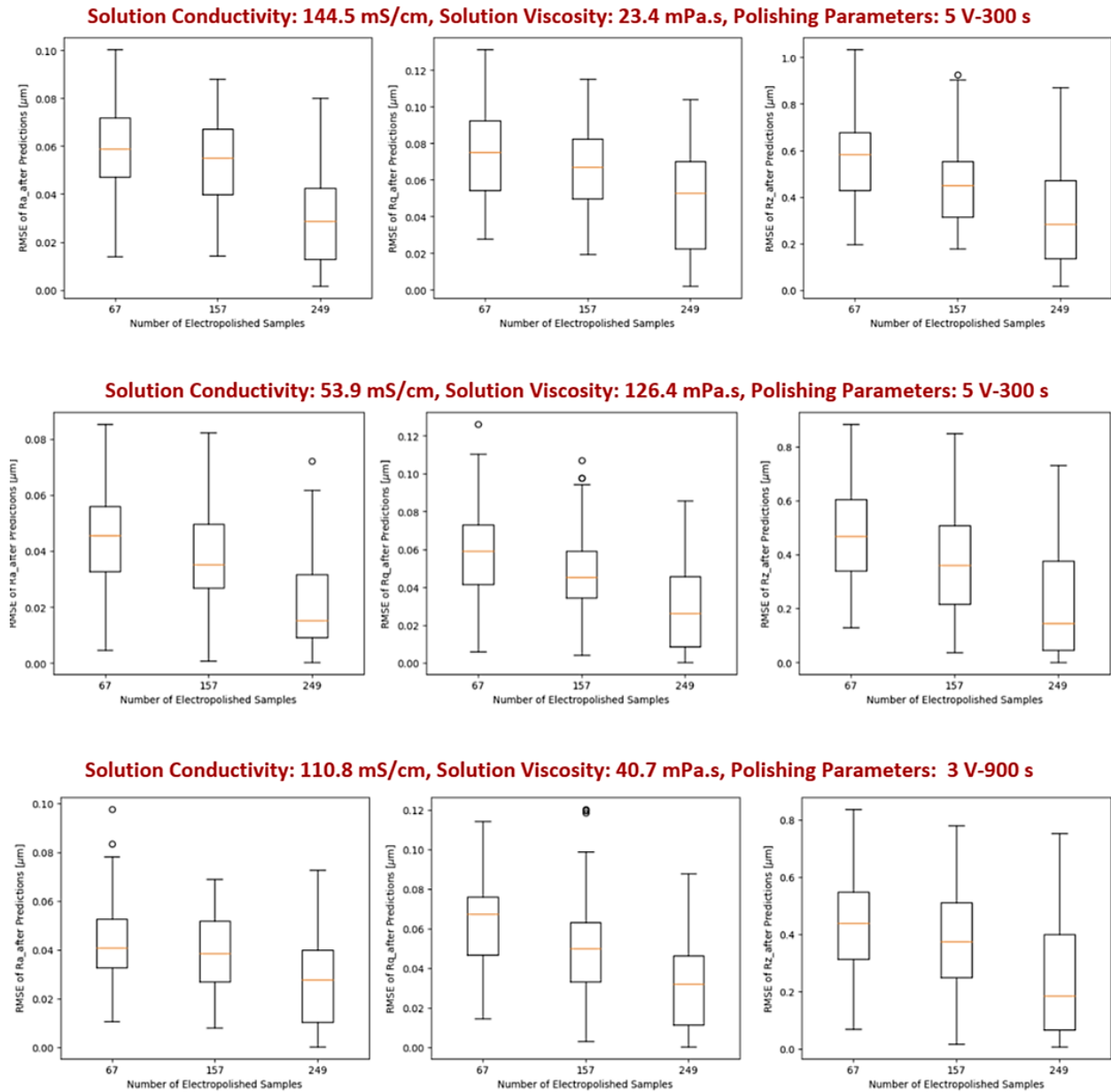


Figure 7.2. Variation of the KNN model RMSE error in prediction of  $Ra_{after}$ ,  $Rq_{after}$ , and  $Rz_{after}$  with increasing the size of the dataset.

## **7.4. Software architecture for actual deployment of the prediction tool in production**

Actual deployment of the prediction tool in an electropolishing facility can be realized by automated data streaming pipelines. These pipelines allow for real-time ingestion, processing, and analysis of production data as it flows through the system. Therefore, they enable prompt response to changing process conditions and rapid decision-making. Data streaming systems require a sophisticated software architecture for controlling the connection and collaboration of various system components as well as collecting, storing, and processing the data. In Figure 7.3 we illustrate a proposed software architecture that can be deployed on-premise (the electropolishing facility) or in the cloud to effectively use the prediction tool developed in this project. In the perception layer, sensors or programmable machines that interact with the physical production environment collect the data from monitoring of equipment, processes, and events. The connection layer connects various system components with different data formats, communication protocols, and interfaces. It employs a combination of hardware and software tools to ensure effective communication and smooth data flow between various system components. The acquired data is then forwarded to the aggregation layer, where Apache Kafka distributed streaming platform<sup>2</sup> may be used for real-time data ingestion and processing. The messaging pattern between different components of a data streaming architecture determines how data is exchanged and processed within the system. Using Kafka Connect framework, the Kafka cluster connects to external systems to import and export data using the Publish-Subscribe (Pub-Sub) messaging paradigm. In this framework, source connectors receive data from sensors (publishers) and feed them into different topics. Sink connectors gather the data from the topics and make them available to consumers (subscribers) who have expressed interest in a specific topic. In the storage layer, the ingested production data is distributed across a cluster of one or more machines (brokers) that are responsible for storing and managing the data. This way, if one machine fails or needs to be updated, the complete production data will not be lost, and the Kafka cluster continues to function. The data can also be distributed in cloud systems in different locations for extra precaution. Data preparation operations like data cleansing and rearrangement are handled by the computation layer. Sink connectors then transfer the preprocessed data to databases, data warehouses, or other external systems for applications and reporting. The application layer then provides notifications, machine learning algorithms, and visualization tools for monitoring and analyzing real-time data. Finally, the data will be forwarded to the business layer, where insights into the process are generated and acted upon based on predefined criteria. Implementing the prediction tool with such modern architecture can enable time and cost-effective process optimization, automate the quality control process, and reduce the plant's dependence on a qualified workforce willing to work in hazardous polishing environments.

---

<sup>2</sup> Originally developed by LinkedIn, it was donated to the Apache foundation by LinkedIn in 2011.



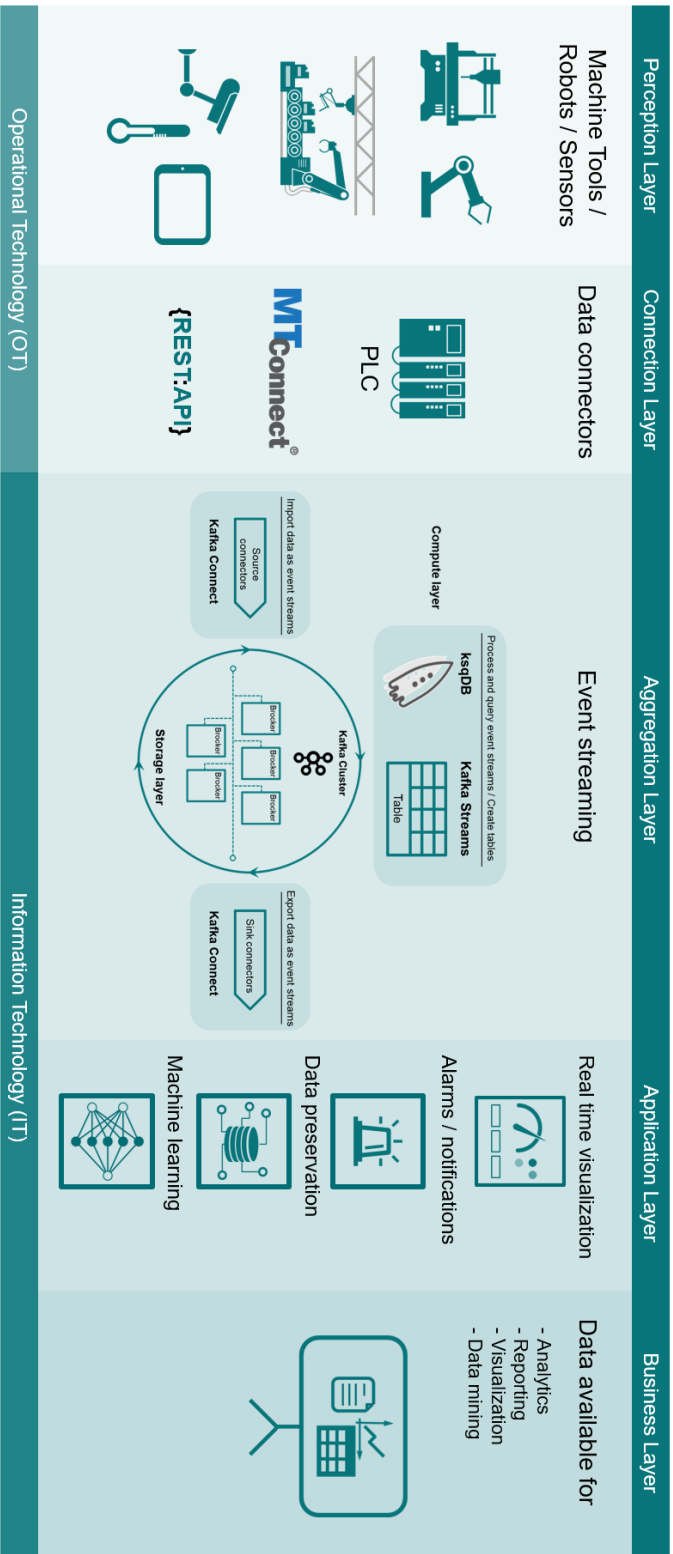


Figure 7.3. Example of a software architecture of actual deployment of the prediction tool in production.

## 8. Conclusion

Throughout this thesis journey, we have advanced our understanding of the effect of electrolyte aging on the outcomes of electropolishing process achieving meaningful insights into the role of bath state and polishing process parameters in determining the ultimate surface finish of the electropolished parts.

Most importantly, we have diligently pursued the objectives set forth in the introduction chapter:

- *Establishing a methodology for quantifying the state of an aging bath and determining relevant electrolyte properties:*

We proposed that, in the context of deteriorating the performance of a polishing bath over extended use, it is more appropriate to replace the concept of bath "age" with bath "state." The latter term offers a clearer reflection of the complex processes a bath undergoes during its service life, whereas the former can be misleading, as the number of treated parts or the total ampere-hours of polishing treatment have a lesser influence on a bath's polishing performance compared to its usage and replenishment history.

We were also able to identify the relevant physicochemical properties of the polishing bath (namely, the specific gravity, electric conductivity, and viscosity), which can effectively characterize its condition at any given point during its service life. These properties were selected not just for their impact on the bath's performance but also for their suitability for rapid and straightforward on-line measurement in industrial electropolishing facilities, eliminating the need for intricate equipment or extensively trained personnel.

- *Exploring the possibility of employing the physicochemical properties considered relevant to the state of the polishing bath for maintaining the consistency of electropolishing results:* After establishing the importance of closely monitoring and controlling the bath's physicochemical properties for achieving consistent and high-quality electropolishing results, it was concluded that these properties are not the sole determinants of the electropolishing process's outcome. It was proven through experimental results that with the same set of polishing parameters, conducting straightforward measures to compensate electrolyte aging, like modification of the applied polishing potential or re-adjusting bath composition, cannot assure uniform polishing results. These properties, however, may be used in conjunction with correct process parameters (such as the polishing voltage and time) to achieve consistent electropolishing outcomes. This conclusion highlighted the necessity for a data-driven approach to identify the suitable process parameters for obtaining a target surface finish at a given bath state.

- *Building a comprehensive dataset of the polishing process parameters and resulting surface qualities:*

We constructed a comprehensive and balanced dataset, incorporating a substantial quantity of data points derived from numerous electropolishing experiments conducted at different bath conditions. The distribution of electric conductivity and viscosity of the polishing baths indicated that adequate instances of each bath state were included without excessive emphasis on any specific state. Analysis of the dataset also revealed the most influential parameters affecting the final surface quality of the electropolished parts.

- *Developing a tool to predict the optimum process parameters for achieving a target surface quality at a given bath state:*

We evaluated a variety of machine learning algorithms to assess their accuracy in summarizing the constructed dataset. Out of the algorithms considered, the Random Forests model emerged as the most accurate, predicting the surface roughness and brightness of the electropolished samples with the lowest Root Mean Square Error (RMSE). This precision of the Random Forests model was shown to match our surface roughness measurement precision, which is the highest precision attainable for a model. The precision of the model in predicting the final surface brightness was also found to be very close to our surface gloss measurement precision.

We also evaluated the prediction tool in terms of its predictive power and generalization capability to unseen scenarios. The tool was found to be highly tolerant of variations in the polishing electrolytes. It was also shown that even in scenarios that significantly deviate from the dataset, the prediction tool remains sufficiently robust to serve as an initial reference point for quickly estimating appropriate polishing parameters.

- *Developing a tool to identify the polishing voltages associated with the occurrence of surface defects at different bath conditions:*

We generated a series of current-voltage plots by recording the polishing current for samples electropolished at various bath states and under different polishing voltages for the same duration. Upon examining the surfaces of these samples, we successfully identified a specific region within their I-V plots that correlates with the occurrence of common surface defects encountered in the electropolishing industry, including the orange peel effect and gassing streaks. We consequently deduced that these current-voltage plots can be employed at various bath states to determine the polishing voltages most likely to induce these surface defects. Upon the application of the developed prediction tool for determining the process parameters required to attain the desired surface finish, these I-V plots can serve as a supplementary tool to avoid using process parameters that might lead to the emergence of surface defects. When combined, these two tools offer a

comprehensive understanding of the electropolishing results for different bath states and process parameters.

## 9. References

1. <https://www.swatch.com/en-ca/swatch-x-you.html>. Accessed on December 18, 2023.
2. <https://www.nike.com/nike-by-you>. Accessed on December 18, 2023.
3. S. Vaidya, P. Ambad, and S. Bhosle, *Procedia Manuf*, **20**, 233–238 (2018).
4. M. Xu, J. M. David, and S. H. Kim, *International Journal of Financial Research*, **9**, 90–95 (2018).
5. S. Kotha, *Strategic Management Journal*, **16**, 21–42 (1995).
6. X. Yao and Y. Lin, *The International Journal of Advanced Manufacturing Technology*, **85**, 1665–1676 (2016).
7. <https://gesrepair.com/mass-production-advantages-and-disadvantages/#advantages>. Accessed on December 18, 2023.
8. R. Hans, <https://www.deskera.com/blog/repetitive-manufacturing/>. Accessed on December 18, 2023.
9. S. Aheleroff, N. Mostashiri, X. Xu, and R. Y. Zhong, *Advanced Engineering Informatics*, **50**, 101438 (2021).
10. M. M. Tseng, R. J. Jiao, and C. Wang, *CIRP Annals*, **59**, 175–178 (2010).
11. W. P. Hsiao and M. C. Chiu, *Advances in Transdisciplinary Engineering*, 698–705 (2014).
12. L. A. Hof and R. Wüthrich, *Manuf Lett*, **15**, 76–80 (2018).
13. I. A. R. Torn and T. H. J. Vaneker, *Procedia Manuf*, **28**, 135–141 (2019).
14. M. M. Piller, Frank T; Tseng, *Handbook of research in mass customization and personalization*, p. 33–34, Singapore Hackensack, N.J World Scientific Pub. Co, (2010).
15. F. Mo, H. U. Rehman, F. M. Monetti, J. C. Chaplin, D. Sanderson, A. Popov, A. Maffei, and S. Ratchev, *Robot Comput Integr Manuf*, **82**, 102524 (2023).
16. <http://www.harrisonep.com/benefits-of-electropolishing.html>. Accessed on December 18, 2023.
17. F. Eozénou, S. Berry, C. Antoine, Y. Gasser, J. P. Charrier, and B. Malki, *Physical Review Special Topics - Accelerators and Beams*, **13**, 1–8 (2010).
18. P. Lochyński, S. Charazińska, E. Łyczkowska-Widłak, A. Sikora, and M. Karczewski, *Advances in Materials Science and Engineering*, **2018** (2018).

19. S. Mohan, D. Kanagaraj, R. Sindhuja, S. Vijayalakshmi, and N. G. Renganathan, *Transactions of the IMF*, **79**, 140–142 (2001).
20. F. Eozenou et al., in *Proceedings of the 12th International Workshop on RF Superconductivity (SRF 2005), Ithaca, New York, USA*, vol. 9, p. 451–454, Ithaca (2005).
21. M. Sawabe, T. Saeki, H. Hayano, S. Kato, M. Nishiwaki, and P. V. Tyagi, in *Proceedings of the 1st International Particle Accelerator Conference (IPAC'10), Kyoto, Japan*, p. 2947–2949 (2010).
22. H. Tercan and T. Meisen, *J Intell Manuf*, **33**, 1879–1905 (2022).
23. <https://www.qualitymag.com/articles/97488-why-automated-machine-learning-boosts-quality>. Accessed on December 18, 2023.
24. P. Zheng, H. wang, Z. Sang, R. Y. Zhong, Y. Liu, C. Liu, K. Mubarak, S. Yu, and X. Xu, *Frontiers of Mechanical Engineering*, **13**, 137–150 (2018).
25. D. Weichert, P. Link, A. Stoll, S. Rüping, S. Ihlenfeldt, and S. Wrobel, *The International Journal of Advanced Manufacturing Technology*, **104**, 1889–1902 (2019).
26. I. Ahmed, G. Jeon, and F. Piccialli, *IEEE Trans Industr Inform*, **18**, 5031–5042 (2022).
27. P. V. Tyagi, M. Nishiwaki, T. Noguchi, M. Sawabe, T. Saeki, H. Hayano, and S. Kato, *Appl Surf Sci*, **285**, 778–782 (2013).
28. B. Chatterjee, *Galvanotechnik*, **71**, 71–93 (2015).
29. <https://www.besttechnologyinc.com/electropolishing-equipment/how-does-electropolishing-work/>. Accessed on December 18, 2023.
30. S. F. Rudy, (2021), <https://finishingandcoating.com/index.php/plating/810-electropolishing-process-considerations>. Accessed on December 18, 2023.
31. D. J. Arrowsmith and A. W. Clifford, *Transactions of the Institute of Metal Finishing*, **58**, 63–66 (1980).
32. P. Lochyński, S. Charazińska, M. Karczewski, and E. Łyczkowska-Widłak, *Sci Rep*, **11** (2021).
33. W. Han and F. Fang, *Int J Mach Tools Manuf*, **139**, 1–23 (2019).
34. G. Yang, B. Wang, K. Tawfiq, H. Wei, S. Zhou, and G. Chen, *Surface Engineering*, **33**, 1–18 (2016).
35. S. H. Kim, S. G. Choi, W. K. Choi, and E. S. Lee, *International Journal of Advanced Manufacturing Technology*, **85**, 2313–2324 (2016).

36. A. M. Awad, N. A. A. Ghany, and T. M. Dahy, *Appl Surf Sci*, **256**, 4370–4375 (2010).
37. E. S. Lee, *International Journal of Advanced Manufacturing Technology*, **16**, 591–599 (2000).
38. L. S. Andrade, S. C. Xavier, R. C. Rocha-Filho, N. Bocchi, and S. R. Biaggio, *Electrochim Acta*, **50**, 2623–2627 (2005).
39. A. M. A. Abouelata, *ARPN Journal of Engineering and Applied Sciences*, **13**, 2422–2428 (2018).
40. G. Yang, B. Wang, K. Tawfiq, H. Wei, S. Zhou, and G. Chen, *Surface Engineering*, **33**, 149–166 (2017).
41. E. Pircher, M. R. Martínez, S. Hansal, and W. Hansal, *Plating and Surface Finishing*, **90**, 74–79 (2003).
42. D. Landolt, *Electrochim Acta*, **32**, 1–11 (1987).
43. R. Yi, J. Ji, Z. Zhan, and H. Deng, *J Mater Process Technol*, **305**, 117599 (2022).
44. T. P. Hoar and J. A. S. Mowat, *Nature*, **171**, 931 (1953).
45. D. Nakhaie, E. Asselin, K. Wang, M. Salasi, and S. Bakhtiari, *Impedance Analysis of a Model Mechanism for Acceptor-Limited Electropolishing*.
46. S. Magaino, *J Electrochem Soc*, **140**, 1365 (1993).
47. Z. Chaghazardi and R. Wüthrich, *J Electrochem Soc*, **169**, 043510 (2022).
48. S. Van Gils, S. Holten, E. Stijns, M. Vancaldenhoven, H. Terryn, and L. Mattsson, *Surface and Interface Analysis*, **35**, 121–127 (2003).
49. H. Adelkhani, S. Nasoodi, and A. Jafari, *Int. J. Electrochem. Sci*, **4**, 238–246 (2009).
50. A. M. Awad, E. A. Ghazy, S. A. Abo El-Enin, and M. G. Mahmoud, *Surf Coat Technol*, **206**, 3165–3172 (2012).
51. S. Van Gils, C. Le Pen, A. Hubin, H. Terryn, and E. Stijns, *J Electrochem Soc*, **154**, C175 (2007).
52. M. Haïdopoulos, S. Turgeon, C. Sarra-Bournet, G. Laroche, and D. Mantovani, *J Mater Sci Mater Med*, **17**, 647–657 (2006).
53. M. I. Ismail, *J Appl Electrochem*, **9**, 471–473 (1979).
54. M. Haïdopoulos, S. Turgeon, C. Sarra-Bournet, G. Laroche, and D. Mantovani, *J Mater Sci Mater Med*, **17**, 647–657 (2006).

55. J. Kim, J.-K. Park, H. K. Kim, A. R. Unnithan, C. S. Kim, and C. H. Park, *J Nanosci Nanotechnol*, **17**, 2333–2339 (2017).
56. D. Brent, T. Alyssa Saunders, F. Garcia Moreno, and P. Tyagi, in *Proceedings of the ASME 2016 International Mechanical Engineering Congress and Exposition, IMECE2016*, p. V002T02A014 (2016).
57. M. Mahardika, M. A. Setyawan, T. Sriani, N. Miki, and G. S. Prihandana, *Machines*, **9** (2021).
58. P. S. Kao and H. Hocheng, in *Journal of Materials Processing Technology*, vol. 140, p. 255–259 (2003).
59. M. M. Fallah, M. A. Attar, A. Mohammadpour, M. Moradi, and N. Barka, *Mater Res Express*, **8** (2021).
60. C.-C. Lin and C.-C. Hu, *Electrochim Acta*, **53**, 3356–3363 (2008).
61. M.-L. Doche, J.-Y. Hihn, C. Rotty, A. Mandroyan, G. Montavon, and V. Moutarlier, in *Proceedings of the 30th International Conference on Surface Modification Technologies (SMT30), Milan, Italy, 29th June - 1st July, 2016*, (2016).
62. P. Tyagi, D. Brent, T. Saunders, T. Goulet, C. Riso, K. Klein, and F. G. Moreno, *The International Journal of Advanced Manufacturing Technology*, **106**, 1337–1344 (2020).
63. H. Hocheng and P. S. Pa, *Effective Form Design of Electrode in Electrochemical Smoothing of Holes*, p. 995–1004, (2003).
64. K. B. Hensel, *Metal Finishing*, **98**, 440–448 (2000).
65. E.-S. Lee, *Machining Characteristics of the Electropolishing of Stainless Steel (STS316L)*, p. 591–599, (2000).
66. M. B. García-Blanco, M. Díaz-Fuentes, E. Espinosa, A. M. Mancisidor, and G. Vara, *Transactions of the IMF*, **99**, 274–280 (2021).
67. A. Acquesta and T. Monetta, *Adv Eng Mater*, **23**, 2100545 (2021).
68. E. Łyczkowska, P. Szymczyk, B. Dybała, and E. Chlebus, *Archives of Civil and Mechanical Engineering*, **14**, 586–594 (2014).
69. H. Surmann and J. J. Huser, *Automatic electropolishing of cobalt chromium dental cast alloys with a fuzzy logic controller*, p. 1099–1111, (1998).
70. C. L. Faust, *Metal Finishing*, **82**, 29–31 (1984).
71. F. Éozénou, Y. Gasser, J. Charrier, S. Berry, C. Antoine, D. Reschke, and C. De Saclay, in *Proceedings of 14th International Workshop on RF Superconductivity (SRF 2009), Berlin, Germany*, p. 781–785 (2009).



72. P. Lochyński, S. Charazińska, E. Łyczkowska-Widłak, and A. Sikora, *Metals (Basel)*, **9** (2019).
73. J. B. Durkee, *Galvanotechnik*, **100**, 1573–1577 (2009).
74. B. Krishna and R. Wuthrich, *ECS Trans*, **97**, 505 (2020).
75. P. Lochyński, S. Charazińska, M. Karczewski, and E. Łyczkowska-Widłak, *Sci Rep*, **11** (2021).
76. F. Eozénou, A. Aspart, C. Antoine, and B. Malki, *EU contract number RII3-CT-2003-506395: "Electropolishing of Niobium : best EP Parameters."*
77. P. V. Tyagi, M. Nishiwaki, T. Noguchi, M. Sawabe, T. Saeki, H. Hayano, and S. Kato, in *Proceedings of 2nd International Particle Accelerator Conference (IPAC'11), San Sebastián, Spain*, p. 292–294 (2011).
78. G. M. El-Subruiti and A. M. Ahmed, *Kinetic Study of Corrosion of Copper in Phosphoric Acid Tert-Butanol Electropolishing Mixtures*, p. 151–166, (2002).
79. M. Datta and D. Vercruyse, *J Electrochem Soc*, **137**, 3016 (1990).
80. L. Neelakantan and A. W. Hassel, *Electrochim Acta*, **53**, 915–919 (2007).
81. F. Éozénou, S. Berry, Y. Gasser, J. Charrier, and C. De Saclay, in *Proceedings of 14th International Workshop on RF Superconductivity (SRF 2009), Berlin, Germany*, p. 776–780 (2009).
82. F. Eozénou, S. Berry, C. Antoine, Y. Gasser, J.-P. Charrier, and B. Malki, *Physical Review Special Topics - Accelerators and Beams*, **13** (2010).
83. F. Éozénou, M. Bruchon, and J. Gantier, in *Proceedings of 13th International Workshop on RF Superconductivity (SRF2007), Beijing, China*, p. 313–317, Beijing (2003).
84. F. Éozénou, Y. Gasser, J. Charrier, S. Berry, C. Antoine, and D. Reschke, *LOW-VOLTAGE ELECTRO-POLISHING OF SRF CAVITIES*.
85. P. Lochyński, P. Wiercik, S. Charazińska, and M. Ostrowski, *Archives of Environmental Protection*, **47**, 18–29 (2021).
86. S. Charazińska, P. Lochyński, and E. Burszta-Adamiak, *Journal of Water Process Engineering*, **42**, 102169 (2021).
87. F. Eozénou, C. Antoine, A. Aspart, S. Berry, J. F. Denis, and B. Malki, *Efficiency of electropolishing vs bath composition and aging : first results*, (2005).
88. P. Lochyński, M. Kowalski, B. Szczygiel, and K. Kuczewski, *Polish Journal of Chemical Technology*, **18**, 76–81 (3916).

89. J. Destefani, (2007), <https://www.pfonline.com/articles/clean-economical-electropolishing>. Accessed on December 18, 2023.
90. P. Asokan, R. Ravi Kumar, R. Jeyapaul, and M. Santhi, *The International Journal of Advanced Manufacturing Technology*, **39**, 55–63 (2008).
91. Z. Li, H. Ji, and H. Liu, **122**, 893–899 (2010).
92. F. Ji, C. Chen, Y. Zhao, and B. Min, *Micromachines*, **12** (2021).
93. C.-M. Hsu, *Engineering Optimization*, **36**, 659–675 (2004).
94. D. Alves Goulart and R. Dutra Pereira, *Comput Chem Eng*, **140**, 106909 (2020).
95. C. D. Ellis, M. C. Hamilton, J. R. Nakamura, and B. M. Wilamowski, *IEEE Trans Compon Packaging Manuf Technol*, **4**, 1380–1390 (2014).
96. Y. Yoon, M. J. Kim, and J. J. Kim, *Electrochim Acta*, **399**, 139424 (2021).
97. [https://archive-resources.coleparmer.com/Manual\\_pdfs/59770-10.pdf](https://archive-resources.coleparmer.com/Manual_pdfs/59770-10.pdf). Accessed on December 18, 2023.
98. <https://pandas.pydata.org/>. Accessed on December 18, 2023.
99. <https://scikit-learn.org/stable/>. Accessed on December 18, 2023.
100. <https://matplotlib.org/>. Accessed on December 18, 2023.
101. <https://numpy.org/>. Accessed on December 18, 2023.
102. A. Latifi, M. Imani, M. T. Khorasani, and M. D. Joupari, *Surf Coat Technol*, **221**, 1–12 (2013).
103. R. Wüthrich and J. D. Abou Ziki, *Micromachining Using Electrochemical Discharge Phenomenon: Fundamentals and Application of Spark Assisted Chemical Engraving*, William Andrew, (2015).
104. R Schleicher, (2021), <https://alleghenysurface.com/2021/06/overcome-electropolishing-finishing-woes-with-a-solid-plan-and-clean-chemistry/>. Accessed on December 18, 2023.
105. <https://www.kemet.co.uk/blog/lapping/surface-finishing-technologies-process-types-and-methods>. Accessed on December 18, 2023.
106. Kirby R. and Mulhollan G., *A Brief Report on a Brief Examination of the Electropolished GTF Cathode*, Stanford, (1999).
107. <https://waykenrm.com/blogs/electropolishing-vs-mechanical-polishing/>. Accessed on December 18, 2023.
108. <https://www.delstar.com/characteristics-of-the-electropolishing-process>. Accessed on December 18, 2023.

109. <https://www.unifiedalloys.com/blog/stainless-electropolishing>. Accessed on December 18, 2023.
110. <https://www.sansmachining.com/summary-of-common-problems-in-electropolishing/>. Accessed on December 18, 2023.
111. W. Schwartz and J. H. Lindsay, *Electropolishing.*, p. 8–12, (2003).
112. P. Lochyński, S. Charazińska, E. Łyczkowska-Widłak, and A. Sikora, *Metals (Basel)*, **9** (2019).
113. P. Lochyński, S. Charazińska, M. Karczewski, and E. Łyczkowska-Widłak, *Sci Rep*, **11** (2021).
114. L. Ponto, M. Datta, and D. Landolt, *Surf Coat Technol*, **30**, 265–276 (1987).
115. M. Datta and D. Vercruyse, *J Electrochem Soc*, **137**, 3016 (1990).
116. F. Nazneen, P. Galvin, D. W. M. Arrigan, M. Thompson, P. Benvenuto, and G. Herzog, *Journal of Solid State Electrochemistry*, **16**, 1389–1397 (2012).
117. F. M. Abouzeid and H. A. Abubshait, *Arabian Journal of Chemistry*, **13**, 2579–2595 (2020).
118. S. C. Chen, G. C. Tu, and C. A. Huang, *Surf Coat Technol*, **200**, 2065–2071 (2005).
119. C. A. Huang and C. C. Hsu, *The International Journal of Advanced Manufacturing Technology*, **34**, 904–910 (2007).
120. H.-K. Hwang and S.-J. Kim, *Surfaces and Interfaces*, **37**, 102730 (2023).
121. S. Magaino, *J Electrochem Soc*, **140**, 1365 (1993).
122. B. Krishna and R. Wuthrich, *ECS Trans*, **97**, 505 (2020).
123. A. M. Awad, N. A. A. Ghany, and T. M. Dahy, *Appl Surf Sci*, **256**, 4370–4375 (2010).
124. E. S. Lee, *International Journal of Advanced Manufacturing Technology*, **16**, 591–599 (2000).
125. N. Eliaz and O. Nissan, *J Biomed Mater Res A*, **83A**, 546–557 (2007).
126. G. M. El-Subruiti and A. M. Ahmed, *Kinetic Study of Corrosion of Copper in Phosphoric Acid Tert-Butanol Electropolishing Mixtures*, p. 151–166, (2002).
127. S. M. Aguilar-Sierra and F. Echeverría E, *J Mater Eng Perform*, **27**, 1387–1395 (2018).

128. Z. Chaghazardi and R. Wuthrich, in *Proceedings of the 72nd Annual Meeting of the International Society of Electrochemistry (Jeju Island, 29 August - 03 September 2021)*, Jeju Island.

129. S. A. Dudani, *IEEE Trans Syst Man Cybern*, **SMC-6**, 325–327 (1976).

## 10. Appendix

In the following examples, various models were compared with regard to their performance in predicting the relative surface roughness of the parts ( $Ra_{rel}$ ,  $Rq_{rel}$ , and  $Rz_{rel}$ ).

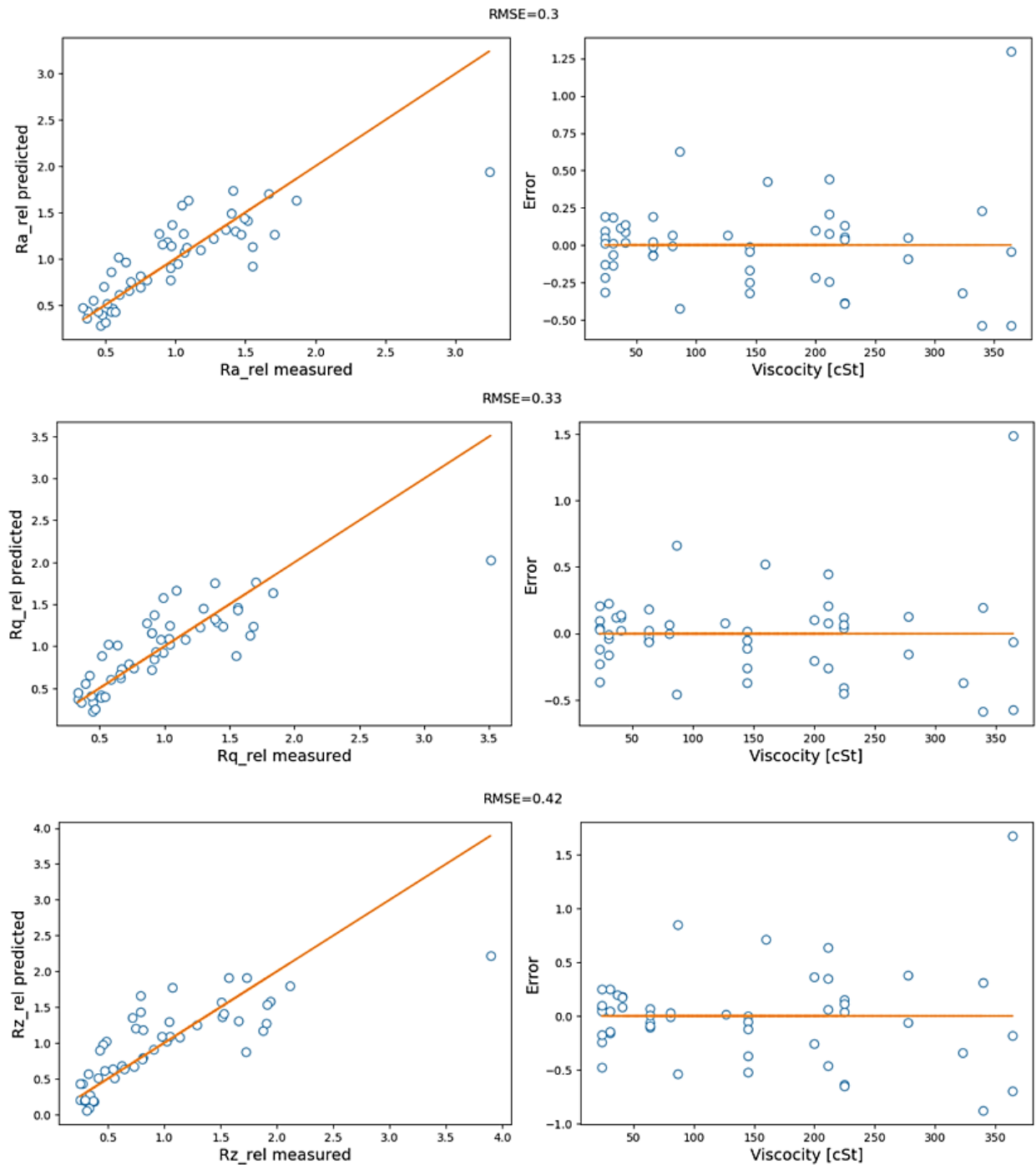


Figure 10.1. The linear regression model used for the prediction of  $Ra_{rel}$ ,  $Rq_{rel}$ , and  $Rz_{rel}$ .

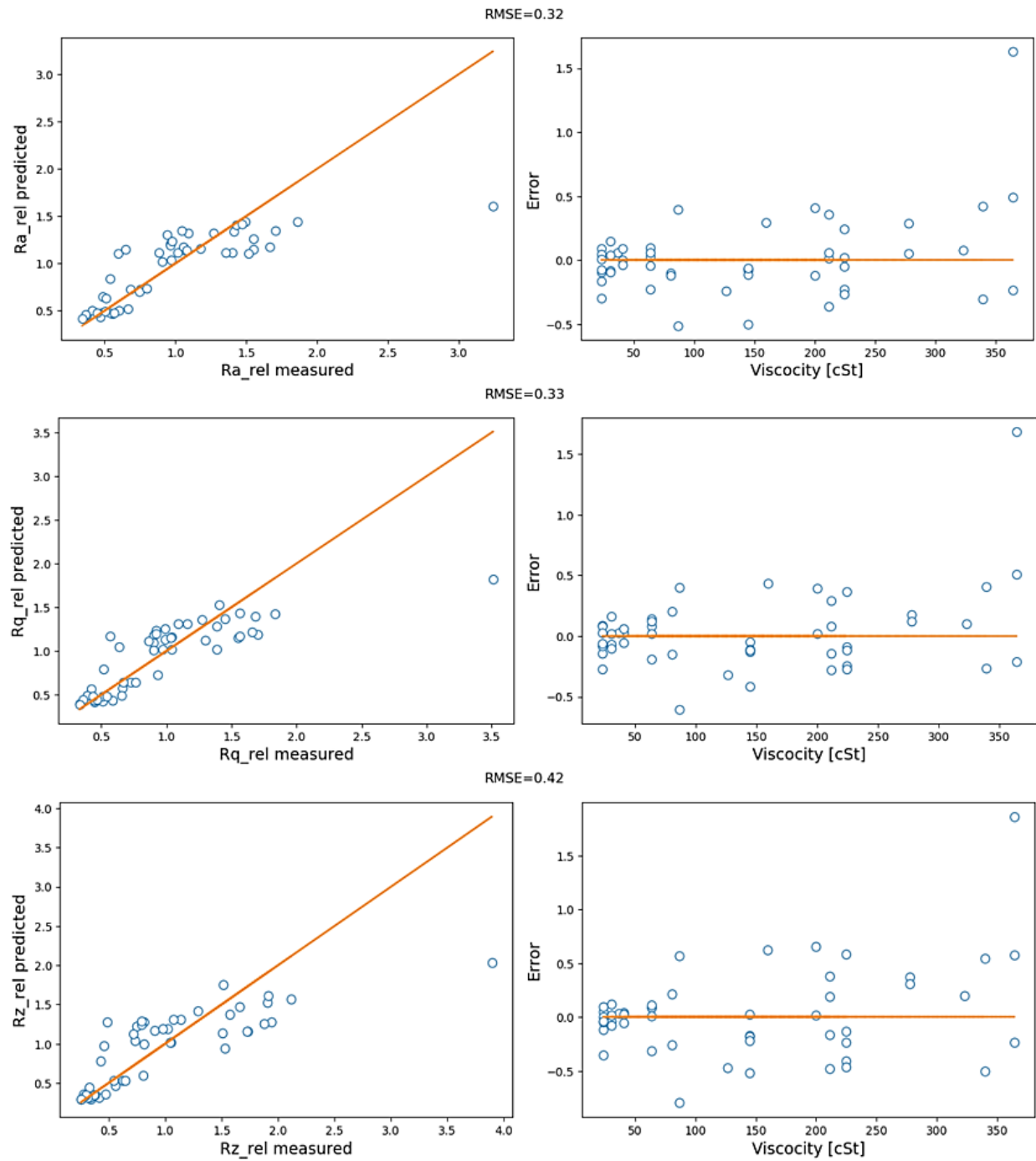


Figure 10.2. The KNN model used for the prediction of Ra-rel, Rq-rel, and Rz-rel.

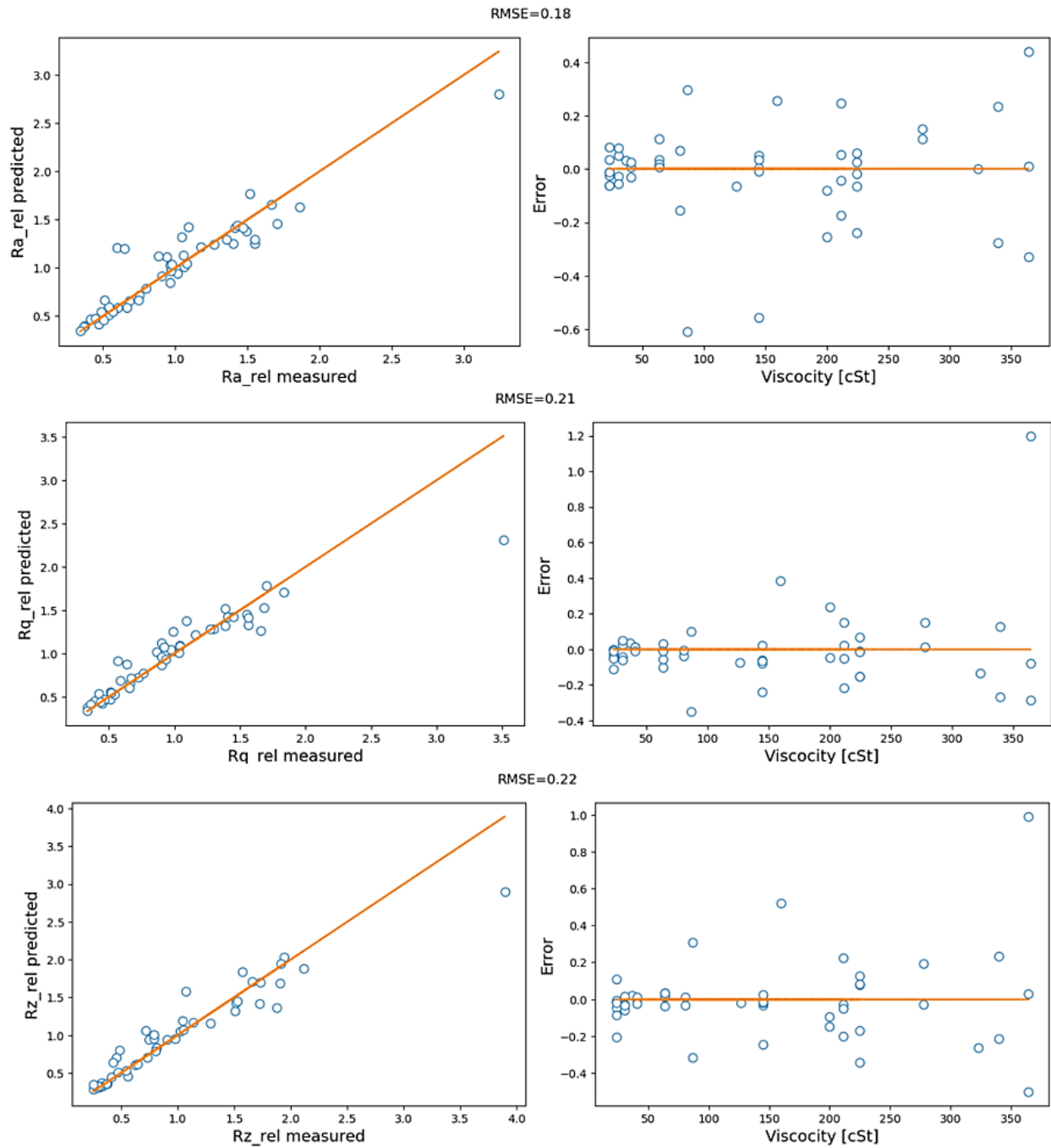


Figure 10.3. The Random Forests model used for the prediction of Ra-rel, Rq-rel, and Rz-rel.

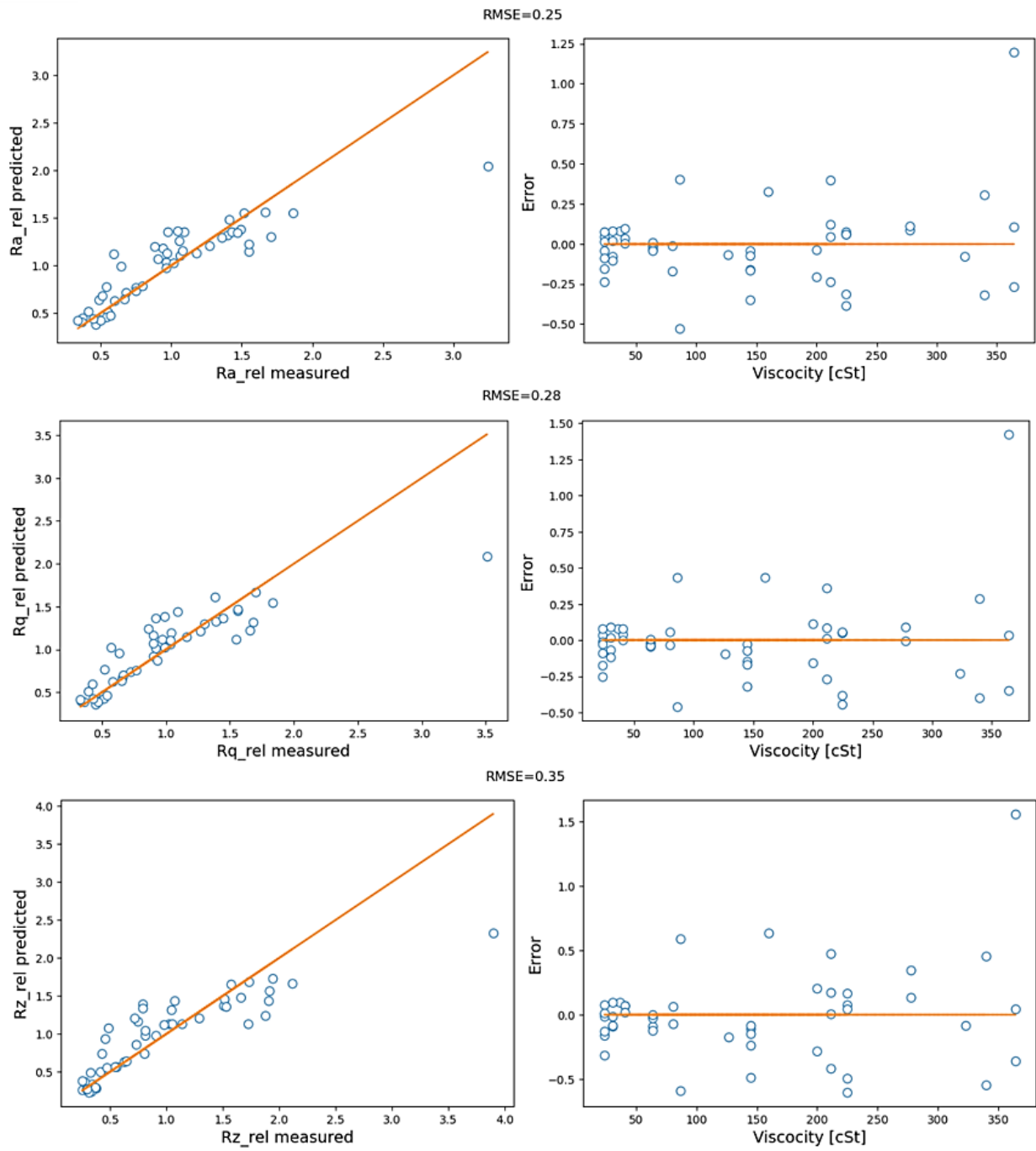


Figure 10.4. The Voting Regressor ensemble used for the prediction of Ra-rel, Rq-rel, and Rz-rel.



Figure 10.5 presents the distribution of the models' Root Mean Squared Error (RMSE) in predicting various target variables across 100 different train-test splits of the dataset. All predictions were executed on the data from the test set.

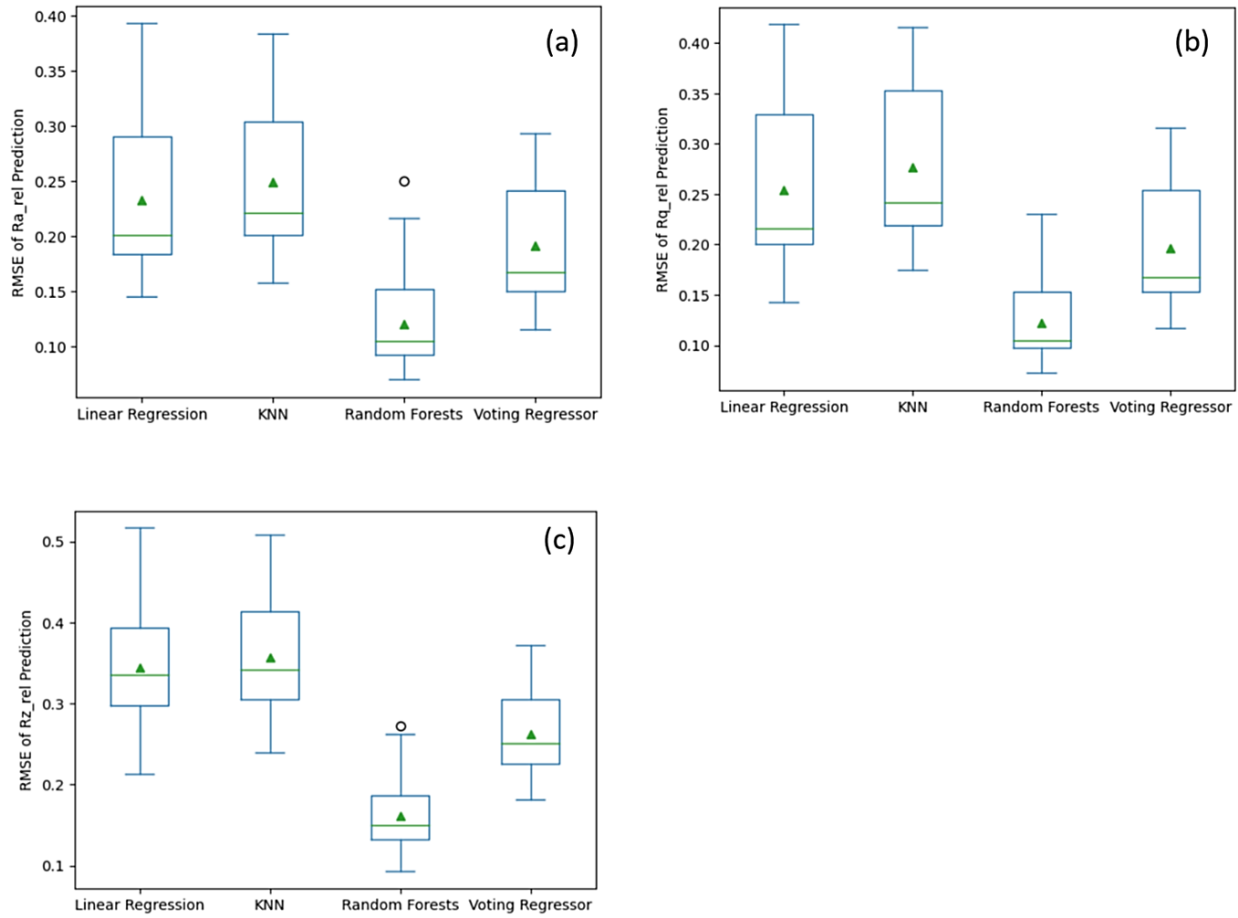


Figure 10.5. RMSE distribution of different models for prediction of Ra-rel, Rq-rel, and Rz-rel on the test set.